CELLULAR AND MOLECULAR MECHANISMS OF *IN VITRO* AND *IN VIVO* INTERACTIONS OF MACROPHAGES WITH THE BIOMATERIAL, POLY(ETHER URETHANE) UREA

A THESIS SUBMITTED

BY

ASHA S. MATHEW

IN PARTIAL FULFILLMENT OF THE REQUIREMENTS

FOR THE DEGREE OF

DOCTOR OF PHILOSOPHY

SREE CHITRA TIRUNAL INSTITUTE FOR
MEDICAL SCIENCES AND TECHNOLOGY
THIRUVANANTHAPURAM – 695 011

APRIL 2007

The thesis

titled

CELLULAR AND MOLECULAR MECHANISMS OF *IN VITRO* AND *IN VIVO* INTERACTIONS OF MACROPHAGES WITH THE BIOMATERIAL, POLY(ETHER URETHANE) UREA

Submitted by

Asha S. Mathew

For the degree of

Doctor of Philosophy

of

Sree Chitra Tirunal Institute
for
Medical Sciences and Technology
Thiruvananthapuram – 695 011

Evaluated and approved

by

Mira Mohanty.
(DR. MIRA MOHANTY)

Name of the guide

Mary Babu
(MARY BABU)

Name of Thesis Examiner

DECLARATION

I, **Asha S. Mathew**, hereby declare that I had personally carried out the work depicted in the thesis titled **"Cellular and molecular mechanisms of *in vitro* and *in vivo* interactions of macrophages with the biomaterial, poly(ether urethane) urea"** under the direct supervision of **Dr. Mira Mohanty**, Scientist G, Division of Implant Biology, Biomedical Technology Wing, Sree Chitra Tirunal Institute for Medical Sciences and Technology, Thiruvananthapuram, Kerala, India, except where external help sought and acknowledged.

Asha S. Mathew

Dr. Mira Mohanty
Scientist G

Histopathology Laboratory
Division of Implant Biology, Biomedical Technology Wing
Sree Chitra Tirunal Institute for Medical Sciences & Technology
Poojapura, Thiruvananthapuram

CERTIFICATE

This is to certify that **Miss. Asha S. Mathew**, in the Division of Implant Biology of this institute, has fulfilled the requirements of the regulations relating to the nature and prescribed period of research for the Ph.D degree of the Sree Chitra Tirunal Institute for Medical Sciences and Technology, Thiruvananthapuram. The work relating to her thesis titled **"Cellular and molecular mechanisms of *in vitro* and *in vivo* interactions of macrophages with the biomaterial, poly(ether urethane) urea"** was carried out under my direct supervision.

Mira Mohanty.

Dr. Mira Mohanty

You are the Vine, I am a small branch.....

.....To Thee I humbly bring this fruit

CONTENTS

Page

ACKNOWLEDGEMENTS

This thesis has taken shape during the past few years, during which I have got the oppurtunity to learn a lot of things. I have been associated with several people in the course of thesis work, to whom I am thankful for reasons worth mentioning.

My research supervisor, ***Dr. Mira Mohanty****, has laid down the platform to stand on and work towards this final dissertation. It is with great appreciation and respect that I thank you Dr. Mira for all the efforts you have put in to make the thesis achieve its present form. On a personal note, I am thankful to you for being there for me on several occasions when I needed your guidance and support.*

I am grateful to ***Dr. K. Mohandas****, Director of our Institute and* ***Dr. G.S. Bhuvaneshwar****, Head BMT wing for permitting me to utilize the excellent facilities in the Institute. Without the coveted research scholarship from* ***Council of Scientific and Industrial Research****, Govt. of India, my dreams on scientific research would not have materialized. The financial assistance from* ***Defence Research and Development Organisation****, Govt of India, is acknowledged. Sincere thanks are due to The Registrar,* ***Dr. A.V. George*** *for the academic support rendered.*

The timely suggestions and valuable comments of the members of ***Doctoral Advisory Committee****, Dr. K. Sreenivasan, Dr.Prabha Balram (Regional Cancer Centre, Thiruvananthapuram) and Dr. P.S. Appukuttan have been of help throughout the study. I thank them for their valuable time and interest in this piece of work. I owe a deep sense of gratitude to* ***Dr. T.V. Kumary****. Whenever I turned to her for help either regarding the use of tissue culture facility or for discussion on the in vitro studies, she has rendered a helping hand.*

Thanks are due to ***Dr. Ajith****, Boston Scientific, USA for the kind gift of commercial polyurethanes and to* ***Mr. C.V. Muraleedharan*** *for the supply of UHMWPE used in this study.*

I am indebted to ***Prof. Luigi Ambrosio, Prof. C. James Kirkpatrick*** *and* ***Prof. Guy Daculsi*** *for the travel awards for two consecutive years by the European Society of Biomaterials, which had enabled me to present my work in the 19th and 20th European Conference on Biomaterials at Sorrento, Italy and Nantes, France. The travel grant from* ***CSIR*** *and* ***DBT****, Govt of India also made my participation in these international conferences possible.*

I have got to mention quite a number of people who have in some way or other helped me during the tenure. ***Dr. Annie John****, I am thankful to you for helping me with TEM analysis, and also for the wonderful tips on life.* ***Dr. G. Pradeepkumar****, (Rajiv Gandhi Centre for Biotechnology, Thiruvananthapuram) has helped me with the MALDI ToF MS analysis.* ***Mrs. Sulekha Baby*** *was there for teaching me the techniques in histology. More than those histology training sessions I thank*

*you for creating the full-of energy atmosphere in the department. **Dr. Anilkumar P.R.**, I am thankful to you for teaching me how to use different tools in computer. The formatting of this thesis was made much easy with the template you have provided. **Viji**, I am thankful to you for patiently making me learn the tissue culture techniques and also for your friendship. I am thankful to all those in different departments of BMT Wing who have helped me by permitting me to do parts of this work in their labs, or by lending me some of the chemicals when I went short of them. I am also thankful to **Dr. H.K. Varma** for the ESEM analysis, **Dr. A.C. Fernandez** for the supply of animals. **Dr. PV. Mohanan** took the pains to give me training on animal experiments. The independent use of the confocal microscope was possible only because of the efficient training provided by **Dr.T.V. Anilkumar**. I am thankful to you **Linda** for the contact angle measurements.*

*This note will become incomplete if I am not expressing my thanks to my **friends**, because they have been a constant source of support for me. My friend **Bernadette K Madathil**, you have been there even before I started with this work, and throughout the period of this study. How can I not mention your name when I put my gratitude down here. **Shiny**, the chatting we had during the long morning walks and the late hour discussions were much inspiring. A note of thanks to you for giving me wings at times when I forgot how to fly. **Bindu** and **Josna**, the good times we had during the last few years has definitely contributed to the making of this thesis. **Mrs. Usha Vasudev, Maya, Neena, Dr. Sabareeswaran, Joseph, Dr. Sajitha, Chitra, Susan, Manitha, Tilak**, you all were there for me whenever there was a need. **Nishi, Divya, Sajeesh, Elizabeth, Smitha, Biji and Anu** you have given me the much wanted companionship.*

***My parents** have been the all-time support and motivators behind my achievements. You have gone through lots of sacrifices for making me comfortable enough to pursue my doctoral study. Though this occassion is not sufficient to express my sense of thankfulness, I thank you both for teaching me the good things that really matter in life.*

When the going was tough, I fell down and when the ride was joyous, I was excited, but one thing is for sure, You kept me safe in Your arms for I could rise after each fall and I could keep my steps steady to reach till here. I kneel before Thee O Lord for everything.

Asha S. Mathew

LIST OF FIGURES

LIST OF TABLES

ABBREVIATIONS

ATR-FTIR	Attenuated Total Reflection – Fourier Transform Infra Red
CASE	Cellular Activation of Signaling ELISA
CE	Cholesterol Esterase
CHAPS	3-[(3-Cholamidopropyl)-Dimethylammonio]-1-Propane Sulfonate
$CoCl_2$	Cobalt chloride
DAB	Diaminobenzidine
DMAc	Dimethylacetamide
DSC	Differential Scanning Calorimetry
DTT	Dithiothreitol
ECM	Extracellular matrix
ED	Ethylene diamine
ELISA	Enzyme Linked Immunosorbent Assay
ESC	Environmental Stress Cracking
ESEM	Environmental Scanning Electron Microscopy
EtO	Ethylene oxide
FAKs	Focal Adhesion Kinases
FBGC	Foreign Body Giant Cells
FBS	Foetal Bovine Serum
GPC	Gel Permeation Chromatography
H_2O_2	Hydrogen peroxide
HCl	Hydrochloric acid
IFN-γ	Interferon gamma
IgG	Immunoglobin G
IL-1	Interleukin 1
IL-6	Interleukin 6
IPG	Isoelectric pH gradient
JNK	c-Jun NH2 terminal Kinase
KCl	Potassium Chloride

LSCM	Laser Scanning Confocal Microscopy
MALDI MS	Matrix Assisted Laser Desorption Ionization Mass Spectrometry
MALDI ToF MS	Matrix Assisted Laser Desorption Ionization Time-of-Flight Mass Spectrometry
MAPK	Mitogen Activated Protein Kinase
MDI	4,4'- methylene di(p-phenyl isocyanate)
MDM	Monocyte Derived Macrophages
MEM	Minimum Essential Medium
MMPs	Matrix metalloproteinases
Mn	Number average molecular weight
Mw	Weight average molecular weight
Na_2HPO_4	Disodium hydrogen phosphate
NaCl	Sodium chloride
NaH_2PO_4	Sodium dihydrogen phosphate
NaOH	Sodium hydroxide
NO	Nitric oxide
OsO_4	Osmium tetroxide
PBD	Polybutadiene
PBS	Phosphate Buffered Saline
PDMS	Polydimethylsiloxane
PEUU	Poly(ether urethane) urea
PKC	Protein Kinase C
PMA	Phorbol 12-myristate 13-acetate
PMMA	Poly(methyl-methacrylate)
Poly HEMA	Poly(2-hydroxyethyl-methacrylate)
PTFE	Polytetrafluoroethylene
PTMEG	Polytetramethylene ether glycol
PTMO	Polytetramethylene oxide
PU	Polyurethane
RT	Room Temperature
SAM	Self assembled monolayer

SDS	Sodium dodecyl sulfate
SEM	Scanning Electron Microscopy
SMM	Surface modifying macromolecules
TCPS	Tissue culture grade polystyrene
TDI	Toluene diisocyanate
TEM	Transmission Electron Microscopy
TEMED	N,N,N'N' tetramethylethylenediamine
T_g	Glass transition temperature
TGF-β	Transforming Growth Factor β
TGF-α	Transforming Growth Factor alpha
TNF-α	Tumour Necrosis Factor alpha
UHMWPE	Ultra High Molecular Weight Polyethylene

SYNOPSIS

History is replete with reports of materials being used to replace body parts. Recent times have witnessed the widespread use of materials as such or in the form of tissue engineered materials for improving the functions of almost all organs and organ systems of the body. The materials which are used for fabricating implantable devices for assisting, replacing or augmenting body parts such as tissues or organs are termed biomaterials. Research in biomaterials field stems in different directions such as development of novel biomaterials, testing the efficacy of biomaterials for various applications, tissue engineering, drug delivery, nanomaterials and medicine. A different aspect which deals with an important challenge in the biomaterials field assumes much importance. That is about the very promising biomaterials which change with long-term residence in the human body and ultimately fail to deliver their intended function. Biomaterials with excellent physicochemical properties which pass all the biocompatibility tests seem to be very promising. However when placed inside the human body in the form of a medical device, in some cases there is long-term failure. Such cases of long-term failure cannot be ignored as incidental because it involves revision surgery, pain and financial implications for the patient. This prompted a time related investigation into the factors involved in biological response to such materials. Of interest was the highly versatile family of polyurethanes.

Chapter 1 gives an introduction to the topic being addressed in the thesis. Biomaterials for assisting cardiovascular system are mainly used in the form of artificial heart valves, vascular grafts, catheters, ventricular assist devices and total artificial heart. A family of such materials which has found widespread use in cardiovascular system in particular is polyurethanes (PUs). The compliance of PUs with the tissue, excellent chemical and mechanical properties suitable for many of the cardiovascular applications makes PUs the material of choice for many implantable biomedical devices. However, biodegradation in the biological system is a matter of concern in the use of PUs for long-term implant devices. This lack of stability at long-term in the biological milieu leads to loss of function and failure of the device. The need to eliminate biodegradation of this very useful material assumes importance in the field of development of materials for medical applications such as long-term implantable devices.

Chapter 2 gives a comprehensive account of the literature related to the study. The suggested causes of polyurethane degradation are calcification, environmental stress cracking, hydrolysis and oxidation. The stability of PU is influenced by the chemistry of the material. Involvement of biological components in the degradation of PUs is also reported. Cholesterol esterase and carboxyl esterase were suggested as potential candidate enzymes for the degradation of different types of PUs. Synergistic effect of plasma components with oxidative action of reactive oxygen species on the environmental stress cracking has been reported.

To overcome the degradation of PUs, several research groups have adopted strategies such as varying the material chemistry by altering the type and ratio of monomers and also by incorporating additives. Eventhough some reports claim the *in vitro* stability of these modified PUs, their long-term biostability relevant for human clinical applications have not been reported. The pursuit for a biostable, biocompatible PU for long-term implants in clinical applications continues. On the other hand, the understanding of sequential events following the interaction of PU with the biological milieu assumes importance. This will be facilitated by delineating the ongoing biochemical interactions and molecular mechanisms in the cell-material niche.

Adsorption of proteins on implant surface from the biological milieu at the site of injury is the first event following implantation. Incoming inflammatory cells adhere to the material surface through adsorbed proteins. Depending upon the nature of adsorbed proteins, signals are transferred to the cells through ligand-receptor interactions at the cell surface. Inflammatory cells, initially neutrophils followed by monocytes and macrophages are predominant at all material-tissue interfaces following implantation in any tissue, such a response being mainly to the surgical procedure. Inflammation is followed by repair with formation of a fibrous capsule around the implant. However, persistence of macrophages at the interface in some cases has led to queries regarding the role of these cells in material failure. The significance of the interrelated phenomena, of material properties and complex cellular interactions with the material, in the cell mediated biodegradation of polyurethane has not yet been elucidated fully. Previous studies have explored certain aspects of cell signaling following cell adhesion on tissue culture polystyrene. However cell signaling events which occur upon interaction of macrophages with PUs is not yet delineated. A detailed understanding of signaling pathways induced by macrophage interaction with PU may assist in the development of

specific inhibitors to prevent macrophage activation. The present study attempts 1) to gain a better understanding of the sequence of cell-material interactions at the polyurethane-tissue interface over a long period of implantation and 2) to delineate the molecular mechanism of cellular activation underlying the surface degradation of PEUU, by an *in vitro* approach.

Chapter 3 describes the experimental approach of the entire study including methodology and materials used. The study was performed in three phases.

In the first phase, a PU, containing ether soft segment, poly(ether urethane) urea herein referred to as PEUU was synthesized and characterized by attenuated total reflectance Fourier transform infrared spectroscopy (ATR-FTIR), Differential Scanning Calorimetry (DSC), Contact angle analysis and Gel Permeation Chromatography (GPC). The PEUU was tested for cytotoxicity by a cell culture method using L929 mouse fibroblast cells. For the *in vivo* experiments PEUU was implanted at an intramuscular site in rat animal model. A sham operation served as the control for the surgical technique. Ultrahigh molecular weight polyethylene (UHMWPE) was used as a control material. The tissues with the implants were retrieved at definite time periods starting with one hour through 180 days post-implantation. Tissue response to sham operation and implantation of UHMWPE were evaluated to assess the response to control. Tissue response to PEUU implants was evaluated by histological as well as immunohistochemical analysis at all time periods of the study. Transmission electron microscopy (TEM) analysis was performed to analyse the ultrastructural details at selected time periods of the study. To study the initial event of protein adsorption on implants, at two days post-implantation, a proteomic approach consisting of two dimensional polyacrylamide gel electrophoresis in conjunction with matrix assisted laser desorption/ionization time of flight mass spectrometry was adopted. The surface changes of retrieved implants were examined by scanning electron microscopy (SEM) analysis. On the basis of the findings from *in vivo* study, interaction of macrophages with PEUU was assessed in detail in the next phase of the study.

In the second phase of the study cell-material interactions were analysed by an *in vitro* method using the murine macrophage cell line RAW 264.7. In this phase, in addition to the in-house synthesized PEUU, UHMWPE, control glass coverslip and a series of six commercial biomedical grade PUs with different chemistries were evaluated. The commercial PUs were also characterized by ATR-FTIR, GPC and contact angle analysis.

Cell adhesion and actin cytoskeletal distribution were evaluated by phase contrast microscopy/environmental SEM and laser scanning confocal microscopy (LSCM). The determination of cytokines IL-6 and IL-1α released at 24 and 48 hours by macrophages was carried out by enzyme linked immunosorbent assay (ELISA).

In the third phase of the study the role of a cell signaling molecule in macrophage activation was studied by detecting protein phosphorylation using a commercial kit based on cellular activation of signaling ELISA (CASE assay).

Chapter 4 includes the results obtained from the various experimental aspects of this study, described under separate headings with deliberations on key aspects. The results of the characterization experiments indicated that the in-house synthesized PEUU had the chemistry characteristic of polyurethanes. Based on its *in vitro* non-cytotoxic nature, PEUU was used for *in vivo* intramuscular implantation in rat animal model. Macrophages were the predominant cell type observed adjacent to the implant site. While the inflammatory response to the control material UHMWPE, had subsided by 60 days of implantation, the presence of macrophages at PEUU adjacent tissue persisted throughout the entire time period studied (180 days). Immunohistochemical analysis of PEUU adjacent tissue confirmed the identity of macrophages. The presence of pro-inflammatory cytokines such as IL-6, IL-1α, IL-1β, TNF- α and IFN-γ at the tissue adjacent to PEUU indicated the active nature of these cells. Absence of lymphocytes was proved by the negative staining for lymphocyte marker. Ultrastructural analysis of tissue at the implant site also substantiated the histological observations. The results of the proteomic study performed with two day post-implantation sample proved the hypothesis that the difference in response elicited against PEUU and UHMWPE could be attributed to the difference in protein adsorption at early time periods.

The intricate mechanisms of cell material interactions were delineated by the cell adhesion pattern and actin cytoskeletal spreading of macrophages on PEUU and commercial PUs *in vitro*. The spreading behaviour exhibited by macrophages at the early time periods of 4, 24, 48 and 72 hours after seeding denoted difference in adhesion pattern between PUs with different chemistry. The results of ELISA confirmed the active status of the macrophages on contact with the polyurethane. The secretion of IL-1α by the macrophages decreased with time, but the decrease was significant only in the case of the control material. The release of IL-6 by cells on PEUU was however less than that on the

commercial PU, Biospan and the control glass coverslip. The CASE assay revealed that the cell signaling molecule JNK (c-Jun NH2 terminal kinase) is phosphorylated in macrophages adherent on PEUU at higher rates in comparison with the glass coverslip and commercial PU. The increase in the phosphorylation of JNK further points that the survival signal in these PEUU adhered cells is high.

Chapter 5 summarizes the whole study and provides the conclusions drawn out. The results of this study indicate the persistence of macrophages adjacent to PEUU at long-term residence in biological tissue with concomitant surface degradation in the implant. The study delineates the active nature of these cells and implicates the role of JNK phosphorylation in activation and survival of macrophages adhered on PEUU. The investigation into the role of a signaling molecule in survival and activation of macrophages on PU surface has not been carried out earlier. The differential protein adsorption on PEUU and the control UHMWPE at an early time period post-implantation indicates the differential signal transmitted to the cells by these adsorbed proteins.

This study assumes significance in that it provides insights into the molecular mechanisms of macrophage activation on PEUU which will be useful to devise methods to prevent the survival of macrophages on PEUU. Selective inhibition of signaling molecules to prevent persistence and activation of macrophages on PUs could be effected to ensure long-term *in vivo* stability of material. This in turn will aid in designing better PUs which could resist degradation in the biological milieu.

As an extension of the study in future, investigations can be carried out to elucidate the entire signaling network behind macrophage activation. Analysis of adsorbed proteins over time for the initial durations could provide information on how the protein adsorption pattern changes with time. The role of JNK activation in survival of macrophages *in vivo* can be confirmed by the use of knockout animals.

Chapter 1

INTRODUCTION

1.1. Biomaterials

Health care has vastly improved to-day due to the developments in technology and availability of materials to replace diseased tissues and organs. From the very early time in human history the practice of using materials for assisting or replacing body parts has started. Recent times have witnessed the widespread use of materials as such or as tissue engineered materials for improving the functions of almost all organs and organ systems of the body. The materials which are used for fabricating implantable devices for assisting, replacing or augmenting body parts such as tissues or organs are termed biomaterials.

By definition biomaterial is "any substance (other than a drug) or combination of substances, synthetic or natural in origin, which can be used for any period of time, as a whole or as part of a system which treats, augments or replaces any tissue, organ or function of the body". Biomaterials fall under different categories such as: polymers, metals, ceramics, natural materials and composite materials which are combinations of the other classes of materials. Polymers have found use in most systems of the body either alone or as composites (Abramson S *et al* 2004).

1.1.1. Polymers as biomaterials

Polymers are used for a variety of biomedical applications including soft and hard tissue implants and as scaffolds for tissue engineering. Synthetic and natural polymers derived from synthetic organic processes or natural sources respectively, are

widely used. Natural polymers may be of plant or animal origin. Cellulose, sodium alginate, natural rubber, chitosan are plant based materials used widely in the field of biomaterials. Collagen, glycosaminoglycans, heparin, hyaluronic acid, tissue based heart valves and sutures fall under the category of animal derived biomaterials. Synthetic polymers can be prepared by addition or condensation polymerization methods. Polymers containing only one type of repeat units are called homopolymers. Poly(methyl-methacrylate) (PMMA), Poly(2-hydroxyethyl-methacrylate) (poly HEMA), polyethylene, polytetrafluoroethylene, polydimethylsiloxane (PDMS), polyvinylchloride, polyethyleneterephthalate are some of the common homopolymers used as biomaterials. Copolymers have two or more repeat units. The copolymers most commonly used as biomaterials are polyurethanes (PU) and poly(glycolide-lactide) copolymers. Depending on the reaction conditions and the reactivity of each monomer type copolymers can be random, alternating, graft or block copolymers.

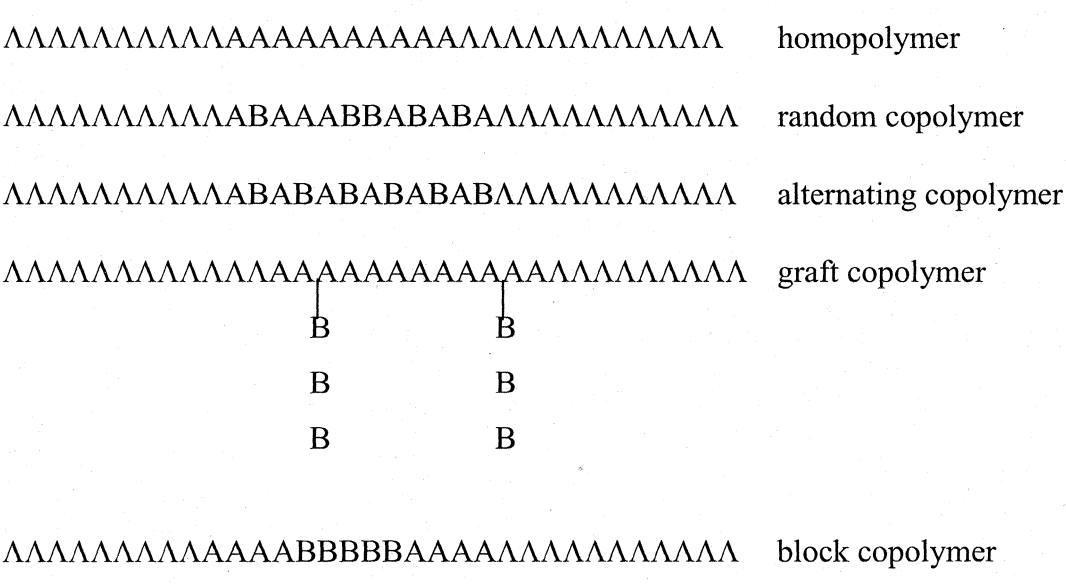

A- repeat unit 1

B- repeat unit 2

Table 1 Polymers used as biomaterials and their applications.

Polymer	Application
PMMA	Intraocular lenses, hard contact lenses
Poly-HEMA	Soft contact lenses
Polyethylene (high density)	Tubing for drains and catheters
Polyethylene (ultrahigh-molecular weight)	Acetabular component in artificial hips, other prosthetic joints
Polypropylene	Sutures and hernia repair
Polytetrafluoroethylene	Vascular grafts
Polyvinylchloride	Blood storage bags, tubings for blood transfusion
Poly(dimethylsiloxane)	Finger joints, heart valves, breast implants, ear, chin and nose reconstruction
Polyethyleneterephthalate	Ligament reconstruction, large diameter arterial grafts
Nylon	Surgical sutures
Poly lactic co glycolic acid	Resorbable surgical suture, orthopaedic fixation devices
Polyurethanes	Pacemaker lead insulations, catheters, vascular grafts, heart assist balloon pumps, artificial heart bladders, wound dressings

1.1.2. Polyurethanes

Polyurethanes (PUs) are block copolymers containing "hard" and "soft" blocks or segments. The hard blocks have glass transition temperature (T_g) above room temperature (RT), hence they behave as glassy or semi-crystalline reinforcing blocks. The hard segment is composed of a diisocyanate and a chain extender. The soft segment is composed of a polyol. The soft blocks have T_g values below RT, hence they give a rubbery character to the material at RT. PU elastomers are segmented polymers, with a two-phase structure of rigid hard segments reinforcing the soft segment matrix.

The heterogenous family of polymers, which contain urethane linkage are known as PUs. However, urethane groups do not necessarily contribute to the major functionality in PUs. The ability to incorporate other functional groups results in a variety of PUs with properties ranging from hard thermosetting materials to soft elastomers. PUs used for biomedical applications generally belong to the thermoplastic elastomeric group having good fatigue and compliance properties. PUs are characterized by the presence of urethane (carbamate) linkages.

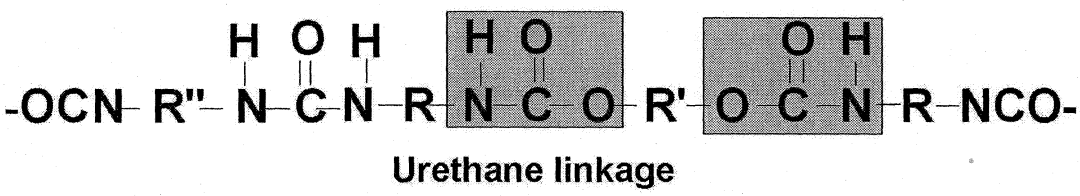

Figure 1 Schematic representation of polyurethane backbone structure urethane linkage is highlighted.

The three major constituents of PUs are diisocyanate, macrodiol and chain extender. According to the type of the three components selected different types of PUs can be synthesized. The options available in selecting the chemistry of PU offer a variety of combinations from which the selections can be made, hence PUs with tailor-made properties can be synthesized accordingly.

Polyurethanes are frequently used for the manufacture of implantable medical devices such as vascular grafts, catheters, artificial heart diaphragms, heart valves and pacemaker lead insulators, defibrillators, neurologic stimulators and mammary prostheses. The performance of PUs in medical device applications is acceptable in terms of its compliance with the tissue and excellent chemical and mechanical properties suitable for many of the cardiovascular applications. In addition to their excellent physical and mechanical properties, PUs fulfill the most important need of a biomaterial, that is compatibility with tissues. However, this compatibility has been found to be unstable over a long term in the biological environment. This lack of stability in the biological milieu leads to loss of function and failure of the device (Chawla AS *et al* 1988). On the other hand this feature of biodegradability has found use in applications such as tissue adhesives, scaffolds for tissue engineering, and drug

delivery devices. In such cases slow degradation of material with simultaneous replacement with tissues is a requisite. Nevertheless, the need to find out the cause of biodegradation of this very useful material assumes importance in the development and improvement of materials for medical applications, especially for long-term implantable devices. The pursuit for a biostable, biocompatible PU for long-term implants in clinical applications continues. Investigation of sequential events following the interaction of PU with the biological milieu is of significance in designing biostable PUs. This will be facilitated by delineating the ongoing biochemical interactions and molecular mechanisms in the cell-material niche.

The significance of the interrelated phenomena, of material properties and complex cellular interactions with the material, in the cell mediated biodegradation of polyurethane has not yet been elucidated fully. An understanding of the tissue response to implanted material is of importance in the study of degradation of PUs *in vivo*.

1.2. Tissue response to injury and foreign bodies

The implantation of a medical implant or prosthesis involves an injury to the tissue. The immediate response to an injury, in which the skin-tissue barrier is breached, will be to prevent loss of blood. This nonspecific response is quite complex which involves activation and aggregation of platelets culminating in a platelet plug. The coagulation pathway is activated and a fibrin clot is formed. The initial event following implantation of a biomaterial is the adsorption of proteins on the material surface. Depending upon material surface energy parameters, protein concentration in the extracellular fluid and blood, and affinity of protein to the surface, proteins adsorb and desorb in sequence. This phenomenon is termed Vroman effect. The adsorbed proteins serve as bridging molecules for the cells to attach on material surface. The inflammatory cell infiltration determines the type of response elicited against the implanted material. Based on the type of biological response elicited, biomaterials are classified as inert, bioactive, bioresorbable and biodegradable.

One of the main aspects of the innate host response will be directed against the invasion of microorganisms and foreign bodies. The complement system

consisting of a set of serum proteins gets activated in a cascade manner and coats the foreign material and targets it for ensuing attack by cells.

The presence of blood, damaged tissue and extra-cellular components of surrounding tissue leads to an accumulation of chemokines, which further causes the movement of inflammatory cells from adjacent blood vessels. The exodus of cells is facilitated by increase in permeability of these vessels. The first cell type to arrive at the site of injury is neutrophils. The neutrophils are involved in phagocytosis of dead tissue and any foreign materials of minute size. This is carried out by the engulfment of tissue debri/material by internalization through cell membrane invaginations, fusion with lysosomes and subsequent degradation/killing. This is effected by reactive oxygen species formed during phagocytosis and bioactive constituents such as myeloperoxidase, cationic peptides (defensins) produced in granules. Neutrophils are short lived and the function of phagocytosis is taken up by macrophages. At the site of injury, release of TGF-β from platelet α granules stimulates recruitment of monocytes. Tissue fibroblasts produce collagen and a scar is ultimately formed.

If the foreign body is small enough for the cells to digest and remove, a repair phase follows the response to the foreign body. If not, chronic inflammation ensues with persistence of macrophages for a longer time. Presence of debri of the material, leakage of chemical constituents or persistence of sterilization residues have been found to initiate an influx of macrophages leading to chronic inflammation over a long period of time.

If the macrophage fails to phagocytose a large foreign object, they undergo frustrated phagocytosis in which they release their vacuole contents extracellularly. This may in turn result in damage to the surrounding tissue. However, it is noted that macrophages form a sealed interface with the material and release their contents in an enclosed environment underneath the cell directly on the material. Macrophages undergoing frustrated phagocytosis, when met with similar cells fuse with each other. The multinucleated cells formed by the fusion of two or more macrophages are known as foreign body giant cells (FBGC). Continued presence of foreign bodies with concomitant recruitment of macrophages and formation of FBGCs leads to a state of chronic inflammation.

1.2.1. Tissue-polyurethane interactions

The monocytes and macrophages adhere to the material surface through receptor-ligand interaction with the adsorbed proteins. Based on this interaction, cells are primed for activation, proliferation, spreading or apoptosis. Hence, the molecular signal transduced to the cell upon contact with the material through the adsorbed protein influences the cell behaviour which determines the response elicited towards implanted PU. The *in vivo* environment presents a complex involvement of different cell types and the cytokine network secreted by them along with the various extracellular matrix proteins and matricellular proteins. It is in this complex biological milieu that the sequence of events progress from wound healing response to chronic inflammation and eventually cell-mediated degradation of implanted polyurethane. The surface expression of cellular receptors and their interaction with protein ligands hence becomes a determinative factor in the biostability of polyurethanes. The biocompatibility and biostability is affected by the cell-material interactions at the tissue-implant interface. Not much information is available on the molecular interactions of soft tissue (especially muscle) with polyether urea urethanes.

The adherent cells upon activation release cytokines which in turn mediate the inflammatory processes. Although several *in vitro* studies have dealt with the effect of cytokines on various cellular processes upon contact with biomaterials, there has been little effort towards understanding the production of cytokines in the complex biological milieu upon implantation of PU, specifically poly(ether urethane)urea.

A polyether urethane urea (PEUU) has been selected as the material of choice for this study because of its relatively good resistance to the common mechanisms of degradation such as hydrolysis and lipid sorption. The major method of PEUU degradation is environmental stress cracking (ESC), in which the contribution of the biological milieu is significant. The cellular response to implanted PEUU and changes in PEUU morphology after implantation in animal model is evaluated. The mechanism of cellular interactions with PEUU is evaluated *in vitro* in comparison with commercial PUs.

The topic is addressed in this thesis starting with the synthesis of the particular polyether urea urethane under study. The characterization of the PEUU was done by

techniques like attenuated total reflectance Fourier transform infrared (ATR- FTIR) spectroscopy, Gel permeation chromatography (GPC) and scanning electron microscopy (SEM). An *in vitro* cytotoxicity test was carried out to assess the cytotoxic potential of PEUU. The implantation studies were carried out in a murine model for various time periods starting from one hour through 180 days. A known biocompatible material UHMWPE served as the control. Sham operation served as the control for the surgical technique. The cellular response to the injury as well as to the implanted materials was analysed by histological evaluation of the retrieved tissue. Immunohistochemical staining for particular cells and cytokines was also carried out on PEUU adjacent tissues. Analysis of adsorbed proteins on explanted material surface was carried out at an early time period. The surface degradation of PEUU was qualitatively analysed by SEM. *In vitro* analysis of cell- PEUU interactions were also carried out in comparison with that on commercial PUs. Cellular activation on the commercial PU, Biospan®, and in house synthesized PEUU was analyzed by measuring the cytokine release. The role of a signaling molecule, c-Jun NH2 terminal Kinase (JNK) in cell activation on PEUU was also investigated. The results obtained for the various aspects of this study are described under separate headings with deliberations on key aspects.

CHAPTER 2

LITERATURE REVIEW

2.1. Biomaterials

The use of materials for implantation in human body began much earlier than the modern awareness and applications of biomaterials were established. In prehistoric times man used non-living materials for regaining loss of structural or functional aspects of the body. The identification of a spear point in the hip bone of a man lived 9000 years ago indicated complete integration of the spear point with the bone. Dental implants were used in Europe around 200 A.D. Linen sutures were used by Egyptians to close wounds. The well defined area of biomaterials science as perceived today has evolved from these ancient practices to the present situation of bionic man. It is now possible, to a certain extent, to custom make and replace diseased organs or tissues, by the efficient use of biomaterials.

Biomaterials fall under different categories of materials such as polymers, metals, ceramics, natural materials, and composite materials formed of any two different classes of materials (Abramson S *et al* 2004). Metals are used mainly in orthopaedic implants and to a certain extent in cardiovascular implants as well. Ceramics, glasses and glass-ceramics are used in dentistry and orthopaedics. Composite materials find use in hard tissue applications. A range of natural materials such as collagen, silk, and cellulose are also used in biomedical applications. Polymers, the largest class of biomaterials are used for a variety of implant devices such as in orthopaedic, dental, soft tissue, cardiovascular and tissue engineering

applications. Polyurethanes, one of the most versatile group of polymers are widely used in biomaterial applications.

2.2. Polyurethanes as biomaterials

Polyurethanes (PUs) have been used in biomedical applications because of their beneficial properties such as fatigue resistance and compliance. The diversity in the available range of constituent raw materials for synthesis of PUs holds out an array of PUs. From these, PUs with tailor made properties can be chosen according to the intended application. Biomedical applications which use PUs include vascular catheters, bladders of left ventricular assist devices, heart valves, total artificial heart, pacemaker lead insulators, breast implants, and wound dressings (Zdrahala and Zdrahala 1999). In addition to the use in long-term devices, PUs have been used in tissue engineered (Saad B *et al* 2000) biodegradable scaffolds and in drug delivery systems (Yang M and Santerre JP 2001). The first reported use of PU in biomedical application dates back to late 1960s, when Boretos and Pierce have mentioned the use of a commercial PU, Biomer® for medical applications (Boretos JW and Pierce WS 1967).

Eventhough Biomer® was accepted as a successful biomaterial, it was withdrawn from the market due to product liability concerns in 1991. The use of polyether based thermoplastic urethane, Pellethane prevailed from late 1970s. Because of yellowing of 4,4'-methylene di(p-phenyl isocyanate (MDI) containing Pellethanes®, aliphatic diisocyanate based PUs were developed. With the increasing need for more biomaterials for different applications, novel PUs were developed. These novel PUs were claimed to have enhancement in performance. However, one of the major concerns in the use of PUs for long-term use as implants is the degradation in biological milieu.

2.2.1. Degradation of polyurethane

Stability of PUs in the biological milieu is not adequate for its successful use as an implantable biomedical device. Surface degradation of cardiac pacemaker lead insulations explanted from patients was evidenced by infrared spectroscopy. Some of the explanted lead insulators exhibited shallow microcracking and some others had

deep crazed breaches (Stokes KB 1997). Polyether urethane implanted for 5 weeks time period in subcutaneous cage model in rats exhibited degradation. Degradation was evidenced in the form of pits and cracks directly under the areas of adhered macrophages and foreign body giant cells (FBGCs) (Zhao Q *et al* 1991). The suggested causes of polyurethane degradation are calcification, environmental stress cracking, hydrolysis and oxidation (Stokes K and McVenes R 1995). Of these, oxidation and hydrolysis are the widely investigated mechanisms of PU degradation.

2.2.1.1. Hydrolytic degradation

Polyesterurethane ureas are susceptible to the hydrolytic action of Proteinase K, chymotrypsin, thrombin and cholesterol esterase, whereas polyetherurethane ureas are susceptible only to proteinase K and cholesterol esterase action. Susceptibilty of PUs to degradation as assessed by *in vitro* radiolabel release indicated hydrolytic degradation. (Labow RS *et al* 1999). Cholesterol esterase (CE) and carboxyl esterase were suggested as potential candidate enzymes for the degradation of different types of PUs (Labow RS *et al* 2002a). Cholesterol esterase is secreted in high levels as monocytes differentiate to macrophages. Polyester and polyether urethanes with hard segments based on toluene diisocyanate (TDI) and ethylene diamine (ED) when incubated with CE showed radiolabel release indicating degradation (Santerre JP *et al* 1993). Santerre *et al* had evaluated the potential of other enzymes relevant in an inflammatory milieu such as cathepsin B, collagenase and xanthine oxidase for radiolabel release from PUs. The results showed that only cholesterol esterase was capable of causing radiolabel release from PUs. This study suggested initiation of degradation at the hard segment regions which are easily accessible by the enzyme. A reduction in radiolabel release was noticed after 28 days, which was attributed to the lack of accessibility of hard segments deep down the surface. Labow *et al* demonstrated hydrolytic degradation of polycarbonate and polyether urethanes by *in vitro* studies (Labow RS *et al* 2001a).

2.2.1.2. Oxidative degradation

Polyether urethanes are susceptible to oxidative damage by reactive oxygen species produced by activated inflammatory cells. Synergistic effect of plasma components with oxidative action of reactive oxygen species on the environmental

stress cracking of Pellethane 2363-80A has been reported (Zhao QH *et al* 1993). At short-term, degradation of polyether urethane occured only at the surface. Cholesterol esterase cleaves urethane linkages which are easily accessible, further degradation could be delayed because of the phase separated nature and hence the urethane linkages may not be accessible by the enzyme. Horse radish peroxidase, an oxidative enzyme was unable to cause degradation of both polyether and polyester urethanes (Santerre JP *et al* 1994). The soft segment of polyether urethane is cleaved by reactive oxygen species which leads to initiation of degradation as embrittled areas which eventually forms cracks on the material surface (Wu Y *et al* 1992). Hydroxyl radicals are responsible for the abstraction of proton from ether and this leads to degradation of PEUU. This process is enhanced by adsorbed α-2 macroglobulin through the formation of highly reactive thiyl radicals from the thiol-ester of α-2 macroglobulin (Schubert MA *et al* 1995). The oxidative degradation of polyetherurethane urea is controlled by the diffusion of oxygen into the polymer (Schubert MA *et al* 1997a). Chemical degradation and mechanical stress synergistically operate towards the ultimate degradation of PUs in the form of environmental stress cracking. Mechanical deformation increases the polymer chain scission initiated by oxidative agent. This leads to the formation of pits and cracks which coalesce together and result in rupture of the polymer (Schubert MA *et al* 1997b).

2.2.1.3. Material chemistry and degradation

Polyurethane chemistry varies depending upon the monomer units and the stochiometry employed. The durability of PUs and the mechanism of PU degradation are influenced by the chemistry of the material. An *in vitro* study by Labow *et al* has analyzed the factors involved in biodegradation of PUs, specifically polyester urethane. The results indicated that the physical and chemical nature of PU, biological components such as the hydrolytic enzyme, cholesterol esterase and the enzymatic reaction product phospholipids all contribute towards biodegradation (Labow RS *et al* 1997). Segmented polyurethanes with aliphatic hydrocarbon soft segments showed better stability, in *in vitro* oxidative environments, over those having soft segments of polytetramethylene oxide (PTMO) (Takahara A *et al* 1991). Polyurethanes with MDI based hard segments had better *in vivo* stability than those with H12MDI hard segments. However, strain induced loss of tensile properties was evidenced in

prestrained PUs, Pellethane, Biomer and other MDI and H12MDI based PUs after 12 weeks of implantation (Hergenrother RW *et al* 1993). Polyurethanes containing polyethylene oxide (PEO), polybutadiene (PBD), or PTMO based soft segments were reported to undergo hydrolytic degradation by the action of the enzyme papain (Takahara A *et al* 1992).

Polyether and polycarbonate urethanes undergo degradation by oxidative mechanisms, wherein proton abstraction from soft segment is the initial event leading to radical formation, crosslinking and/or chain scission. Degradation of soft segment is more pronounced in polyetherurethanes, whereas hard segment degradation is more prominent in the case of polycarbonate urethanes, (Christenson EM *et al* 2004a). Polyether and polycarbonate urethanes degrade oxidatively by the action of sodium hypochlorite when under mechanical stress (Fare S *et al* 1999).

Biodegradation of polyether and polycarbonate urethanes follows a similar pattern *in vivo*, only difference being in the relative kinetics of degradation due to difference in soft segment chemistry. Monocyte adhesion, formation of macrophages and FBGCs on the material surface were the same for both PUs. This suggested an oxidative microenvironment at the cell-polymer interface (Christenson EM *et al* 2004b). A recent study reported that *in vivo* degradation of commercial PUs, both polyether and polycarbonate urethanes were not sufficient for deterioration of bulk properties. This study also proposed that hydrolytic degradation is negligible in comparison with oxidative degradation (Christenson EM *et al* 2006).

2.2.1.4. Effect of hydrogen bonding

Labow *et al* reported the inhibition of hydrolysis when polycarbonate urethane was subjected to an initial oxidative treatment (Labow RS *et al* 2001a). Oxidation led to crosslinking of soft segment in phase separated PUs and hence the degree of oxidation was lesser. The susceptibility of polycarbonate urethanes to hydrolytic degradation is indirectly proportional to the hard segment content. Further, increase in hydrogen bonding within the hard segments improve the stability of polycarbonate PUs (Tang YW *et al* 2001a). Tang *et al* also proposed that the initiation of degradation occurs at sites where less number of hydrogen bonded carbonates and urethanes were located. Polycarbonate urethanes with MDI hard segment were more

stable than those with HMDI and HDI hard segments with equivalent stochiometry. Hydrogen bonding within carbonate and urethane linkages were proposed as determinative factors in stability of polyurethanes (Tang YW *et al* 2001b). Hydrogen bonding improves the stability of polycarbonate urethanes by reducing PUs susceptibility to oxidative treatment and subsequent hydrolysis (Labow RS *et al* 2002b). However, a strong dose response on cholesterol esterase enzyme concentration was noted, especially when hard segment concentration was less (Tang YW *et al* 2003).

2.2.2. Towards developing degradation resistant polyurethanes

Development of PUs with novel combinations of raw materials, incorporation of additives, alteration in stochiometry, and surface modification have been carried out with the aim of improving biostability. An *in vitro* study by Salacinski *et al* reported better stability of a stress free compliant polycarbonate urethane over a commercial polyether urethane in oxidative and hydrolytic conditions (Salacinski HJ *et al* 2002b). The compliant polycarbonate urethane (MyoLink) did not exhibit drastic chemical changes in degradative solutions such as cholesterol esterase and $H_2O_2/CoCl_2$. However degradation of the carbonate soft segment occurred in t-butyl peroxide/$CoCl_2$ solution (Salacinski HJ *et al* 2002a).

2.2.2.1. Use of surface modifying macromolecules

Fluorine containing moieties are used as surface modifying macromolecules (SMM) to reduce degradation of PUs. The hydrolytic degradation by cholesterol esterase is inhibited by fluorine containing SMM incorporated with a polyester urethane (Tang YW *et al* 1997). Polyether urethanes end capped with PDMS did not undergo degradation, over 10 weeks implantation period, due to the protective role of the end caps by reducing the number of adherent macrophages and also by shielding the surface (Mathur AB *et al* 1997). However, it was assumed that over long-term an increase in the acidity at the polymer surface due to cellular activation can make the PU vulnerable to degradation.

2.2.2.2. Protein preadsorption on PU surface

Studies have focused on the effect of cholesterol esterase on degradation of PU in combination with protein preadsorption and the protective role of SMMs in degradation (Jahangir R *et al* 2003). Fibrinogen preadsorption delayed the hydrolytic degradation of PU until 70 days of enzyme treatment in both SMM treated and non-treated PUs. However at later time periods the protective nature of protein preadsorption on degradation was ineffective for the base PU, whereas the SMM modified PU showed relatively greater resistance to biodegradation. Jahangir *et al* also pointed out that eventhough protein adsorption occurs well before other biological interactions with the material, there may be unoccupied sites or "free access zones" on the material surface, remaining uncoated with protein. Hence these areas can provide sites for the action of degradative enzymes.

2.2.2.3. Incorporation of additives and bioactive molecules

Polyurethanes surface modified with Vitamin E incorporated fluorinated SMMs had better resistance to oxidative damage by HOCl, when compared to non-bioactive SMM containing PUs (Ernsting MJ *et al* 2003). Linear and side chain functionalized polyurethanes were synthesized using improved synthetic procedures in order to develop better biomedical PUs (Simonovsky FI 2005 *et al*). Incorporation of antioxidant, Santowhite powder into PEUU resulted in an inhibition of FBGCs formation and also prevented surface cracking (Wu Y *et al* 1991). Vitamin E at 5 wt% incorporated into PEUU reduced the number and activation status of macrophages in comparison with that on bare PEUU (Schubert MA *et al* 1996). Incorporation of dehydroepiandrosterone has reduced the inflammatory response and degradation of polyetherurethane urea (Collier T *et al* 1998). A study by Casas *et al* revealed the reduction in oxidative damage and environmental stress cracking in Pellethane®, (commercial polyetherurethane) incubated with macrophages in presence of both dexamethasone in solution and when incorporated into PU matrix (Cassa J *et al* 1999).

Some research groups claimed biostability of certain PUs. Polyurethanes with polysiloxane soft segments exhibited biostability in a sheep model upto nine months of implantation (Bernacca GM *et al* 2002). Surface enhancement of siloxane was observed after nine months, eventhough there were no signs of degradation and no

deterioration of mechanical properties was noted. Elast-Eon a thermoplastic PU elstomer containing polyhexamethylene oxide and polydimethylsiloxane macrodiols exhibited relatively enhanced biostability in comparison with Pellethane® and Bionate® over 24 months implantation in sheep model (Simmons A *et al* 2004). Even though these reports claimed the stability of PUs, long-term biostability relevant for human clinical applications have not been reported. The pursuit for a biostable, biocompatible PU for long-term implants in clinical applications continues. An understanding of the sequential events following the interaction of PU with the biological milieu will help in devising better methods for preventing degradation. Design of better biostable PUs will be facilitated by delineating the factors and ongoing molecular mechanisms in the cell-material niche.

2.2.3. Biological response to materials

Implantation of a biomaterial leads to a sequence of events in the biological milieu, the first of which is the adsorption of proteins on the implant surface.

2.2.3.1. Protein adsorption

Protein adsorption from the biological milieu on biomaterials is the initial event in material-tissue interaction. Extracellular fluid as well as blood leaked out from injured vessels constitute the source for proteins which adsorb onto implant surfaces. Adsorbed proteins influence adhesion of cells through the cell adhesion motifs on the proteins. Activation of cells upon adhesion to material surface is dependent on the molecular signal transduced by the interaction of cells with adsorbed proteins. Several techniques such as radiolabelling, surface matrix assisted laser desorption ionization mass spectrometry (MALDI MS) (Griesser HJ *et al* 2004), electron spectroscopy for chemical analysis (ESCA), time-of-flight secondary ion mass spectrometry (TOF-SIMS) (Wagner MS *et al* 2003) have been used for studying protein adsorption on biomaterials. Derhami *et al* have used a combined approach of two dimensional gel electrophoresis and Matrix Assisted Laser Desorption Ionization Time-of-Flight Mass Spectrometry (MALDI-ToF MS) for the detection of adsorbed proteins on the surfaces of commercial titanium and tissue culture polystyrene. Intracellular proteins which are differentially expressed by cells adherent on material surfaces were also studied using the same techniques (Derhami K *et al* 2001).

Analysis of multicomponent protein adsorption was possible by TOF-SIMS except for quantitation (Wagner MS *et al* 2003).

Cell adhesion on adsorbed fibronectin was higher on sulfonated surfaces relative to that on non-sulfonated surfaces (Kowalczynska HM *et al* 2002). This study also revealed that cell adhesion on sulfonated surfaces was mediated by $\alpha 5\beta 1$ integrin. The surface chemistry of biomaterial influences the conformation of adsorbed proteins. The accessibilty of integrin binding motifs on the proteins for interaction with integrins varies accordingly. In consequence the cellular response such as spreading, activation, cytokine release alters accordingly (Keselowsky BG *et al* 2003). Ochsenhirt *et al* confirmed the significance of peptide confirmation in specific binding with cell surface ligands. Langmuir-Blodgett supported films containing RGD and PHSRN peptides engaged specific integrin recptors on human umbilical vein endothelial cells depending upon the manner in which they were presented to the integrin molecules (Ochsenhirt SE *et al* 2006).

Pre-adsorbed IgG enhanced long-term macrophage adhesion *in vitro* on an oxygenated, hydrophilic polystyrene modified by a glow discharge method (Jenney CR *et al* 2000a). The enhanced macrophage adhesion was mediated by the Fab, F(ab')2 portions of IgG but not by the Fc portion. The conformation of IgG adsorbed on this surface favoured adhesion of macrophages and this was attributed to the surface chemistry of the polystyrene.

Absorption of fibrinogen was reduced on (polyethylene glycol) PEG–ylated surfaces. Fibronectin adsorption on gold-alkanethiol self assembled monolayer (SAM) surfaces with terminal functionalities such as OH-, CH3, COOH-, NH3 were studied by a modified force field CHARMm, computational modeling method. Even though, all the different parameters affecting protein adsorption on biomaterials in real life situations were not included in this study, it has provided information regarding the molecular mechanisms of adsorption of FN 7-10 type III repeats onto surfaces with different exposed functional groups (Wilson K *et al* 2004). Fibroblast cell deformation and detachment from fibronectin coated dodecanethiolate SAMs under hydrodynamic shear was dependent on fibronectin concentration above a threshold value of 0.23 $\mu g/cm^2$ (Goldstein AS *et al* 2002).

An important consideration in protein adsorption is the controlling role of water in adsorption of proteins to hydrophobic materials (Krishnan A *et al* 2005). Krishnan *et al* also pointed out that protein concentration is an important energetic driver for adsorption to hydrophobic surfaces.

The composition of the adsorbed protein layer varies depending upon the surface chemistry of the material. *In vitro* cellular response to a series of thermoresponsive N-isopropylacrylamide based co-polymer with varied surface chemistry was different in terms of cell adhesion, cytoskeletal organization and cell morphology (Allen LT *et al* 2006).

2.2.3.2. Inflammatory response to biomaterials

The injury caused by the surgical procedure of implantation of a material or device initiates the classical inflammatory as well as wound healing response. Inflammatory response initiated by the implantation of biomaterials involves acute and chronic phases. This response sets off cellular and humoral defense lines in order to neutralize, destroy or wall off the implanted material (Cassa J *et al* 1999).

Neutrophils and monocytes are recruited to the site initially. These cells perform the functions of clearing the wound site off the necrotic tissue, cellular debri and any foreign bodies present. Neutrophils are the first line of defense against foreign bodies. These cells interact with different biomaterials in varied fashion. Neutrophils release reactive oxygen species in order to destroy the biomaterial (Falck P 1995). They get activated on contact with biomaterials and release defensins, which act as chemotaxins for subsequent cells to reach the site (Territo MC *et al* 1989). However, these defensins also cause the deactivation of further incoming neutrophils (Kaplan SS *et al* 1999). Monocytes form the next line of defense. A study by Labow *et al* compared the degradative potential of neutrophils and monocyte derived macrophages on incubation with polyester urea urethane coated coverslips. Release of radiolabel from the PU was found to be significantly more in the case of macrophage seeded PU in relation to neutrophil seeded PU (Labow RS *et al* 2001b). Monocyte derived macrophages phagocytize foreign bodies. These cells adhere to the implant surface through receptor-ligand interactions with the adsorbed proteins.

In the case of a biocompatible material the initial inflammatory response subsides and eventually a thin fibrous capsule is laid by the fibroblast cells which mediate the repair of the injured tissue. The formation of a fibrous capsule around biomaterial implant is dependent upon the chemical as well as physical parameters of the implant. Ward *et al* reported that a thinner implant will result in a thin fibrous capsule. The fibrous capsule formed was less dense in the case of porous implants than solid implants irrespective of the material chemistry (Ward WK *et al* 2002). The acute inflammatory response elicited is influenced by the net surface charge on biomaterial. A study by Hunt *et al* showed that PUs with 20% negative charge on the surface induced less neutrophil response than those with 10% and 30% negative charges (Hunt JA *et al* 1996).

2.2.3.3. Immune system

Immune response of the body is elicited by the presence of foreign antigens such as invading bacteria or fungi and virally infected cells. Two components of the immune system participate in the response towards these antigens (Voet and Voet 1995). They are the cellular and humoral immune response. Cellular immune response is mediated by immune cells such as macrophages, T and B lymphocytes. Humoral immune response is mediated by antibodies secreted by the B lymphocytes. This type of a response is a specific immune response towards specific antigens.

However, in majority of cases, implantation of a biomaterial does not elicit a typical specific immune response but rather a nonspecific inflammatory response. This response is mediated by components of the innate immune system neutrophils, monocytes and macrophages. Tissue-material interactions and the associated inflammatory response is mediated mainly by macrophages (Anderson JM *et al* 1999).

2.2.3.4. Macrophages

Macrophages are phagocytic cells involved in removal of worn out cells, cellular debri, invading pathogens and any other foreign body. These cells originate from the mononuclear phagocyte system. One set of precursor cells in the bone marrow differentiate into monocytes which circulate in the blood. In tissues monocytes get differentiated to form macrophages. Macrophages are the tissue

counter parts of monocytes. They are widely distributed in different organs of the body wherein they perform specialised functions.

Macrophages recognize any foreign body invading the system as non-self through certain pattern recognition receptors. Subsequently these cells bind to the foreign body by means of integrin molecules on the cell membrane. After binding, the foreign body is phagocytized if it is less than 10 μm in diameter. Larger molecules are engulfed by foreign body giant cells (FBGC) which are formed by the fusion of two or more macrophages in an attempt to destroy the foreign body. In the case of an infection macrophages process the internalized antigen and present it to the effectors of adaptive immunity such as T and B lymphocytes. This elicits a heightened response to the infection which enables the host to combat the infection. Xia and Triffitt (2006) listed the secretory products of activated macrophages which are the modulators or mediators of inflammatory and immune response.

Microbicidal and cytotoxic	
Reactive oxygen intermediates	Superoxide, hydrogen peroxide, hydroxyl radical, hypohalites, chloramines.
Reactive nitrogen intermediates	Nitric oxide, nitrites, nitrates
Oxygen-independent	Neutral proteases, acid hydrolases, lysozyme, defensins
Tumoricidal	Hydrogen peroxide, NO, TNF-α, C3α, proteases, arginase, thymidine
Tissue damaging	Hydrogen peroxide, NO, TNF-α, neutral proteases
Fever inducing	Pyrogenic cytokines-IL-1, TNF-α, IL-6
Inflammatory regulators	
Bioactive lipids	Prostaglandins (PGE2, PGF2α), prostacyclin (PGI2), thromboxanes, leukotrienes (LTB4, LTC4, LTD4, LTE4)
Bioactive oligopeptides	Glutathione
Complement components	C1, C4, C2, C3, C5, Factors B, D, P, I, H

Clotting factors	V, VII, IX, X, prothrombin, plasminogen activator, plasminogen activator inhibitors
Cytokines	IL-1, IL-6, IL-8, TNF-α, IFN-γ, macrophage inflammatory proteins, regulatory growth factors (M-CSF, GM-CSF, G-CSF, PDGF)
Neutral proteinase	Elastase, collagenase, angiotensin convertase, stromelysin
Proteinase inhibitors	α-macroglobulin, α-1 proteinase inhibitor, plasmin and collagenase inhibitors
Acid hydrolases	Acid proteases (cathepsin D and L) peptidases, lipases, lysozyme and other glycosidases, ribonucleases, phosphatases, sulphatases
Stress proteins	Heat shock proteins
Immune response regulators	
Innate immune response (MIF)	Macrophage migration inhibitory factor
Adaptive immune responses	IL-12, IL-18
Tissue regeneration	
Tissue reorganization	Elastase, collagenase, hyaluronidase
Angiogenesis	bFGF, TGF-α, GM_CSF, VEGF, IL-8, human angiogenic factor, angiotrpopin, substance P
Mitogens for fibroblasts, keratinocytes and osteoblasts	TGF-α, TGF-β, FGF-1, 2 & 4, HB-EGF and BMP-2
Others	Apolipoprotein E, IL-1 inhibitors, purine and pyrimidine derivatives.

2.3. Macrophage response to biomaterials

Implantation of a biomaterial invokes a wound healing response initially to restrain the effects of the injury caused by the wound. Simultaneously an inflammatory response is elicited towards the implanted biomaterial. Monocytes and macrophages mediate this inflammatory response to a great extent. Particulate wear debri of polymethylmethacrylate or ultrahigh-molecular-weight polyethylene in patients with total hip arthroplasty induce macrophage activation (Maguire JK *et al* 1987). Subcutaneous implantation of Dacron and expanded polytetrafluoroethylene in rats has also shown the inflammatory response mediated by macrophages (Wenig BM *et al* 1990). Macrophages adherent on PU were reported to be involved in the surface degradation (Zhao Q *et al* 1990).

The macrophage response to implanted biomaterials is very important in deciding its fate in the host system (Schlosser M *et al* 2002). Upon contact with the material surface, macrophages actually interact with the adsorbed proteins and accordingly elicit particular responses. Macrophages are stimulated by external stimuli which modify many of its functions such as migration, adhesion, aggregation, chemotaxis, phagocytosis, and production of inflammatory mediators. Both *in vitro* and *in vivo* experiments have been carried out by various research groups to study the macrophage response to various biomaterials. The involvement of macrophages in wound healing as well as in the healing response to biomaterials was revealed by *in vivo* studies, on the other hand *in vitro* studies delineated the facets of macrophage activation (Bernatchez SF *et al* 1997).

2.3.1. Monocyte/macrophage adhesion

In vitro studies show that serum protein depletion and surface chemistry can modulate cellular behavior on material surfaces (Collier TO and Anderson JM 2002). Monocyte adhesion on an RGD modified glass surface was higher than that on a dimethylsilane modified surface in IgG depleted serum but no significant difference was noted when fibronectin and vitronectin were depleted. However, the increased monocyte adhesion was noted only at the initial time of zero and three days, which became comparable at 10 days on both surfaces. Moreover RGD modified surface did not significantly affect FBGC formation or apoptosis of adherent cells (Collier TO

and Anderson JM 2002). Studies of *in vitro* monocyte interactions with artificial surfaces coated with albumin and fibrinogen at early time periods showed that albumin coated surfaces induced apoptosis on more cells (Werthen M *et al* 2001). Polyethyleneterephthalate surfaces modified with polyethylene glycol showed reduced adhesion of macrophage-like U937 cells, when preadsorbed with fibrinogen (Ademovic Z *et al* 2006).

An *in vitro* study indicated that leucocyte adhesion was decreased with increase in shear stress. Complement component C3a derived peptides were found to be mediating higher adherent macrophage density than C5a or fibronectin derived peptides (Kao WJ 2000). Macrophages isolated from inflammatory exudates of cage implants with different biomaterials such as PU, PDMS, polyetherimide and polyetheretherketone all showed expression of major histocompatibility (MHC) class II molecule. This indicated an activated nature of the macrophage in response to these biomaterials (Petillo O *et al* 1994).

2.3.2. Monocyte/macrophage activation

The cytokines secreted by adherent macrophages collectively mediate the course of response to the biomaterial by up/down regulation of wound healing and inflammatory response. Secretion of cytokines by macrophages steered the course of the response to biomaterial by promoting inflammation or wound healing (Brodbeck WG *et al* 2002). Pro-inflammatory cytokines promote chemotaxis, cellular activation and lead to a heightened inflammatory response. The cytokines IL-1, TNF-α, IL-8, IL-6, are considered as proinflammatory and anti-wound healing. Interleukin-1β activates inflammatory cells such as macrophages and wound healing cells such as fibroblasts. TNF and IL-1 were reported to prime superoxide ion production by macrophages and neutrophils (Warren JS *et al* 1988, Kharazmi A *et al* 1988). Activated macrophages produce TNF-α which has got mediator role in inflammatory as well as immune responses (Leibovich SJ *et al* 1987). Chapekar *et al* reported enhanced production of TNF-α by RAW 264.7 cell line in response to PTFE particles and bacterial cell wall components lipopolysaccharide (LPS) and lipotechioc acid (LTA) (Chapekar MS *et al* 1996).

Brodbeck *et al* reported that in the absence of IL-4 the ability of surfaces to promote induction of apoptosis was inversely related to its ability to promote adhesion. Poly (benzyl N.N-dimethyl dithio-carbamate co styrene) (BDEDTC) coated PET films photograft copolymerized with Polyacrylamide, sodium salt of polyacrylic acid or methiodide of poly(dimethyl amino propyl acrylamide) (DMAPAAmMel) when incubated with human monocytes, it was found that these hydrophilic surfaces showed reduced cell adhesion. However for adherent cells, the fusion of macrophages to FBGC was increased from seven days to ten days on all surfaces. Induction of apoptosis was higher on hydrophilic surfaces both in the presence and absence of IL-4 (Brodbeck WG *et al* 2001). The inflammatory response to Ti particles assessed by a protein array method to detect the cytokine release using an *in vitro* system of mouse monocytic macrophage (RAW 264.7) cell line revealed a subtle and gradual increase in TNF-α and MIP-2, a slight elevation in IL-6 and no changes in TGF-β upto 72 hrs (Li Y *et al* 2005).

Cell adhesion onto PU was found to be greater when compared to that on Ti and cell culture treated polystyrene. The number of apoptotic cells were higher on PU than the other two materials. However secretion of IL-10, an anti-inflammatory cytokine was found to be greater on Ti, which is a known biocompatible material (Gretzer C *et al* 2003). This study also pointed out that the manner by which material surfaces were modified with peptides (directly or with Star PEO linkers) influenced the cytokine release by adherent cells.

2.3.3. FBGC formation on biomaterial surfaces

Monocyte differentiation to macrophage and subsequent fusion of macrophages to form foreign body giant cells is dependent upon the surface on which the cells adhere. A study by Collier *et al* showed that macrophages fuse to form FBGC on N-(2 aminoethyl)-3-aminopropyltrimethoxysilane surface but not on an interpenetrating polymer network of polyacrylamide and poly(ethylene glycol) (Collier TO *et al* 2004). *In vitro* studies reported the modulation of macrophage behaviour and FBGC formation by adsorbed serum proteins (Jenney CR *et al* 2000b). Preadsorbed immunoglobulin (IgG) promoted long-term macrophage adhesion, whereas von Willebrand factor (vWF) inhibited the adhesion. Preadsorbed vitronectin (VN) did not have much effect on FBGC formation.

2.4. Macrophages in relation to polyurethanes

Macrophages adhere on implanted PU surface and release enzymes or reactive species which results in degradation of PU *in vivo*. A cage-implantation study by Zhao *et al* revealed that inflammatory response to pre-stressed Pellethane increased over 21 days. This was concomitant with cracking and rupture of the implant (Zhao Q *et al* 1990). Foreign body giant cells adhere on PU surface and cause degradation of material directly beneath it (Zhao Q *et al* 1991). Polyurethane implanted in subcutaneous cage model in rats over 10 weeks showed formation of FBGCs. However incorporation of Santowhite powder decreased leucocyte adhesion with concomitant decrease in FBGCs. (Zhao Q *et al* 1992). Silicone modification of PUs was reported to direct the fate of macrophages adherent on PU surface towards fusion of cells and apoptosis (Jones JA *et al* 2004). The formation of FBGC by the fusion of macrophages on PUs was mediated by IL-4 (Kao WJ *et al* 1995). Hydrophilic polyurethane (Mitrathane®) fragments, produced by milling, have been found to degrade in the peritoneal cavity of mouse in a 180 days study. The smaller polymer fragments were found to be phagocytized by macrophages (Maurin N *et al* 1997). Leaching of low molecular weight oligomers from PU was considered as the first event leading to macrophage mediated degradation at long term (Xi T *et al* 1994).

Polycarbonate urethanes were susceptible to hydrolytic degradation by the action of monocyte derived macrophages (Labow RS *et al* 2001). The *in vitro* degradation studies of PU employed monocyte derived macrophages (MDM). Matheson *et al* (2002) evaluated the efficacy of U937 cell line for PU degradation studies. This cell line was found to be a model cell system with comparable esterase activity as that of MDMs for radiolabel release from a PU based on HDI, poly(1,6-hexyl 1,2-ethyl carbonate) diol and butane diol. Eventhough the cell line required phorbol 12-myristate 13-acetate (PMA) activation for differentiation, they did so as early as 72 hours as opposed to 14 days required by MDMs (Matheson LA *et al* 2002). During the differentiation of monocytes to macrophages cholesterol esterase (CE) is produced. Biomaterial surface chemistry influences the production of CE by monocytes. A study by Labow *et al* showed that polycaprolactone and PTMO based PUs with 2,4- toluene diisocyanate and ethylene diamine differed in their ability to induce production of CE by monocytes in culture. (Labow RS *et al* 1998).

Ma *et al* reported the ability of PU particles to induce macrophage activation as measured by TNF-α release. Macrophage viability and activity was dependent upon the concentration of particles and ratio of soft to hard segment in the PU. Macrophage activation increased with particle concentration and hardness of PU (Ma N *et al* 2002).

2.5. Cell signaling

Macrophage interaction with biomaterials results in intracellular events which manifests as fusion of cells, secretion of specific enzymes, cytokines and/or other reactive molecules. Intracellular signaling involves a cascade of molecular events mediated by extracellular matrix molecules, cell surface receptors, cytoskeletal proteins and other intracellular molecules.

2.5.1. Morphological manifestations of cell signaling

Intracellular signaling events in macrophages during inflammatory response have been studied by several groups. However intracellular signaling following macrophage interaction with PUs have not been investigated. Development of adhesive structures and cytoskeletal reorganization were significant in functional specializations by macrophages during inflammatory responses (Defife KM *et al* 1999). Cytoskeletal reorganization and development of adhesive structures were involved in the process of monocyte differentiation into macrophages and also during IL-13 induced FBGC formation. The study revealed the formation of podosomes on the ventral surface of macrophages and punctuate core of f-actin, gelsolin, L-plastin and ring organization of vinculin, talin, paxillin at 3 days of culture. With the addition of IL-13, podosomes restructured into lamellipodia and uropods in macrophages on clean coverslips, whereas on dimethylsilane surface, podosomes were present on the extreme periphery of FBGC.

2.5.2. Cell migration

Migration of cells is significant in inflammatory response because the cells have to travel towards the site of inflammation. Actin cytoskeleton plays an important role in cell migration and motility. GTP binding proteins, members of the intracellular signaling cascade, control the polymerization of actin filaments. Rho, Rac and Cdc42

are small GTPases which mediate the signal transduction pathways leading to formation of focal complexes. It was reported that Rho and Rac mediates the formation of stress fibres and filopodia/lamellipodia respectively (Nobes CD and Hall A 1995). Podosomes and invadopodia are feet like structures which form on the bottom surface of leading edge of migrating cells. These structures contain actin and enzymes capable of degrading extracellular matrix (ECM) thus aiding in cell migration.

Another area where cell migration becomes significant is the wound healing process. Cells migrate over degraded ECM and participate in reconstitution of the damaged tissue at the wound site. Matrix metalloproteinases (MMP) are enzymes capable of degrading the ECM proteins. These MMPs are very important for tissue remodeling and homeostasis (Steffensen B *et al* 2001).

2.5.3. Role of integrins in signaling cascade

The assembly of ECM is influenced by cells via anchoring ECM molecules, by cell surface receptors such as integrins, thus favouring self assembly of the secreted ECM molecules (Wu C *et al* 1995). In turn, the ECM influences cellular behaviour including differentiation and survival (Lin CQ and Bissell MJ 1993, Ruoslahti E and Reed JC 1994). Integrins are also crucial in cell adhesion and related signalling events. Integrin molecules present on the cell surface associates both intracellular and extracellular events through integrin-ligand interaction either in an inside-out or an outside–in manner. Downstream association of integrins with Shc resulted in cell survival and cell cycle progression in CHO cells (Wary KK *et al* 1996). Integrins upon ligand binding results in the formation of focal adhesion sites which are the focal points where cytoskeletal proteins and extracellular matrix proteins concentrate. Integrin binding to ligand leads to clustering of integrins and association of multiple proteins at the intracellular region. Such intracellular complexes contain p130Cas, paxillin, Src, talin, α-actinin and vinculin.

2.5.4. Focal adhesion

Focal adhesion sites accommodate intracellular proteins such as focal adhesion kinases (FAKs). Integrin clustering leads to phosphorylation of FAK. The FAKs acts in conjunction with downstream protein kinases which act in a cascade

manner eventually leading to cell adhesion, cell death or cell migration depending upon the specific signal transmitted. Jun Kinase-1 (JNK-1), a member of the mitogen activated protein kinase (MAPK) family, was considered to be the downstream effector of cell death mediated by poly(ADP ribose) polymerase-1 (PARP-1). (Alano CC and Swanson RA 2006). Adhesion of osteoblast cells to bioceramics was reported to be mediated by integrins. Integrin associated downstream signal transduction pathways involved FAK phosphorylation and signaling molecules such as Shc which were upregulated on Mg+ modified Bioceramics (Zreiqat H *et al* 2002). Self assembled monolayers of alkanethiols on gold functionalized with FNIII7-10 (fragment reconstituting the primary and secondary structure of the cell binding motifs) resulted in higher adhesion strength and FAK activation in osteoblast cells by engaging $\alpha v\beta$ 3 integrin. (Petrie TA *et al* 2006).

2.5.5. Intracellular signaling

Interaction of cell surface integrins with fibronectin results in phosphorylation of protein kinases such as protein tyrosine kinase and protein serine/threonine kinase. A study by Kao *et al* revealed that phosphatidylinsitol 3 kinase (PI3-kinase)-protein kinase C (PKC)-MAPK signaling cascade was involved in macrophage adhesion on fibronectin coated surfaces. This study also showed that the signaling cascade mediated by fibronectin-integrin interaction were distinct on polyethylene glycol and tissue culture polystyrene surfaces (Kao WJ and Liu Y 2003). Earlier studies have shown that PKC was an important factor involved in signal transduction mediated by integrin binding (Vuori K and Ruoslathi E 1993). Investigation of the intracellular protein expression by U937 monocytic cell line adhered on albumin adsorbed and fibronectin adsorbed tissue culture polystyrene (TCPS) surfaces was carried out using liquid chromatography coupled with Mass spectrometry (LC/MS) followed by database search (Kao WJ and Zuckerman ST 2006). The results of this study underscored the fact that macrophage activation, may be altered by difference in signaling pathways activated on contact with different ligands adsorbed on biomaterial surface.

Macrophages are found to phagocytize particles bound by immunoglobulin molecules through Fc-γ receptor crosslinking. This event is mediated by the intracellular signaling molecule Syk which is critical in the formation of polymerized

actin cups responsible for internalizing the particles. Syk deficient cells failed to facilitate internalization of particles by the dissolution of the formed actin cup (Crowley MT *et al* 1997). Adhesion of monocytes resulted in the activation of extracellular signal-regulated kinases (ERK) and subsequent TNF-α production (Rosengart MR *et al* 2000). The events following the differentiation of monocytes to macrophages is dependent upon the specific stimuli involved (Rao KM 2001).

Cell signaling events which occur upon interaction of macrophages with PUs has not been delineated. Elucidation of signaling pathways and molecules involved in manifestation of cellular response to adhesion and activation on PUs is an important aspect of understanding the cell-PU interaction. The manifestations of macrophage response to biomaterials include proliferation, adhesion, spreading and activation. Mitogen activated protein kinases (MAPKs) are a significant part of the signaling cascade in many of these cellular processes. A member of the MAPK family, c-Jun NH2 terminal Kinase (JNK) phosphorylates several transcription factors including PU.1. It is reported that PU.1 is an important regulatory factor for macrophage development and function (Valledor AF *et al* 1998). Activation of JNK is an important event in the transition through G2/M checkpoint in cell cycle and hence is significant for proliferation, differentiation and survival of murine macrophages (Himes SR *et al* 2006). The requirement of JNK signaling for survival of macrophage cell line, RAW264.7 involves Bcl-xL expression (Sevilla *L et al* 1999).

Inspite of the progress in awareness of the interrelationship between material chemistry, adsorbed proteins and cell signaling pathways in eliciting specific response to specific materials, methods for prevention of failure of implants remains elusive. As Gallagher *et al* puts it "the inability to improve on the failure rates of biomaterials is due in major part to the poor definition of events that comprise cell-biomaterial interaction." (Gallagher WM *et al* 2006). The significance of the interrelated phenomena, of material properties and complex cellular interactions with the material, in the cell mediated biodegradation of polyurethane has not yet been elucidated fully. In this context the study of cell-material interactions assumes importance. The present study focuses on the *in vivo* and *in vitro* interactions of macrophages with PEUU.

2.6. Objectives of the present study

The present study attempts 1) to gain a better understanding of the sequence of events at the polyurethane-tissue interface over a long period of implantation and 2) to delineate the molecular mechanism underlying the activation of macrophages on PEUU in comparison to that of other commercial PUs by an *in vitro* approach.

The present work describes the cellular and molecular basis of cell activation on implanted polyether urea urethane (PEUU), with the specific objectives to:

- delineate the biological events sequentially, upon implantation of PEUU
- identify the surface changes in the material over different time periods of implantation.
- elucidate the role of cytokines in steering the course of cellular response elicited against implanted PEUU, by analysis of the cytokine profile.
- analyse early protein adsorption onto implanted PEUU in order to explicate the role of adsorbed proteins in the cellular response.
- investigate the plausible signaling pathway of cell activation on contact with material by *in vitro* method.

CHAPTER 3

MATERIALS AND METHODS

3.1. Materials

3.1.1. Raw materials for in-house synthesized polyurethane

The poly(etherurethane) urea (PEUU) was synthesized from 4,4'- methylene di(p-phenyl isocyanate) (MDI) (Sigma-Aldrich Chemie, Germany), ethylene diamine (Sigma-Aldrich Chemie, Germany) and polytetramethylene ether glycol (PTMEG) (Aldrich chemical company, USA). N, N'-Dimethylacetamide (S.d fine chemicals, India) was used as the solvent for the reaction. Dibutyltin dilaurate (Merck, India) was used for catalyzing the reaction.

3.1.2. Biomaterials used in this study

Six commercial polyurethanes, in-house synthesized PEUU and ultrahigh molecular weight polyethylene (UHMWPE) were evaluated *in vitro* in order to study the macrophage response to the materials.

1. Biospan®, a segmented polyurethane based on an aromatic polyether urethane urea with a hard segment of MDI and mixed diamines. The soft segment consisted of polytetramethylene oxide (PTMO). Stabilizer package consisting of an antioxidant and a copolymer of decyl methacrylate and diisopropylaminothyl methacrylate was also present.

2. PurSil™ AL (Hardness 80A), polyether urethane with MDI hard segment chain extended with 1,4-butane diol and a PTMO soft segment. Surface modifying end groups formed by the incorporation of silicone (20%) was present in the polymer backbone together with polyether soft segments. The polymer chains were terminated by the 0.2 wt% PDMS surface-modifying end groups.

3. PurSil™ AL-20 75A (Hardness 75A) had the same chemical composition as PurSil™ AL (Hardness 80A).

4. Elasthane™ , a polyether urethane with MDI hard segment chain extended with 1,4-butane diol and a PTMO soft segment.

5. CarboSil™ 20, a silicone polycarbonate urethane with polydimethylsiloxane incorporated into the polymer soft segment with hydroxyl-terminated polycarbonate, poly (1, 6-hexyl-1, 2-ethyl carbonate) diol. The hard segment consisted of MDI and low molecular weight glycol chain extender. The copolymer chains were terminated with silicone surface-modifying end groups.

6. Bionate® 80A, A thermoplastic polyurethane formed as the reaction product of a hydroxyl-terminated polycarbonate, poly(1,6-hexyl-1,2-ethyl carbonate) diol, an aromatic diisocyanate MDI, and a low molecular weight glycol butane diol (chain extender).

7. In-house synthesized PEUU.

8. Ultra High Molecular Weight Polyethylene (UHMWPE) served as the control material.

3.1.3. Preparation of Phosphate Buffered Saline (pH 7.4)

Sodium Chloride	-	8 grams
Sodium phosphate, dibasic anhydrous (Na_2HPO_4)	-	1.15 grams
Potassium Chloride	-	0.2 grams
Potassium phosphate, monobasic anhydrous (KH_2PO_4)	-	0.2 grams

Distilled water - 1 litre

The chemicals were weighed out and dissolved in distilled water, pH was adjusted to 7.4 with a pH meter, and made upto one litre with distilled water.

3.1.4. Preparation of Sorensen's phosphate buffer

Stock A - 0.2 M Na_2HPO_4

Stock B - 0.2 M NaH_2PO_4

Sorensen's phosphate buffer (0.1 M) was prepared by mixing 40.5 ml of stock A and 9.5 ml of stock B.

3.1.5. Preparation of 3% gluteraldehyde

The stock 8% gluteraldehyde (Polyscience, USA) was diluted to 3% using Sorensen's phosphate buffer.

3.1.6. Histology

3.1.6.1. Neutral buffered formalin

Disodium hydrogen phosphate anhydrous (6.5 g) (Merck, India), Sodium dihydrogen phosphate monohydrate (4 g) (Merck, India), 100 ml of formaldehyde 37-41% (Merck, India) and 900 ml distilled water. The salts were dissolved by stirring, pH of the solution was adjusted to 7 and made upto one litre.

3.1.6.2. Preparation of Harris's Haematoxylin

Haematoxylin (Merck) was dissolved in absolute alcohol by stirring in a magnetic stirrer. Potasium alum (Merck) was dissolved in water by gentle heating with the help of an electric heater (Bajaj electricals, Pune). Haematoxylin solution was poured into the alum solution while it was hot and allowed to boil rapidly. This was stirred using a glass rod. Mercuric oxide and sodium iodate were slowly added to it. The reaction vessel was then plunged into a basin of cold water. Glacial acetic acid was added to the reagent and filtered.

3.1.6.3. Preparation of Eosin stain

Eosin (spirit soluble) (Merck, India) was mixed with isopropyl alcohol in a ratio of 10:1000 (gm/ml) using a magnetic stirrer.

3.1.6.4. Preparation of acid alcohol

Seven hundred millilitres of isopropyl alcohol was made upto 1000 ml with distilled water. From this 10 ml was discarded and 10 ml of con. HCl (Merck, India) was added to it.

3.1.6.5. Preparation of Scott's tap water

Potassium bicarbonate	-	2 grams
Magnesium sulphate	-	20 grams
Distilled water	-	1 litre

Potassium bicarbonate was dissolved in a little of water. Magnesium sulphate was dissolved in water in a separate beaker. Dissolved bicarbonate was poured into the magnesium sulphate solution and mixed well. The solution was then made upto one litre with water.

3.1.6.6. Preparation of Mayer's egg albumin

Egg white	- 50 millilitre
Glycerin	- 50 millilitre
Thymol	- 100 milligrams

Egg white was made up to 100 ml with glycerin and mixed well with the help of a magnetic stirrer. Thymol was added to it and stored at 4°C.

3.1.6.7. Poly-L-Lysine coated slides

Poly-L-Lysine solution (0.1% w/v in water) (Sigma-Aldrich, USA) was diluted 1:10 with deionised water. This was then coated on clean microslides by smearing the solution on the slide. The slides were then kept for drying at 56°C in an incubator (M.C. Dalal & Co., India).

3.1.6.8. Immunostaining Kit

UltraTech HRP (DAB) Streptavidin-Biotin Detection System PN IM2765 (Beckman Coulter, USA.)

3.1.6.9. Primary Antibodies

Mouse anti rat CD 68 (MCA 341R) purified IgG, ED1 (Serotec, UK)

Mouse anti rat CD 163 (MCA 342R) purified IgG, ED2 (Serotec, UK)

Anti-IL-1α (R-20) :sc-1254 (Santa Cruz Biotechnology Inc., USA)

Mouse anti-IL-1β (MCA 1397) (Serotec, UK)

Anti-IL-6 (M-19):sc-1265 (Santa Cruz Biotechnology Inc., USA)

Anti-TNF α (N-19) :sc-1350 (Santa Cruz Biotechnology Inc., USA)

Mouse anti rat IFN-γ (MCA 1301) (Serotec, UK)

Mouse anti rat CD4 (MCA 55G) (Serotec, UK)

3.1.7. Two dimensional Polyacrylamide gel electrophoresis

3.1.7.1. Preparation of acrylamide/bis acrylamide

Acrylamide	-	14.6 grams
N,N'-methylene-bis Acrylamide	-	0.4 grams

Dissolved in deionised water. Made upto 50 ml and stored at 4°C.

3.1.7.2. Preparation of 1.5 M Tris-HCl, pH-8.8

Tris base	-	18.15 grams

Dissolved in deionised water and pH was adjusted to 8.8 using con. HCl. Made up to 50 ml with deionised water.

3.1.7.3. Preparation of 0.5 M Tris-HCl, pH-6.8

Tris base	-	3 grams

Dissolved in deionised water and pH adjusted to 6.8 using con. HCl. Made up to 50 ml with deionised water.

3.1.7.4. Preparation of 10% (w/v) SDS

Sodium dodecyl sulfate (SDS) - 1 gram

Dissolved in 10 ml deionised water with gentle vortexing.

3.1.7.5. Preparation of 10% (w/v) ammonium persulfate

Ammonium persulfate - 100 milligrams

Dissolved in one ml deionised water.

3.1.7.6. Preparation of Sample buffer

Deionised water	-	3 millilitres
0.5 M Tris-HCl, pH6.8	-	1 millilitres
Glycerol	-	1.6 millilitres
10% SDS	-	1.6 millilitres
Dithitreitol (DTT)	-	0.4 millilitres
Bromophenol blue in water 0.5%	-	0.4 millilitres

3.1.7.7. Preparation of 5x electrode running buffer

Tris base	-	45 grams
Glycine	-	216 grams
SDS	-	15 grams

Dissolved in deionised water and made up to three litre. Diluted 300 ml 5x stock with 1.2 litre deionised water for electrophoretic running.

3.1.7.8. Rehydration buffer

For 10 ml of solution:

Urea 8 M - 4.8 grams

CHAPS 2%	-	200 milligrams
Bio-Lytes(0.2%)	-	20 milligrams
DTT	-	77 milligrams

3.1.7.9. Equilibration buffer I

For 50 ml solution:

DTT	-	1 gram
SDS	-	1 gram
Urea	-	18 grams
1.5 M Tris-HCl (pH8.8)	-	12.5 millilitre
Glycerol	-	10 millilitre

3.1.7.10. Equilibration buffer II

For 50 ml solution:

Iodoacetamide	-	1.25 grams
SDS	-	1 gram
Urea	-	18 grams
1.5 M Tris-HCl (pH8.8)	-	12.5 millilitre
Glycerol	-	10 millilitre

3.1.7.11. Formulation for SDS-polyacrylamide gel (7.5%)

Acrylamide/bis acrylamide	-	25 millilitre
Distilled water	-	48.5 millilitre
1.5 M Tris-HCl, pH 8.8	-	25 millilitre
10% (w/v) SDS	-	1 millilitre
10% ammonium persulfate	-	500 µl
TEMED	-	50 µl
Total monomer	-	100 millilitre

3.1.7.12. Silver staining reagents

Hypo	- $Na_2S_2O_3$ 20 mg/100 ml deionised water
$AgNO_3$	- 500 mg/250 ml. 75 µl formaldehyde (HCHO) was added to each 100 ml of $AgNO_3$ solution.
Devoloper	- 2% $NaCO_3$. 50 µl of HCHO was added to chilled 100 ml of $NaCO_3$ solution.
Stop solution	- citric acid 2.1 g/100 ml

3.1.7.13. Solutions for In-gel trypsin digestion

100% Acetonitrile

100 mM Ammonium Bicarbonate

Wash Solution: 50% acetonitrile and 50 mM Ammonium bicarbonate

Reduction solution: 10 mM DTT in 100 mM Ammonium bicarbonate

Alkylation solution: 50 mM Iodoacetamide in 100 mM Ammonium bicarbonate

Trypsin solution: 20 µg/ml in 50 mM Ammonium bicarbonate

Extraction solution: 0.1% trifluoro acetic acid (TFA) and 50% Acetonitrile

3.1.8. *In vitro* studies

3.1.8.1. Cell culture medium

Minimum essential medium eagle (Sigma, USA) supplemented with 10% fetal bovine serum (FBS) (Gibco BRL, India) (pH 7.4), Streptomycin (100 µg/ml) (Sigma, USA), Penicillin (100 IU/ml) (Sigma, USA), sodium bicarbonate (29.3 ml of 7.5% w/v added to 1 litre) (Himedia, India) and L-glutamine (10 ml of 200 mM added to one litre MEM) (Sigma, USA).

3.1.8.2. Cell lines

Mouse fibroblast cell line L929 (ATCC, USA) was used for the *in vitro* cytotoxicity testing of the PEUU.

Mouse monocyte-macrophage cell line RAW 264.7, purchased from NCCS, India was used for the analysis of *in vitro* macrophage activation on PEUU as well as commercial PUs.

3.1.8.3. Enzyme Linked Immunosorbent Assay (ELISA) for cytokine analysis

Interleukins, IL-1α and IL-6 secreted into the culture medium were analyzed using specific ELISA kits (Biosource Inc., USA).

3.1.8.4. Cell activation analysis

The activation of macrophages upon contact with the materials were studied using the CASE kit (Super array Biosciences, USA).

3.2. PHASE I- METHODOLOGY

3.2.1.1. Polyurethane synthesis

The hard segment consisted of 4,4"-methylene di (p-phenyl isocyanate) (MDI) and ethylene diamine. The polyol used was polytetramethylene ether glycol (PTMEG) of molecular weight 2000. The constituents MDI and PTMEG were reacted in a molar ratio of 2:0.5 for three hours at 70°C. The prepolymer formed was then cooled to 30°C and ethylene diamine was added at a molar concentration of 1.5 and the reaction was allowed to continue at 70°C for three more hours until the reaction system attained a viscous nature. The reactions were carried out under nitrogen atmosphere. The solvent employed was dimethylacetamide and the reaction was catalysed in the presence of 0.1 wt% dibutyltin dilaurate. The PEUU solution was poured into a glass dish and dried in a vaccum oven at 60°C for 24 hours to remove the excess solvent. The film of PEUU was redissolved in DMAc, precipitated in distilled water, washed well and dried. The process was repeated till it was free of unreacted monomers (milky wash turned clear). The cleaned polymer was cast into approximately one milli meter thick film on a clean glass dish. The final PEUU film was again washed by stirring in n-hexane followed by distilled water twice each for a total of two hours.

3.2.1.2. Characterization

Characterization of the PEUU was carried out by the following methods.

3.2.1.3. Attenuated total reflectance-Fourier transform infrared (ATR-FTIR) spectroscopy

The synthesized PEUU was characterized by Attenuated total reflectance-fourier transform infrared (ATR-FTIR) spectroscopy. The spectrum was taken with Model Impact 410 FTIR Spectrometer (Nicolet Inc., Madison, USA). A horizontal ATR accessory containing Zn-Se crystal was used for obtaining the ATR spectrum. The spectrum was obtained by averaging 50 scans.

3.2.1.4. Gel Permeation Chromatography (GPC)

The molecular weight was estimated by Gel Permeation Chromatography (GPC) system (Milford, USA) consisting of 486 Waters Tunable UV Detector, 510 Pump and 7725 Rheodyne injector. Separation was effected using a set of Waters μ-Styragel columns (105, 104, 103 Å). DMAc was used as the mobile phase (0.8 ml/min). Polystyrene molecular weight standards were used for calibration. The column effluents were monitored at 254 nm.

3.2.1.5. Scanning Electron Microscopy (SEM)

The PEUU was sputter coated with gold (Ion Sputter Model E101 Hitachi, Japan) and the surface morphology was observed using a scanning electron microscope (S2400 Hitachi, Japan) at an accelerating voltage of 15 kV.

3.2.1.6. Differential Scanning Calorimetry (DSC)

The glass transition temperature of the PEUU was determined by a test method based on ASTM E-1356-98 using Differential Scanning Calorimeter (DSC 2920 TA Instruments Inc., USA). Nitrogen gas (99% purity) was purged at a rate of 50 ± 5 ml/min. The temperature range of measurement was from -50°C to 150°C at a heating rate of 20°C/minute.

3.2.1.7. Contact angle analysis

The wettability of in-house synthesized PEUU was analysed by contact angle measurements. The measurements were done at room temperature using a video based automatic contact angle measuring instrument (Model OCA, Dataphysics, Germany)

equipped with SCA-20 software. Contact angle measurements were performed to evaluate the hydrophobicity/hydrophilicity of the material in air with deionized water bubble probe.

3.2.2. *In vitro* cytotoxicity testing

3.2.2.1. Cell culture

Mouse fibroblast cell line L929 was maintained in RPMI 1640 (Himedia, Pune, India) medium supplemented with 10% FBS (Sigma, USA), 100 IU/ml penicillin and 100 µg/ml streptomycin. The cell culture was incubated at 37 ± 2°C in a humidified atmosphere containing 5% carbon dioxide with change of medium at an interval of three days.

3.2.2.2. Cytotoxicity-direct contact test.

The PEUU film was cut into six millimeter diameter discs and sterilized by ethylene oxide (EtO) treatment. After sterilization the samples were allowed to aerate for 10 days, in order to ensure removal of residual EtO. The sterilized samples were placed on a confluent monolayer of L929 mouse fibroblast cells. Ultra high molecular weight polyethylene (UHMWPE) and copper were used as the negative and positive controls respectively. After 24 hours of incubation at 37 ± 2°C the cultures were examined with an inverted phase contrast microscope (Leitz DMIL, Leica, Germany).

3.2.3. *In vivo* experiment

3.2.3.1. Implantation

Skeletal muscle was chosen as the site of implantation. This mimics the clinical tissue-material interface as seen around the PU in some medical devices. The PEUU sample was cut into pieces of 1x1x10 millimeter size and sterilized by EtO treatement. The sterilized samples were implanted in the gluteal muscle of Wistar strain young adult rats. The animals were divided into 15 groups, for 15 different time periods of evaluation. Each group had 6 animals. The approval of the Institutional Animal Ethics Committee was obtained for the experiment. Animals were anesthetized by intramuscular injection of Xylazine (5 mg/kg body weight) and Ketamine (100 mg/kg body weight). Before carrying out the implantation procedure,

the animals' fur was clipped on both legs on the dorsal side. The skin was swabbed with surgical disinfectant (70% alcohol) and a 1.5 cm incision was made. The gluteus muscle was exposed, a clean incision was made in the muscle and the materials were implanted inside the muscle. The wound in the muscle was closed with catgut and the skin was sutured externally with a nylon suture. Two samples were implanted per animal, one on each gluteus muscle. The implantation procedure was done based on ISO-10993-6. The animals were given proper post-implantation care according to the guidelines of the Institutional Animal Ethics Committee and were provided with food and water *ad libitum*. Sham operation was performed to evaluate the initial wound healing response. A known biocompatible material, UHMWPE was implanted as a control material.

3.2.3.2. Explantation

The sham operated animals were sacrificed at 1 hour, 4 hours, 7, 10 and 15 days after surgery. The control material UHMWPE was explanted at 1, 2, 12, 18, 30 and 60 days post-implantation. The PEUU samples were retrieved at 1 hour, 4 hours, 1, 2, 7, 10, 12, 15, 18, 30, 60, 90, 120, 150 and 180 days post-implantation. Implants with the surrounding tissue were explanted and representative materials and tissues from each time period were allocated for different downstream analyses. Representative tissues retrieved at 7, 15 and 60 days post-implantation were processed for TEM analysis. One set of materials were removed carefully from the explanted tissue and processed for SEM analysis. Another set of representative samples were kept for analysis of adsorbed proteins. The tissues surrounding the implants were used for the histological assessment of tissue response.

3.2.3.3. Snap freezing of tissues for immunohistochemistry

Soon after sacrifice of animals, one set of explanted tissues with PEUU implant were grossed carefully and snap frozen in isopentane (S.d fine chemicals, India) cooled in liquid nitrogen (-180°C). The isopentane allowed better conduction of heat, hence the tissue was efficiently snap frozen. The tissues were put in labeled containers and kept in -80°C deep freezer till the time of sectioning.

3.2.3.4. Histology

The tissue samples were processed for light microscopic evalauation of tissue response to implants by the following methods.

3.2.3.4.1 Processing and embedding of tissues for paraffin block preparation

One set of the tissues retrieved upon sacrifice of the animals were fixed in neutral buffered formalin. The retrieved tissues were grossed, into small pieces with approximately one centimeter tissue around the implant site. Implants were pulled out gently and kept for further analyses.

The tissue pieces were put in tissue cassettes with proper labels and were allowed to remain in formalin for 24 hours. The processing of fixed tissues was carried out in ascending grades of isopropyl alcohol (Merck), Chloroform (Ranbaxy) and Paraffin wax (with Ceresin) with congealing point of 60°C. Processing was carried out in the following solutions in an automatic tissue processor (Leica Model TP1020, Germany)

Neutral buffered formalin	- 10 minutes
80% isopropyl alcohol	- 2 hours
95% isopropyl alcohol	- 2 hours
95% isopropyl alcohol	- 1 hour
100% isopropyl alcohol	- 1 hour
100% isopropyl alcohol	- 1 hour
100% isopropyl alcohol	- 1 hour
100% chloroform	- 1 hour
100% chloroform	- 1 hour
100% chloroform	- 2 hours
Paraffin wax	- 2 hours
Paraffin wax	- 2 hours

At the end of processing, the tissue capsules were transferred to the cassette bath in the tissue embedder (Leica Paraffin embedder Model EG 1160, Germany).

The paraffin in the paraffin tank and the cassette bath was maintained at 62°C ± 3°C when the tissues were transferred to the embedder. The embedding ring was labeled in accordance with the labels in the tissue cassettes. The mould was half filled with paraffin from the paraffin dispenser of the embedder. The tissue was oriented and placed in the paraffin mould in such a way that the cutting surface includes the cross section of implant area. The labelled embedding ring was placed on the mould and the embedding ring was filled with paraffin and the entire mould was placed in the cold plate maintained at 4°C. The embedding ring was removed when the paraffin was completely solidified. The tissue block was kept in refrigerator until cutting.

3.2.3.4.2 **Section cutting of paraffin embedded tissues**

The paraffin blocks were sectioned on an automatic rotary microtome (Leica motorized rotary microtome Model RM 2155, Germany). The blocks were trimmed initially to expose the tissue completely. The trimming mode was then switched off and section thickness was adjusted to five micrometer. The sections were floated onto water (45°C) in a floatation bath (Leica Histobath, Model HI 1210, Germany). Mayer's egg albumin was applied on clean glass slides and the floating section was picked up onto the slide. The sections were then stained with haematoxylin and eosin.

3.2.3.4.3 **Haematoxylin and Eosin staining**

Staining was carried out in an automatic stainer (Leica autostainer XL Model ST 5010, Germany). Prior to staining, slides were loaded in staining rack. The staining was carried out as follows.

Oven (56°C)	- 1 hour
Xylene I	- 10 minutes
90% isopropyl alcohol	- 3 minutes
70% isopropyl alcohol	- 3 minutes
Tap water	- 3 minutes
Harri's haematoxylin	- 10 minutes
Tap water	- 3 minutes
Scott's tap water	- 3 minutes

Tap water	- 3 minutes
70% isopropyl alcohol	- 1 minute
1% eosin	- 10 minutes
100% isopropyl alcohol I	- 1 minute
100% isopropyl alcohol II	- 1 minute
Xylene II	- 10 minutes
Xylene III	- 10 minutes

The slides were then mounted in DPX mountant and cover slip was applied carefully to avoid formation of bubbles.

3.2.3.5. Cryostat sectioning

The snap frozen tissues were taken out of the -80°C deep freezer, oriented properly and embedded in tissue freezing medium (Jung Leica microsystems, Germany) on chucks. The chuck with the tissue was then fixed on the cryostat microtome (Leica, Model CM 3050 S, Germany). The operating temperature was set at -22°C and the chamber temperature was set at -19°C. Tissue was trimmed till the implant site was reached and then 10 µm thick sections were taken. The tissue sections were adhered onto Poly-L-Lysine coated slides and were stored at -80°C deep freezer until immunostaining.

3.2.3.5.1 Immunohistochemical staining

The frozen tissue sections were allowed to dry on slides under desiccant for four hours at room temperature. Immediately before staining the sections were fixed in cold acetone at -20°C for 10 minutes. Slides were rehydrated in phosphate buffered saline (PBS) for 10 minutes, wiped carefully around tissue sections and circled with DAKO pen to form a well. Immunostaining was performed using the UltraTech HRP (DAB) Streptavidin-Biotin Detection System PN IM2765 (Beckman Coulter, USA.). Briefly, H_2O_2 was added to the rehydrated tissue sections and incubated in a humidity chamber for 10 minutes. This was done to eliminate endogenous peroxidase activity. The H_2O_2 was washed by rinsing with PBS three times. The slides were wiped around the sections and treated with Protein Blocking Agent, to reduce non-specific binding

of antibodies, and incubated in a humidity chamber for 10 minutes. The excess liquid was wiped off from the sides of sections and incubated sequentially with:

- Primary antibody (as the case is) which binds to specific tissue antigens, and the slides were incubated in a humidity chamber for one hour. In the case of negative control slides, instead of primary antibody, PBS was added and kept for one hour. The sections were then rinsed with PBS thrice and wiped around the sections carefully.

- Biotinylated secondary antibody, which binds to the primary antibody was added and incubated for 20 minutes in a humidity chamber. The sections were rinsed with PBS three times.

- Streptavidin-peroxidase reagent, which binds to the secondary antibody was added and incubated for 20 minutes in a humidity chamber. Streptavidin binds to the biotin on the secondary antibody and peroxidase serves as the indicator enzyme. The sections were again rinsed three times with PBS.

- Peroxidase substrate (H_2O_2) and chromogen solution, Diaminobenzidine (DAB) were added and incubated for five minutes. The slides were rinsed with distilled water, flooded with distilled water and incubated for one minute.

The sections were then incubated with Harris' haematoxylin for one minute, flooded with Scott's tap water for 30 seconds and rinsed gently with tap water. The sections were air dried and mounted with mounting medium (Cytoseal™ 60, Richard-Allan scientific, USA).

3.2.3.6. Light microscopy evaluation

The haematoxylin and eosin stained paraffin sections and immunostained frozen sections were evaluated by light microscopy using a trinocular microscope (Nikon Eclipse E600, Japan). All images were captured using a digital camera (DXM1200F, Nikon, Japan) with an ACT-1 software.

3.2.3.7. Transmission Electron Microscopy (TEM)

3.2.3.7.1 Fixation

The tissue samples for transmission electron microscopy (TEM) grossed into one mm^3 size were fixed in 3% gluteraldehyde in Phosphate buffer (Sorensen pH 7.4)

for more than 24 hours at 4°C. Processing of the samples for TEM was started after washing the samples with phosphate buffer at 4°C, four changes of 10 minutes each. Thereafter samples were post-fixed in 1% OsO_4 for two hours at 4°C. OsO_4 acted as a fixative cum primary stain. The samples were again washed four times in Sorensen's phosphate buffer, four changes of 15 minutes each and kept in distilled water for five minutes.

3.2.3.7.2 **Dehydration**

Dehydration of samples were carried out in ascending grades of acetone in the following order.

50% acetone I -10 minutes in cold

50% acetone II -10 minutes in cold

70% acetone I -10 minutes in cold (stored overnight in refrigerator)

70% acetone II -10 minutes at room temperature (RT)

90% acetone I -10 minutes at RT

90% acetone II -10 minutes at RT

100% acetone I -10 minutes at RT

100% acetone II -10 minutes at RT

Dry acetone (acetone mixed with $CuSO_4$)-10 minutes

After dehydration samples were cleared in propylene oxide for 10 minutes.

3.2.3.7.3 **Infiltration**

Infiltration of sample with Polybed 812 (Epon resin) (Polyscience Inc., USA) was carried out as follows.

Propylene Oxide: Resin in 3:1 ratio for 1½ hours

Propylene Oxide: Resin in 1:1 ratio for 1½ hours

Propylene Oxide: Resin in 1:3 ratio kept overnight in vacuum.

The next day samples were kept in full resin for one hour in vaccum.

3.2.3.7.4 **Embedding**

Samples were embedded in moulds containing a mixture of resin (Poly/bed 812 with dodecenyl succinic anhydride (DDSA), Nadic methyl anhydride (NMA-Hardener), and Dimethylaminomethyl phenol (DMP-Accelerator) in appropriate ratios as per the kit instructions (Polyscience Inc., USA) and placed in an oven at 60°C for three days for polymerization of the resin blocks.

3.2.3.7.5 **Semithin sectioning**

The blocks were sectioned on a microtome (Lieca Ultracut Model UCT, Germany) using glass knife to obtain sections of one micrometer thickness.

3.2.3.7.6 **Toluidene blue staining**

Semithin plastic sections were transferred onto the drop of water on a glass slide and stained with 1% Toluidene Blue stain. The glass slide was then heated on a hot plate for few seconds and thereafter the sections were washed with distilled water, air dried and mounted with DPX mountant. The sections were viewed with a trinocular microscope (Eclipse E600, Nikon, Japan). Images were captured using a digital camera (DXM1200F, Nikon, Japan) with ACT-1 software.

3.2.3.7.7 **Ultra thin sectioning**

Once the area of interest was identified from the semithin sections, the block surface was trimmed for ultrathin sectioning. Ultrathin sections with a thickness of 50 – 70 nm were cut using a diamond knife (Diatome®) and sections were taken on to the shiny side of copper grid (300 mesh size).

3.2.3.7.8 **Staining for TEM**

The ultra thin sections were stained in Uranyl acetate, by immersing the grids with the section side up, for two hours. This was followed by washing the sections in methanol – water mixture (100%, 80%, 50%). Thereafter the sections were stained for 10 minutes in Lead Citrate in 0.1N NaOH (prepared in CO_2 free water). Grids were floated on the drop of stain with the section side facing down, placed in a carbon

dioxide-free petri dish (by placing NaOH pellets). Thereafter grids were washed in four changes of distilled water and air dried. Stained ultrathin sections were observed under the electron microscope (Model Hitachi H- 600) at an accelerating voltage of 75 kV and photographs (Kodak Illford film) were captured.

3.2.3.8. Analysis of surface morphology of explanted materials

The explanted materials were fixed in 3% glutaraldehyde. The fixed samples were dehydrated in ascending grades of ethanol and dried in the liquid phase with isoamyl acetate. Critical point drying was carried out (Critical point dryer Model HCP-2 Hitachi Science Systems, Japan) in liquid CO2 at 150 kg/cm^2. The samples were sputter coated with gold (Ion Sputter Model E101 Hitachi, Japan) and observed using a scanning electron microscope (S2400 Hitachi) at an accelerating voltage of 15 kV.

3.2.3.9. Two dimensional electrophoresis

3.2.3.9.1 Sample preparation

The PEUU and UHMWPE retrieved from the animal upon sacrifice were washed in deionised water thrice to remove unadsorbed proteins and to lyse cells. The materials were kept in 300 µl rehydration buffer. The samples were stored at -80°C until electrophoresis was carried out.

3.2.3.9.2 IPG strip rehydration

The sample was thawed and sonicated in a sonicator to elute the proteins into the buffer. The protein sample in the rehydration buffer was loaded onto isoelectric pH gradient (IPG) strips, pH 3-10, linear, 17 cm, (BIO-RAD) and the strips were allowed to rehydrate with the sample overnight at room temperature. Mineral oil was layered on top of the strips to ensure there was no evaporation of sample and drying of IPG strips.

3.2.3.9.3 Iso electric focusing

Mineral oil was drained from the IPG strip, rehydrated with the sample and the strip was placed gel side down on isoelectric focusing tray maintaining the correct

polarity after placing wet wicks on the electrodes. Isoelectric focusing (IEF) was performed in the following steps:

Step 1	- 250V, 20 minutes with a linear voltage ramp
Step 2	-10,000V, 2.5 hours with a linear voltage ramp
Step 3	-10,000V, 40,000 Volt-hours at a rapid voltage ramp.

When the electrophoresis was complete IPG strip was removed from the focusing tray and kept in equilibration tray with gel side up and kept at -80°C until the second dimension electrophoretic run.

3.2.3.9.4 **IPG strip equilibration**

The IPG strips were equilibrated in equilibration buffer I and II for 10 minutes each before second dimension electrophoresis was started.

3.2.3.9.5 **SDS PAGE**

After the first dimension electrophoretic run IPG strips were loaded onto 7.5% polyacrylamide gel. Second dimension electrophoretic run was performed on a PROTEAN II XL cell (BIO-RAD, USA).

3.2.3.9.6 **Visualization**

The gel was fixed in methanol – acetic acid fixative (40% methanol and 10% acetic acid) for 40 minutes and washed in deionised water thrice for two hours. It was soaked in hypo for one minute, washed quickly with water twice and put in $AgNO_3$ for 20 minutes on shaker. This was followed by quick washing thrice in deionised water. Devoloper was added and decanted in one minute. More developer was added and kept shaking until protein spots were visible. Stop solution was added and rinsed with water.

3.2.3.9.7 **Gel analysis**

The gels were photographed with the help of a gel scanner and were stored in 50% methanol until spots were manually excised.

3.2.3.9.8 **In-gel trypsin digestion and MALDI spotting**

Protein spots in the stained gel were excised manually and transferred into sterile microcentrifuge tubes. Gel pieces were washed with 500 µL of wash solution (50% acetonitrile, 50 mM ammonium bicarbonate) and incubated at RT for 15 minutes with gentle agitation (vortex mixer on lowest setting). The solution was pipetted out. The gel pieces were washed with 500 µL of wash solution (15 minutes each) until the dye had been completely removed. The gel pieces were then dehydrated in 100% acetonitrile for five minutes. When dehydrated, the gel pieces had an opaque white color and significantly smaller in size. Acetonitrile was removed with a pipette and gel was completely dried at room temperature for 10-20 minutes. To the gel pieces, 500 µL of wash solution was added and incubated at RT for 15 minutes with gentle agitation. This process was repeated two more times.

The gel pieces were rehydrated with a minimal volume of protease (trypsin) digestion solution and digested overnight at 37° C.

The supernatant was transferred (containing tryptic peptides) to sterile centrifuge tube. 25 µL of extraction solution (60% acetonitrile, 1% TFA) was added to gel pieces and supernatant was transferred (containing additional tryptic peptides) to tube. The gels were extracted with an additional 25 µL of extraction solution for 10 minutes and supernatant was transferred to tube. The pooled extracted peptides were dried by lyophilisation.

The sample was reconstituted in water and mixed with MALDI matrix alpha-cyano-4-hydroxycinnamic acid matrix (10 mg/mL in 50% acetonitrile, 0.1% TFA) and spotted on MALDI plate. The spots were allowed to dry completely followed by MALDI mass spectrometry analysis.

3.2.3.9.9 **Database analysis**

The molecular masses of peptides were matched with that in the database allowing a peptide mass tolerance of one Da and one missed cleavage. The database search was performed on a Matrix Science Mascot search engine. (http://www.matrixscience.com/cgi/search_form.pl?FORMVER=2&SEARCH=PMF).

3.3. PHASE II METHODOLOGY

3.3.1. Molecular weight analysis of commercial PUs

The molecular weights of the commercial PUs (Table 2) used in this study was analyzed by GPC.

3.3.2. Effect of cell culture medium on polyurethane surface chemistry

The in-house synthesized PEUU, UHMWPE and the commercial PUs (Table 2) were analyzed for changes in material properties such as wettability and surface molecular rearrangement after incubation in cell culture medium (MEM) for 30 days. The materials were immersed in sterile cell culture medium and incubated at 37±2°C for 30 days. After treatment period the materials were washed thoroughly with distilled water and dried completely. The materials were then evaluated by contact angle analysis and ATR-FTIR spectroscopy.

Table 2 Materials used in *in vitro* analyses

Material	Specification
Biospan®,	MDI, PTMEG, diamine
PurSil™ AL (Hardness 80A)	MDI, PTMEG, diol -PDMS
Pursil™ AL-20 75A	MDI, PTMEG, diol- PDMS
Elasthane™	MDI, PTMEG, diol
Carbosil™ 20	MDI, HEC, diol-PDMS
Bionate® 80A	MDI, HEC, diol
in-house synthesized PEUU	MDI, PTMEG, diamine
UHMWPE	

3.3.3. *In vitro* cell culture studies

3.3.3.1. Cell culture

Mouse macrophage cell line, RAW 264.7 was used for all the experiments in the investigation of cell-material interactions. The cell line was frozen and stored until the cell culture studies were carried out. The stocked cells were thawed and grown in MEM containing 10% FBS at 37°C under a humidified 5% CO_2 atmosphere. The

medium was changed at an interval of two days until the cells attained near confluency.

In-house synthesized PEUU, commercial PUs and UHMWPE were cut into 1 cm^2 sizes. All the PUs were cleaned by washing in n-hexane followed by 2% SDS, and six changes of distilled water for 30 minutes each. The materials were dried at 60°C and gas sterilized with EtO.

After one passage the confluent cells were harvested by gentle scraping with a cell scraper and suspended to a final density of $2x10^4$ cells/cm^2 in MEM with 10% serum and were seeded onto in-house synthesized as well as commercial PUs and UHMWPE. Glass coverslips of the same size were used as a control. The cell cultures were incubated for 4, 24, 48 and 72 hours.

3.3.3.2. Analysis of cell adhesion

The morphology of cells adhered on the materials were analyzed at 4, 24, 48 and 72 hours. For this, at the end of cell culture, medium was pipetted out and the materials with cells were washed with PBS (pH 7.4) three times, five minutes each. This was done to ensure that non-adherent cells were removed. The materials were then fixed in appropriate fixative.

3.3.3.2.1 Phase contrast microscopy

All the commercial PUs and glass coverslips were fixed in 4% paraformaldehyde and examined under inverted phase contrast microscope (Leitz DMIL, Leica, Germany). Digital micrographs were acquired using a digital camera (DFC 280, Leica, Germany) equipped with a Q-win software.

3.3.3.2.2 Environmental Scanning Electron Microscopy (ESEM)

Evaluation of cell adhesion on in-house synthesized PEUU was not possible by phase contrast microscopy because of its opaqueness. Hence in order to evaluate the cell adhesion pattern on PEUU, ESEM was carried out in the low vacuum mode. Representative samples of Biospan® and glass coverslips were also examined with ESEM for comparison. The in-house synthesized PEUU Biospan® and glass coverslips with adherent cells were fixed in 3% gluteraldehyde and examined with an

ESEM (Quanta 200, FEI, Netherlands). The selection of Biospan® was due to the fact that it had a composition similar to in-house synthesized PEUU.

3.3.3.3. Immunofluorescence analysis

All the materials seeded with cells were stained by an immunofluorescence method. The cells were washed with PBS three changes, five minutes each followed by fixation in 4% paraformaldehyde. Just before starting the staining procedure the material with cells were washed with PBS two changes five minutes each. The cells were permeabilized with Triton X100 (0.1% in PBS) for 10 minutes. To prevent non specific binding of antibodies the cells were blocked with 1% bovine serum albumin (Bio-rad, USA) in PBS for 15 minutes. This was followed by washing with Triton X100 (0.1% in PBS) for two minutes. The cells were incubated with phalloidin conjugated with tetramethylrhodamineB isothiocyanate (Fluka, USA) at a final dilution of 1:1000 for 30 minutes. Finally the cells were washed with PBS two changes five minutes each. The material was mounted on microscopic glass slides with aqueous permanent mountant (Dako cytomation, USA). These were then viewed using a trinocular microscope (Nikon Eclipse E600, Japan) in the fluorescence mode. All images were captured using a digital camera (DXM1200F, Nikon, Japan) with an ACT-1 software.

3.3.3.4. Laser scanning Confocal Microscopy (LSCM)

The immunofluorescence stained preparations were used for LSCM evaluation. The actin cytoskeletal spreading of the adherent cells were analyzed by a laser scanning confocal microscope (Carl Zeiss 510 Meta, Germany). An excitation wave length of 543 nm was employed (He-Ne 543 laser) and emission wavelength was detected with a bandpass filter (BP 560-615 nm). Confocal images were captured and Z-sectioning was performed in order to view the actin cytoskeletal arrangement in three dimension.

3.3.3.5. Enzyme Linked Immunosorbent Assay (ELISA) for interleukins 1 and 6

The interleukin -1α and interleukin -6 secreted into the culture medium by RAW 264.7 cells grown on in-house synthesized PEUU, Biospan® and glass coverslips were quantitated by ELISA. Interleukin secreted into the medium was

assayed at 24 and 48 hours after incubation. The time period selection was made on the basis of the actin cytoskeletal spreading behaviour exhibited by the cells at the different time periods. The medium was stored at -80°C until ELISA was performed. The release of pro-inflammatory mediators IL-6 and IL-1α into the medium was assayed using commercial ELISA kits (Biosource Immunoassay Kit, Biosource International Inc. USA). Briefly, the IL-6 and IL-1α molecules bound to the antibody coated wells of the ELISA plate were sandwiched with the secondary antibody conjugated with avidin-horse radish peroxidase. The bound avidin-HRP was allowed to react with tetramethylbenzidine substrate. Once the colour has developed, stop solution was added. The absorbance was measured at 450 nm using a microplate reader Model Infinite F 200 (Tecan, Austria) equipped with a software Magellan version 6.1.

3.4. PHASE III METHODOLOGY

3.4.1. Cellular assay for intracellular signaling molecule, c-Jun NH2 terminal Kinase (JNK)

Intracellular signaling in RAW 264.7 cells adherent on material surface was assessed by measuring the extent of phosphorylation of JNK, a mitogen activated protein kinase.

3.4.1.1. Cell culture for Cellular Activation of Signaling ELISA (CASE)

The RAW 264.7 cells were grown to near confluency in culture flask in MEM with 10% FBS. On the day before the experiment the cells were changed to serum free medium and kept overnight. This was done to ensure that activation of JNK is accurately measured. On the day of the experiment the cells were gently scraped off the culture flask. This was divided into two groups and to one group JNK inhibitor, SP600125 was added at a concentration of 20 mM and the cells were incubated for one hour. The use of the inhibitor, SP600125, permitted to check the involvement of cross-talks in the signal transduction cascade in JNK activation.

The cells were seeded in individual wells of a 24-well plate onto Biospan®, PEUU and glass coverslip at a density of $5x10^4$ cells/cm^2. After incubating the cells for two hours to ensure adhesion of cells, medium was added to all wells to make a

final volume of 200 µl. To the wells containing cells with inhibitor, the volume of medium was adjusted to get a final inhibitor concentration of 20 µM. The culture was incubated for 24 hours at 37°C in a humidifed 5% CO_2 atmosphere. The assay was performed using triplicates of all the three materials for analysis of phosphorylated JNK, pan protein and phosphorylated JNK in presence of inhibitor for JNK.

3.4.1.2. CASE assay

The cell activation analysis was carried out with a commercial CASE kit (Cellular activation of signaling ELISA). The use of the commercial kit was advantageous because of the fact that the phosphorylation could be assessed even without cell lysis and subsequent protein purification. This facilitated a much error free determination of JNK phosphorylation. Briefly, at the end of 24 hours the cell culture medium was removed and cells were washed with PBS (pH 7.4) and fixed with 4% formaldehyde. The fixed cells were washed with washing buffer and incubated for 20 minutes with quenching buffer. The cells were washed again and antigen retrieval buffer was added. Antigen retrieval was performed in a microwave oven with 30% power. Non-specific antibody binding was blocked by adding blocking buffer. After washing, the primary antibody to pan JNK or to phospho-JNK was added to appropriate wells and incubated for one hour. The cells were washed after the incubation period and secondary antibody was added to all wells and incubated for one hour. At the end of the incubation period the cells were washed with washing buffer and PBS. To each well, 100 µl of developing solution was added and the development of colour was stopped by the addition of stop solution. The absorbance at 450 nm was read in a microplate reader Model Infinite F 200 (Tecan, Austria) equipped with a software Magellan version 6.1.

3.4.1.3. Determination of relative cell number

After the CASE assay was performed, the assay solution was removed and cells were washed with washing buffer and distilled water one after the other. Cell staining buffer was added to each well and incubated for 30 minutes. The wells were washed twice with distilled water and 100 µl 1% SDS added to each well and incubated for one hour in a shaker. The absorbance was read at 595 nm in a microplate reader. The antibody readings from CASE were normalized to the relative

cell number by taking the ratio of absorbance at 450 nm to absorbance at 595 nm for each well.

3.4.1.4. Extent of relative phosphorylation

The extent of relative phosphorylation was calculated using the formula

Extent of JNK phosphorylation = A/B

Where,

$A = X_1/Y_1$

$B = X_2/Y_2$

X_1 = aborbance at 450 nm in phospho-JNK wells

Y_1 = absorbance at 595 nm in phosphor-JNK wells

X_2 = aborbance at 450 nm in pan-JNK wells

Y_2 = absorbance at 595 nm in pan-JNK wells

3.4.1.5. Statistical analysis

Contact angle analysis, ELISA for cytokines and CASE assay experiments were performed in duplicate or triplicate and repeated two times. Differences between groups were analyzed using student's t test. Data are represented as mean ± SD. Differences with $p<0.05$ were considered significant.

Chapter 4

RESULTS AND DISCUSSION

4.1. PHASE I

4.1.1. Characterization of in-house synthesized PEUU

The in-house synthesized PEUU was characterized by the following techniques:

4.1.1.1. ATR-FTIR spectroscopy

The FTIR spectroscopy is a powerful tool for characterizing chemical groups within a compound and has been used for the characterization of PUs. The ATR-FTIR spectrum of PEUU is shown in Figure 3. The C=O urea peak is found at 1642 cm^{-1} and the ether, C-O-C peak is observed at 1102 cm^{-1}. The peak at 2937 cm^{-1} is assigned to the asymmetric stretching of β-methylene from PTMEG. The peak at 2851cm^{-1} is assigned to the symmetric stretching of β-methylene and asymmetric stretching of α-methylene from PTMEG. The peak at 2795 cm^{-1} is due to the symmetric stretching of methylene group from PTMEG. The 1730 cm^{-1} peak is assigned to the stretching of non-H bonded carbonyl from urethane. The shoulder of the peak at 1710 cm^{-1} is assigned to the H bonded carbonyl from urethane. The 1412 cm^{-1} peak is due to the C-C stretching in benzene ring. The peak at 1366 cm^{-1} is from the wagging methylene from PTMEG. The absence of 2270 cm^{-1} peak denotes the absence of physisorbed free isocyanates in the polymer as well as free isocyanate end groups. The characteristic frequencies of functional groups found in polyetherurethanes are

observed in the peaks of the FTIR spectrum of the synthesized PEUU. The spectrum compares well with that of commercial PUs confirming the identical chemistry.

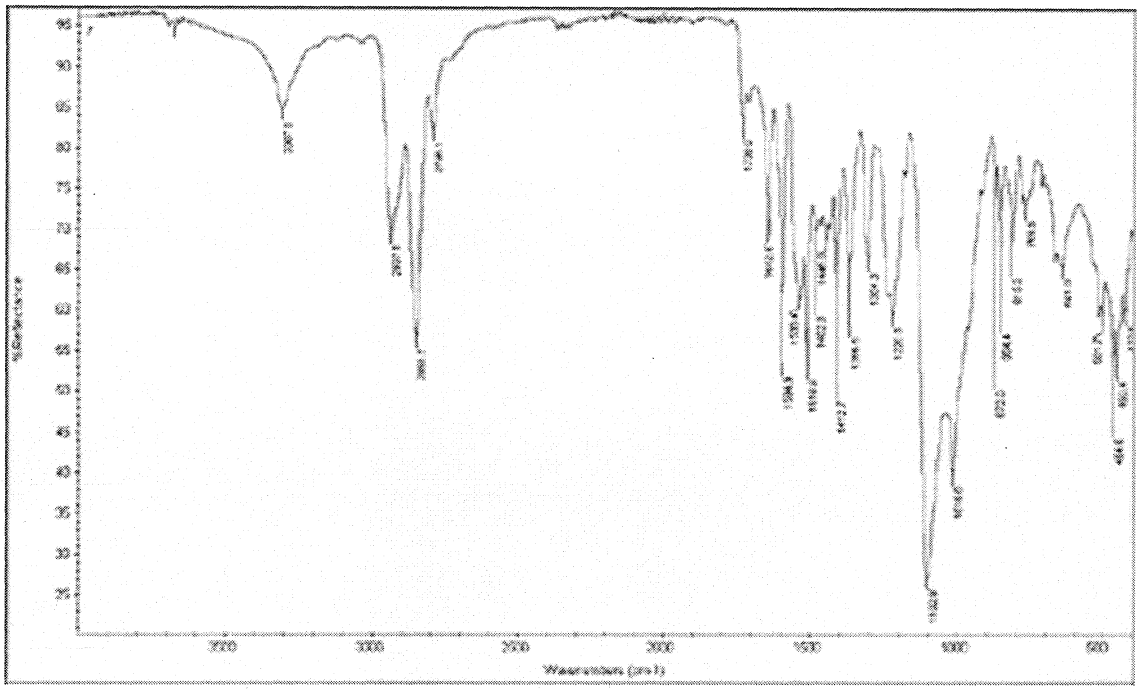

Figure 3 ATR-FTIR spectrum of in-house synthesized PEUU

4.1.1.2. GPC

The in-house synthesized PEUU achieved molecular weight averages comparable to the commercially available PUs of similar structural features. The number average molecular weight (Mn) of the PEUU is found to be 94882 with weight average molecular weight (Mw) of 162564 and polydispersity index of 1.7.

4.1.1.3. SEM

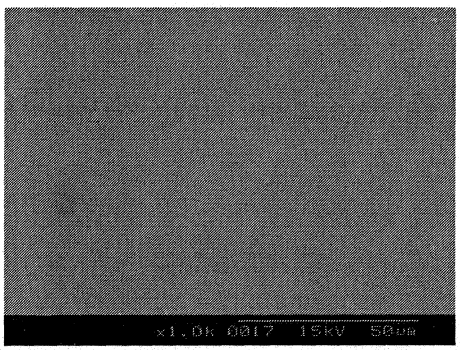

Figure 4 Scanning electron micrograph of in-house synthesized PEUU

The surface of in-house synthesized PEUU had a smooth morphology as shown in the scanning electron micrograph (Figure 4).

4.1.1.4. DSC

The glass transition temperature (T_g) of the PEUU is found to be at -2.95°C as evidenced from the DSC thermogram (Figure 5). In commercial PUs of similar chemistry, T_g is much lower. The upward shift of T_g of the in-house synthesized PEUU is probably due to phase mixing.

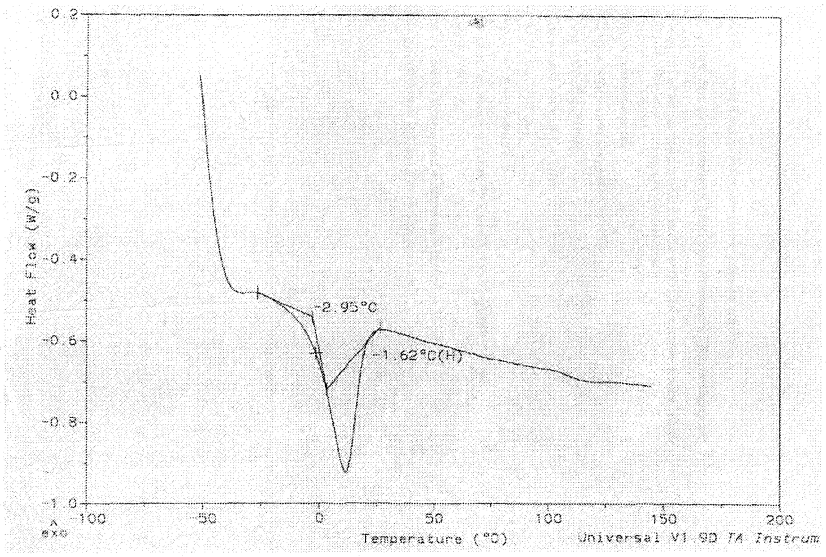

Figure 5DSC thermogram of in-house synthesized PEUU

4.1.1.5. Contact angle analysis

The contact angle value of in-house synthesized PEUU is found to be 81.5 ± 1.74 reflecting the hydrophobic nature of the surface (Figure 6).

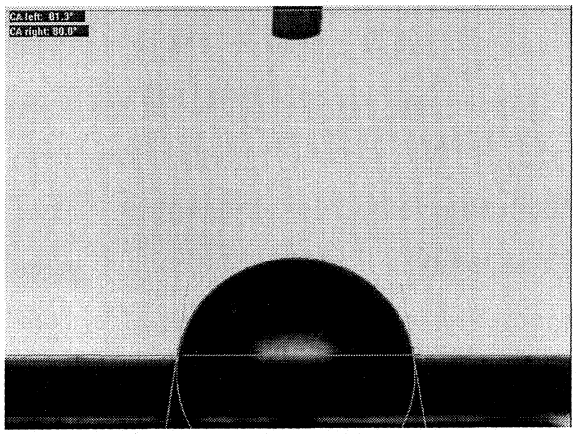

Figure 6 Contact angle measurement of in-house synthesized PEUU

4.1.2. *In vitro* cytotoxicity testing

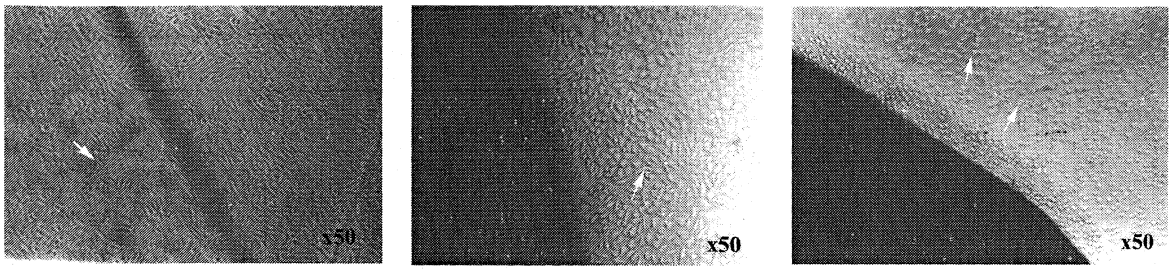

(a) (b) (c)

Figure 7 Light micrographs of L929 fibroblasts incubated with (a) PEUU, (b) negative control and (c) positive control following 24 hours culture.

In vitro cytotoxicity testing was performed for screening of materials prior to *in vivo* experiments. L-929 mouse fibroblast cells in culture retained their spindle morphology at the end of 24 hours incubation with PEUU (Figure 7a) and the negative control UHMWPE (Figure 7b). The cells lost their spindle morphology when incubated with the positive control (Copper) (Figure 7c). Cellular responses to PEUU, negative and positive controls were scored as 0, 0 and 3, respectively. The positive control copper, is cytotoxic and hence the cells became round in morphology. The change in normal morphology of cells indicates that the cells have undergone deteriorative processes leading to cell death. In the case of the negative control, the cells did not exhibit any change in their normal morphology. This indicated the non-cytotoxic nature of the material. The cell morphology remained unchanged in the case of PEUU also. Based on the non-cytotoxic nature of PEUU it was selected for implantation in animal model.

4.1.3. Histological analysis

All the animals used in the study were healthy throughout the experimental period. Gross examination of the implant site did not show infection. **Histological observations at the sham operated site** showed the presence of erythrocytes and leucocytes at one hour post-surgery (Figure 8a). This indicates fresh haemorrhage caused by the wound. Neutrophils were the predominant cells. Tissue debri constituted by disrupted extracellular matrix and damaged cells were also present at the wound site. The blood vessels adjacent to the wound site showed signs of diapedesis. Leucocytes were found marginating towards the endothelial lining of the vessels, indicating an ongoing migration of blood cells towards the injured tissue.

Four hours after surgery also neutrophils were present at the injured site. Far less number of monocytes were also noted in comparison to that of neutrophils. Leucocytes were found to adhere to the vessel wall in blood vessels adjacent to the site of injury (Figure 8b). By seven days, the sham operated site showed resolution of the inflammatory phase with few inflammatory cells and fibroblasts (Figure 8c). This was evidenced by the reorganized nature of the tissue which was disrupted by the injury. The number of inflammatory cells had reduced at 10 days (Figure 8d). At 15 days post-surgery, the sham operated tissue had remodeled and the inflammatory response had subsided (Figure 8e).

The tissue response to UHMWPE (a biocompatible material, used as a control) was characterized by the presence of neutrophils and monocytes at one day post-implantation (Figure 9a). The tissue adjacent to the implant site was infiltrated with these inflammatory cells and leaked out erythrocytes due to the injury to adjacent vascular tissue. Neutrophils are the first line of inflammatory cells recruited at the biomaterial implanted site (Falck P 1995). Similar response was seen at two days post-implantation also (Figure 9b). Absence of neutrophils and presence of macrophages was noted at the tissue adjacent to the implant site at 12 days post-implantation (Figure 9c). The inflammatory response had subsided by 18 days post-implantation (Figure 9d). Fibroblasts were present at the implant adjacent tissue and this was characteristic of remodeling phase. A healing response with formation of a fibrous capsule was noted at 30 days post-implantation (Figure 9e). By 60 days post-implantation, the tissue adjacent to UHMWPE showed a thin fibrous capsule. Macrophages were absent at this stage (Figure 9f). Absence of macrophages around UHMWPE clearly indicates the resolution of the initial inflammatory phase and the transition to repair phase mediated by fibroblasts.

The tissue response to PEUU implants was similar to that of the response to sham operation at one and four hours after surgery (Figure 10 a and 10 b). The histological picture continued into the first and second day with an increase in the number of neutrophils. At one day post-implantation, the tissue adjacent to the PEUU implant site was infiltrated with erythrocytes and leucocytes (Figure 10 c). Neutrophils constituted the majority of leucocyte population which persisted at two days post-implantation (Figure 10 d). The tissue appeared organized into a remodeling

matrix by seven days (Figure 10 e), which continued at 10 days post-implantation also (Figure 10f). The connective tissue matrix seen at the interface of the implant and host tissue indicates the beginning of remodeling phase (Figure 10 e and 10 f). Inflammatory cells, predominated by macrophages were also noted. A similar picture with persistence of macrophages was observed at 12, 15 and 18 days post-implantation (Figure 10 g, 10 h and 10 i). A fibrous capsule similar to that seen around the UHMWPE implant also formed around the PEUU implants at 30, 60 and 90 days post-implantation (Figure 10 j, 10 k and 10 l). However a notable feature was the identification of macrophages at the interface with the PEUU implants in comparison to that around UHMWPE where macrophages were absent at the same time period. Macrophages were continued to be noted even at 120,150 and 180 days (Figure m, n, o).

The response to a material, which is biocompatible with adjacent tissues, volves initial inflammation followed by the formation of a fibrous capsule around e implanted material. Inflammation persists for longer time periods in response to xic or otherwise incompatible materials (Williams DF and Roaf R 2000). The ological environment which interacts with biomaterials includes cells, secretory oducts of cells such as interleukins and cytokines, growth factors, extracellular atrix and blood components. When a biomaterial comes in contact with the ological milieu *in vivo* or *in vitro* one or more of the above constituents interact and cit an apposite response.

Cellular interactions with the implant is mediated by the secretory products of e cells and other extracellular factors which impart signals to the cells. These are portant determinants of ultimate fate of the material in the host. The autocrine and racrine influence of lymphocytes on macrophage response to biomaterials was also ed in literature (MacEwan MR *et al* 2005).

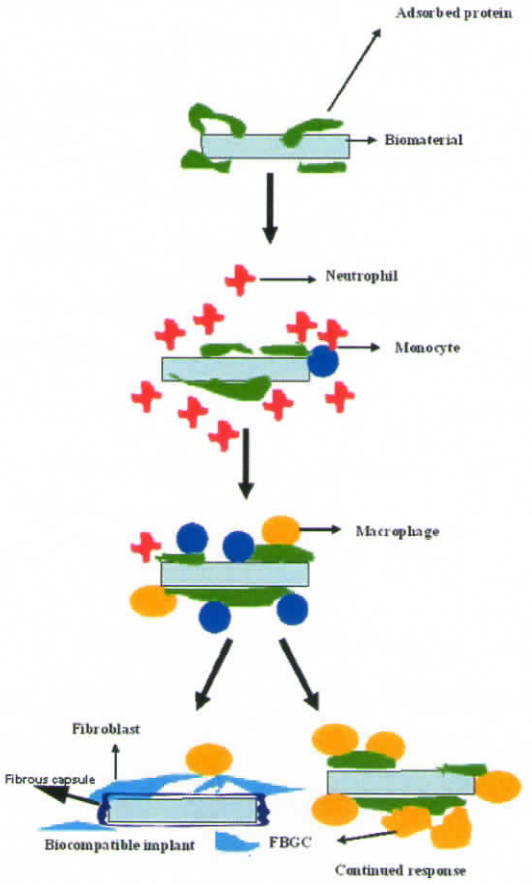

gure 2 Schematic representation of tissue response to implants

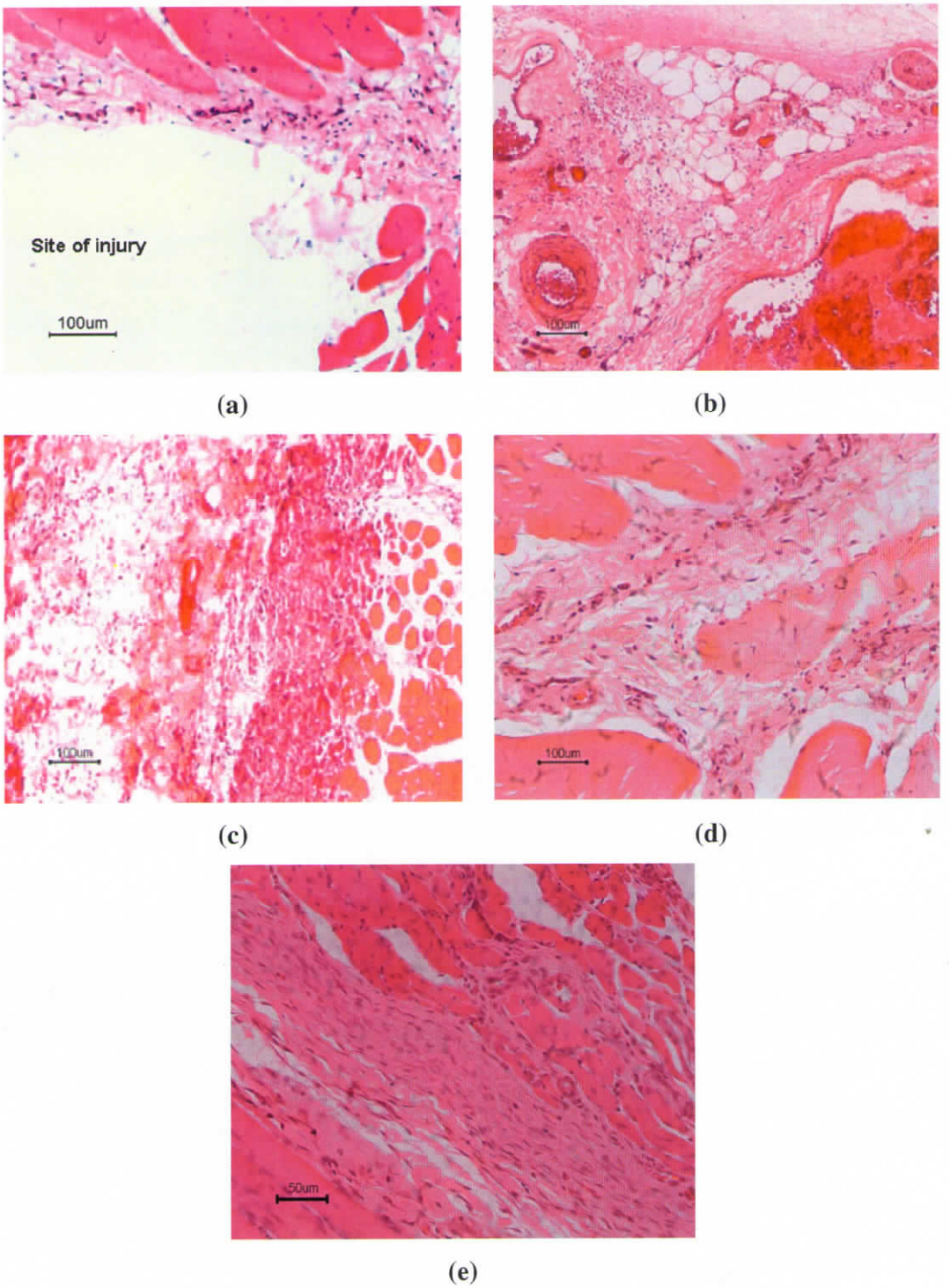

Figure 8 Light micrographs of tissue response to sham operation at (a) 1 hour, (b) 4 hours, (c) 7 days, (d) 10 days, and (e) 15 days post-surgery.

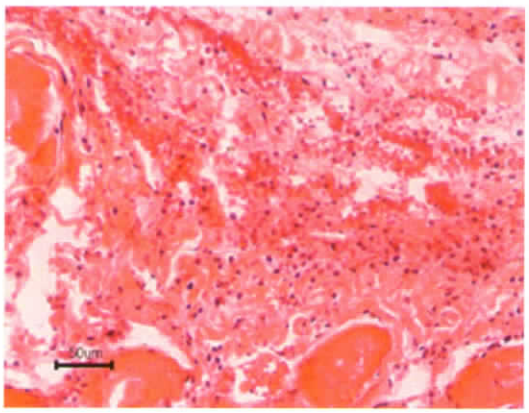

(a)

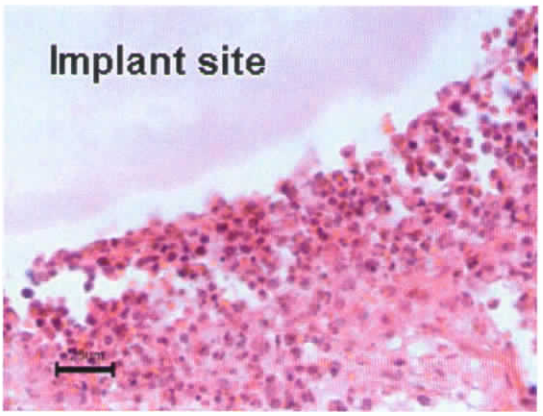

(b)

(c)

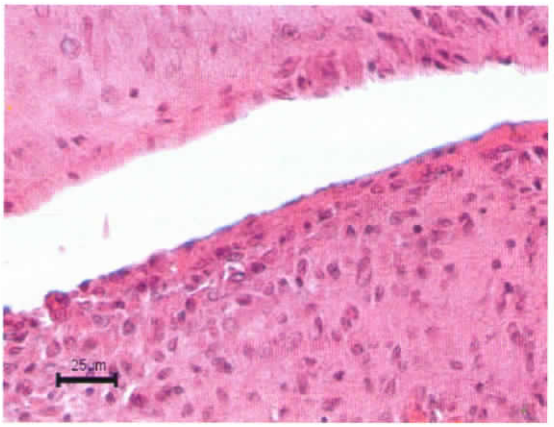

(d)

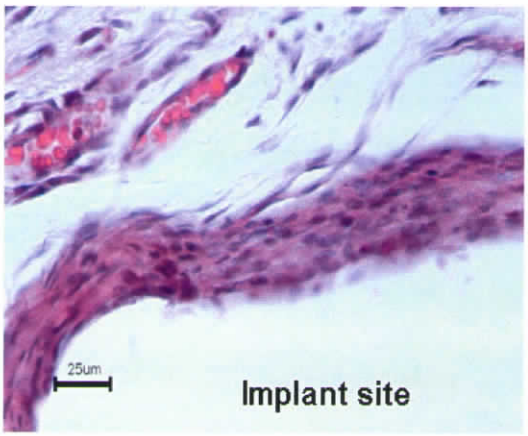

(e)

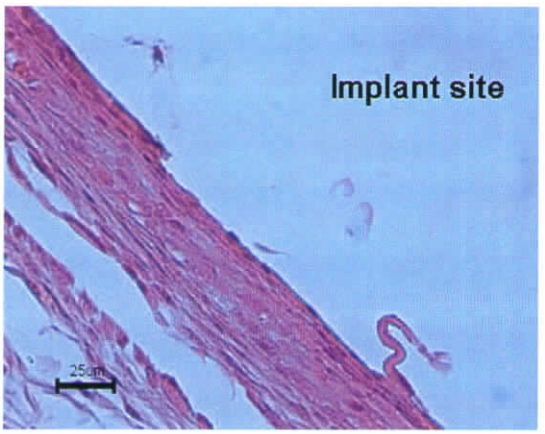

(f)

Figure 9 Light micrographs of tissue response to UHMWPE (a) 1 day, (b) 2 days, (c) 12 days, (d) 18 days, (e) 30 days, and (f) 60 days post-implantation.

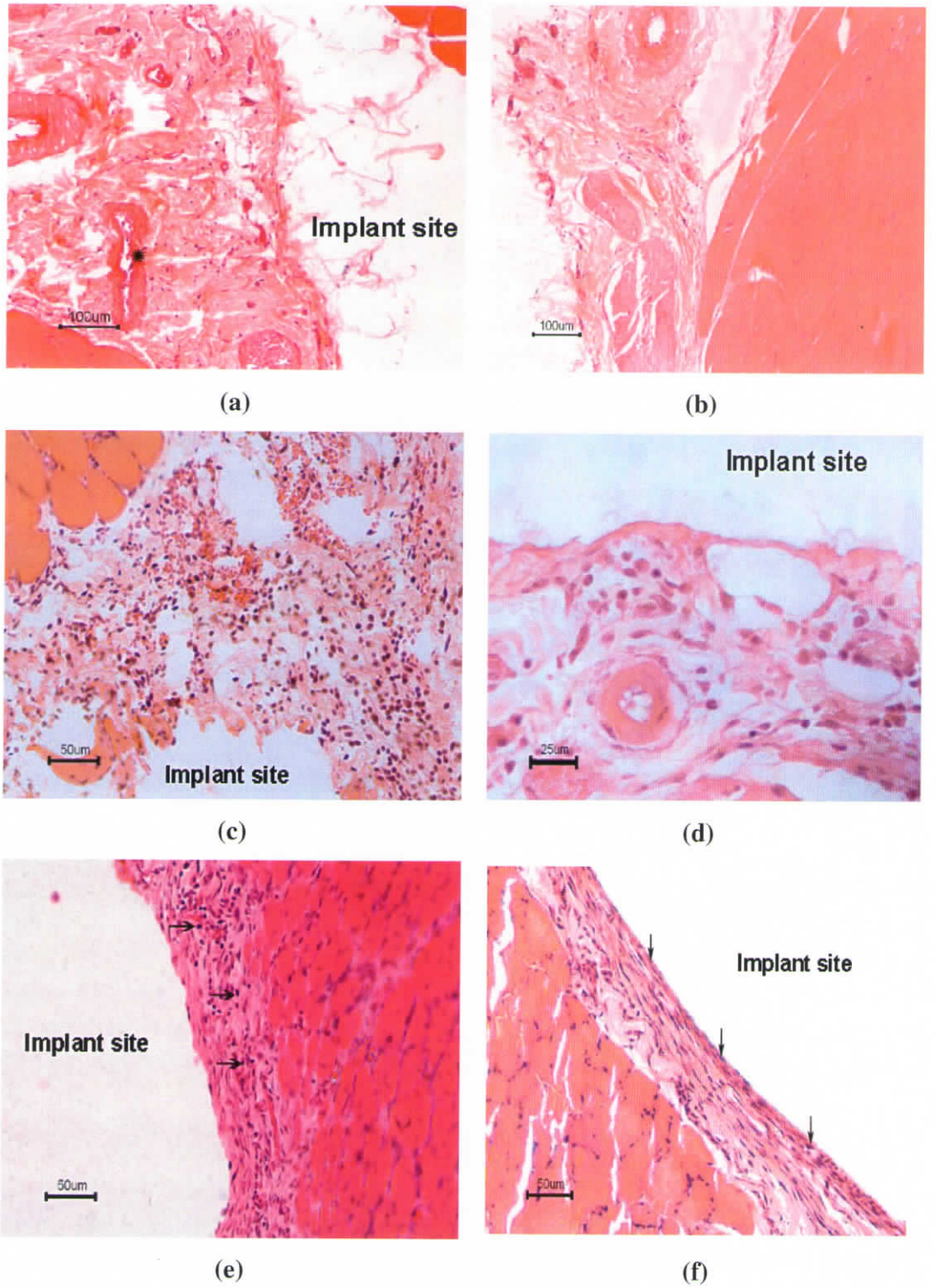

Figure 10 Light micrographs of tissue response to PEUU (a) 1 hour, (b) 4 hours, (c) 1 day, (d) 2 days, (e) 7 days, and (f) 10 days post-implantation.
(* denotes leucocytes marginating towards endothelial lining of blood vessels, arrows indicate macrophages).

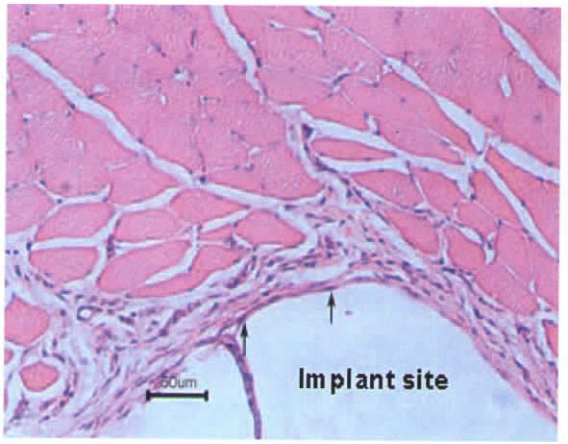

(m)

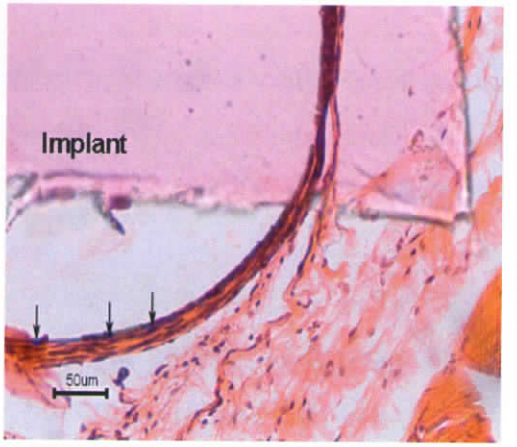

(n)

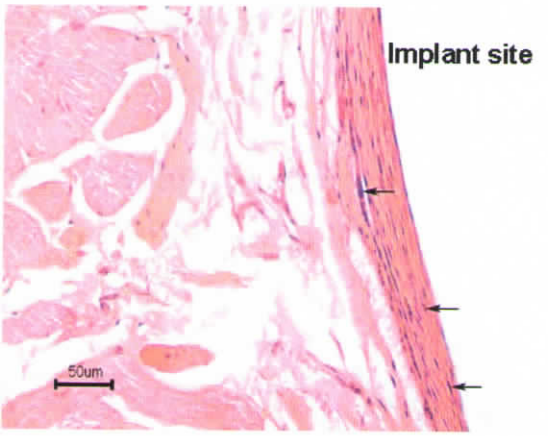

(o)

Figure 10 Light micrographs of tissue response to PEUU (m) 120, (n) 150, and (o) 180 days post-implantation. (arrows indicate macrophages).

Earlier, tissue response to implanted biomaterials, including PUs, were studied by analyzing the cellular constituents of exudates from cage implantation models. In a cage implantation model, the material is placed in a cage made of stainless steel. The entire cage with the material is implanted in the tissue. Cellular response studies were conducted on the exudates collected in the cage. Such models introduce a variant, that is the response is to the cage material. For analyzing tissue response to the material being investigated, eliminating the use of an additional cage material would be more appropriate. Furthermore, the presence of macrophages albeit few at longer time periods, would be difficult to assess in the scant to nil exudate at long-term in a cage model.

To ascertain that tissue response is specifically only to the material being studied, in this study PEUU was implanted directly in the muscle, but not in a cage. The experimental features in this study differ from earlier studies in that 1) PEUU was implanted as such 2) skeletal muscle was the site of implantation. While most of the earlier studies were carried out in subcutaneous tissue, the present study analyzes the cellular response to PEUU implanted in skeletal muscle. As stated earlier, considering that majority of implantable medical devices interact with muscle tissue, the choice of muscle as implantation site is relevant. It is important to test materials at the site of eventual clinical application because of the fact that foreign body response is influenced to a large extent by the local implant microenvironment (Luttikhuizen DT *et al* 2006). The extracellular matrix (ECM) is important in deciding the cellular behaviour. It provides structural support to tissues and is also involved in the control of cell growth and establishment of tissue microenvironment (Ambrosio L *et al* 2002). The responses elicited by tissues vary depending upon their vasculature, anatomic location and metabolic status. Eventhough other studies have probed degradation of polyether urethanes with different stochiometry, our study specifically looks into the surface degradation of a particular PEUU through 180 days in relation to the cellular response. The material surface chemistry greatly varies upon changing the stochiometry and chemistry of components.

The tissue response in the initial period of implantation followed acute reaction, as is usually observed at a site of injury. This was characterised by a cellular infiltration of numerous neutrophils and monocytes around the implant site. At the earlier time periods, the cellular response elicited was similar for PEUU and UHMWPE. The increase in the number of macrophages at 10 days following implantation is also characteristic of the normal healing process which later on leads to encapsulation of implant by a collagenous capsule at 30 days. Normal wound healing in rats ceases after the initial inflammatory response, eventually forming a non-cellular fibrous capsule around the implant site at 4-12 weeks. The course of inflammation was followed by a resolution phase, which was evidenced by the reorganizing matrix, at 15 days post-surgery in the sham operated control. The inclusion of a sham operated control provides information about the tissue response to the surgery alone. This has helped in discriminating the actual response to the implant and that to the injury alone. The initial non-specific response to the injury is

underscored, because it has contributed to the specific response to the implants as implantation time progressed.

With increase in implantation time the cellular response to PEUU and UHMWPE seemed to differ. The inflammatory response to UHMWPE had subsided and reached a repair phase characterized by the presence of fibroblast rich capsule surrounding the implant by 60 days (Figure 8f). However the tissue response to PEUU did not subside with the initial inflammatory reaction. The inflammatory cellular response to PEUU continued with increase in implantation time. The presence of inflammatory cells near the implant site in the later time periods is attributed to the defensins released from activated neutrophils at the early time periods, which act as chemotaxins. In the present study the presence of macrophages in addition to the fibroblasts and fibrocytes in the fibrous capsule around the PEUU implant is noteworthy. The macrophages were located particularly at the tissue-material interface. Earlier works by Zhao *et al* reports the presence of foreign body giant cells (FBGCs) even at one week post-implantation in subcutaneous tissue (Zhao Q *et al* 1991). This could be due to the increased number and activity of cells in the cage implantation model.

The persistent presence of macrophages in the thick fibrous capsule in the later time periods, as observed in histological sections indicates a continuing cell-material interaction around the implanted PEUU. Macrophages direct the inflammatory response to implants (Brodbeck *et al* 2003). The observed persistence of macrophages at the tissue-PEUU interface in contrast to the absence of any inflammatory cell at the tissue-UHMWPE interface at long-term prompted an investigation into the functional nature of these inflammatory cells adjacent to PEUU implants. Modulation of the deleterious host inflammatory response which results in ultimate failure of PU implants will be effected by further delineating the cellular activation status.

4.1.4. Ultrastructural analysis

Light microscopy analysis of semithin sections stained with toluidene blue also revealed the cellular response elicited at the sham operated tissue (Figure 11 a), tissue adjacent to PEUU implant (Figure 11 b) and UHMWPE (Figure 11 c) at 7 days. After identifying the site from the semithin sections, ultrathin sections were prepared

for detailed analysis of ultrastructural features at the site. The ultrastructural details of the tissue-material interface was analysed by TEM. Fibroblasts (F) with adjacent collagen fibres (C) were noted in the sham operated tissue (Figure 12 a). The fibroblasts were active which was indicated by the presence of mitochondria (MC) (Figure 12 b). The fibroblasts are recruited to the site of injury when the remodeling phase is initiated. The recruitement of fibroblasts is in response to the chemotactic microenvironment. A similar picture was seen at the UHMWPE tissue-interface (Figure 12 c).

The tissue adjacent to the PEUU implant contained macrophages (M) adjacent to blood vessel (BV) (Figure 12 f). The macrophages were found to have ruffled cytoplasm (Ruf) (Figure 12 e) and fenestrations (Fen) (Figure 12 h). The active nature of macrophages was indicated by the presence of rough endoplasmic reticulum (RER) (Figure 12 g, Figure 12 i) and mitochondria (MC) (Figure 12 i) in the cell cytoplasm.

Semithin sections stained with toluidene blue, for the 15 days group at the sham operated tissue (Figure 13 a), tissue adjacent to PEUU implant (Figure 13 b) and UHMWPE (Figure 13 c) facilitated identification of the sites for obtaining ultrathin sections for ultrastructural analysis.

At 15 days post-implantation, plump fibroblast (Fp) (Figure 14 a) and collagen bundles indicating the repair of injury was noted at the sham operated site. Foreign body giant cells (FBGC) with more than one nucleus (N), were seen adjacent to the PEUU implant as is seen in the representative micrograph (Figure 14 c, Figure 14 d). Rough endoplasmic reticulum (RER) was present in the cytoplasm indicating the active metabolic nature of the cells (Figure 14 d). At the same time, the tissue adjacent to UHMWPE contained fibroblasts (F) which were metabolically active. The active nature of cells was evident from the presence of rough endoplasmic reticulum (RER) in the cells (Ghadially FN 1982). The presence of collagen (C) fibres adjacent to the fibroblasts is indicative of a remodeling phase (Figure 14 e and 14 f).

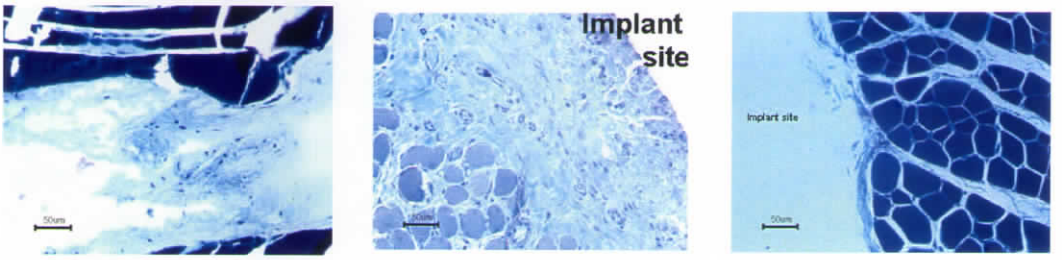

(a) (b) (c)

Figure 11 Photomicrographs of toluidene blue stained semithin plastic sections of tissues at 7 days post-implantation (a) sham operated tissue, (b) PEUU and (c) UHMWPE.

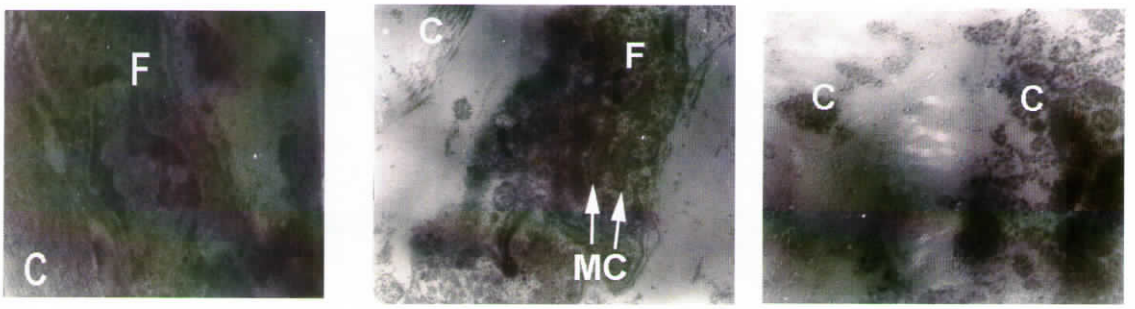

(a) Original magnification x 30,000 (b) Original magnification x 25,000 (c) Original magnification x 60,0000

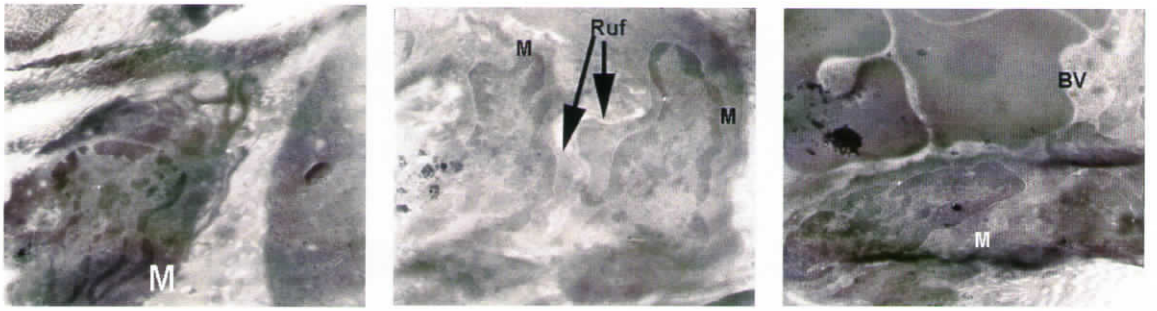

(d) Original magnification x 20,000 (e) Original magnification x 25,000 (f) Original magnification x 25,000

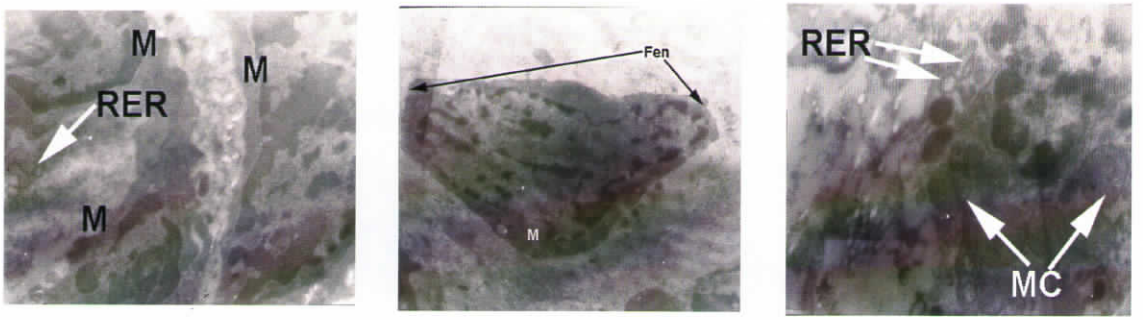

(g) Original magnification x 20,000 (h) Original magnification x 10,000 (i) Original magnification x 25,000

Figure 12 Transmission electron micrographs of ultra thin sections of tissues at 7 days post-implantation (a), (b) sham; (c) UHMWPE; (d) to (i) PEUU.
C-collagen, F-fibroblast, MC-mitochondria, M-macrophage, Ruf-ruffled morphology, BV-blood vessel, RER- rough endoplasmic reticulum, Fen-fenestrations.

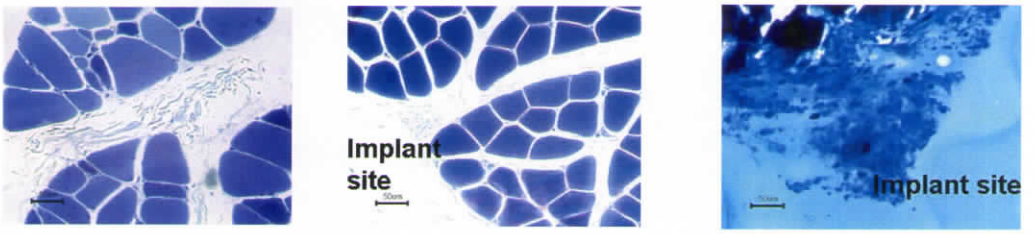

(a) (b) (c)

Figure 13 Photomicrographs of toluidene blue stained semithin plastic sections of tissues at 15 days post-implantation (a) sham operated tissue, (b) PEUU and (c) UHMWPE.

(a) Original magnification x 40,000

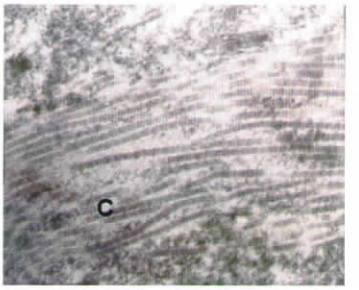

(b) Original magnification x 20,000

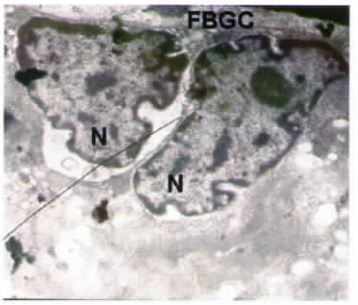

(c) Original magnification x 25,000

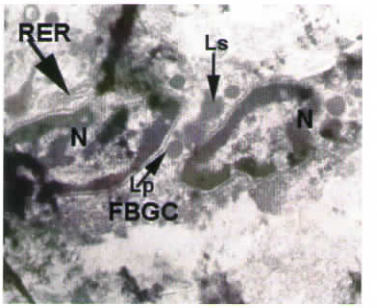

(d) Original magnification x 15,000

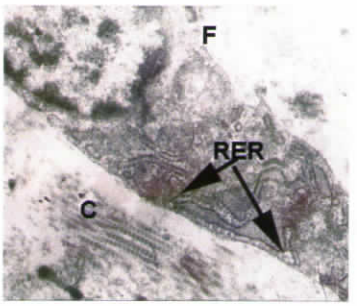

(e) Original magnification x 15,000

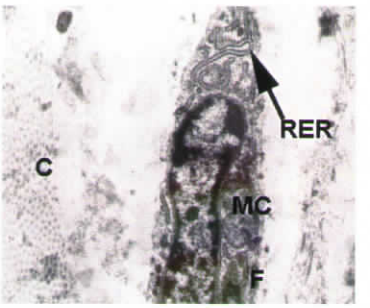

(f) Original magnification x 17,000

Figure 14 Transmission electron micrographs of ultra thin sections of tissues at 15 days post-implantation (a), (b) sham; (c), (d) UHMWPE; (e), (f) PEUU.
Fp- plump fibroblast, C-collagen, N-nucleus, FBGC-foreign body giant cells, RER-rough endoplasmic reticulum, Lp-primary lysosomes, Ls-secondary lysosomes, F-fibroblast, MC-mitochondria.

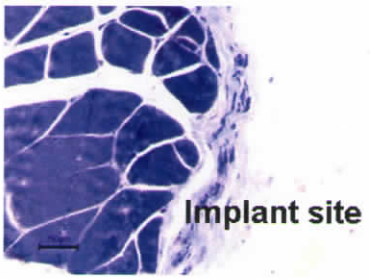

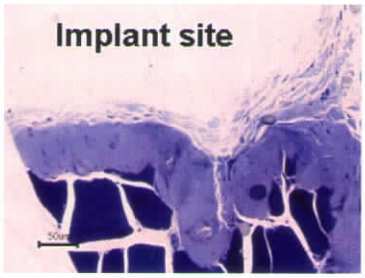

(a) (b)

Figure 15 Photomicrographs of toluidene blue stained semithin plastic sections of tissues at 60 days post-implantation (a) PEUU and (b) UHMWPE.

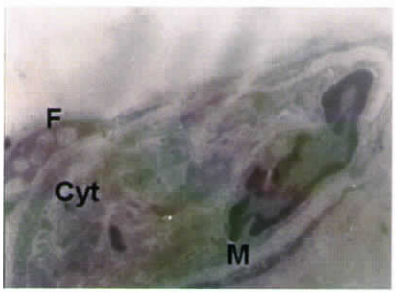

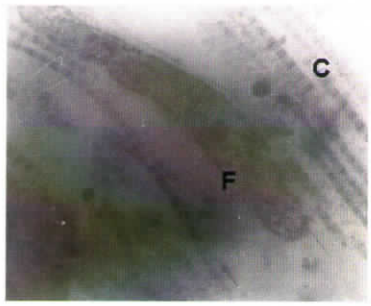

(a) Original magnification x 15,000 (b) Original magnification x 60,000

Figure 16 Transmission electron micrographs of ultra thin sections of tissues at 60 days post-implantation (a) PEUU and (b) UHMWPE.
F-fibroblast, Cyt-cytoplasm, M-macrophage, C-collagen.

The light micrographs of semithin sections of tissues adjacent to PEUU (Figure 15 a) and UHMWPE (Figure 15 b) assisted in the identification of site of implantation at 60 days. Though fibroblasts were seen at the interface along with collagen bundles at both PEUU (Figure 16 a) and UHMWPE (Figure 16 b) -tissue interface, macrophages were also seen only at the PEUU-tissue interface. The observations of TEM analysis further confirms the continued macrophage response elicited against PEUU as noted in haematoxylin and eosin stained tissue sections.

4.1.5. Analysis of surface morphology of explanted materials

Analysis of surface morphology of the explanted materials was done in order to find out if there is any surface degradation. The surface of PEUU did not exhibit much change after 2 days of implantation (Figure 17 a.) from what was observed prior to implantation (Figure 4). Whereas UHMWPE was covered with a loose network of ECM (Figure 17 b). At 30 days post-implantation numerous pits were noted on the

PEUU with occasional cells (Figure 17 c.). At the same time period the UHMWPE surface did not show any structural changes. Focal areas of adhered cells were also noted (Figure 17 d). These cells did not exhibit the ruffled morphology of activated cells. In addition to pits, cracking of the PEUU surface was observed at 60 days post-implantation (Figure 17 e). Large cells were noted adjacent to these cracks. A smooth ECM with spindle cells coated the UHMWPE at 60 days (Figure 17 f). The PEUU retrieved at 90 days (Figure 17 g.) showed pits, adherent cells and ECM covering the surface. The UHMWPE retrieved at the same time period exhibited an ECM coating embedded with cells (Figure 17 h). The formation of a fibrous capsule around the UHMWPE, and absence of surface morphological changes indicates the normal response to a biocompatible material.

The surface morphological changes in PEUU were followed to longer time periods. The pits on the surface of PEUU were apparent beneath the ECM coating with embedded cells on the ECM at 120 days (Figure 17 i). At 150 days post-implantation smaller apparently recent pits with adjacent cells were noted (Figure 17 j) which had increased at 180 days post-implantation (Figure 17 k). Extensive cracking of the implant surface was also noted.

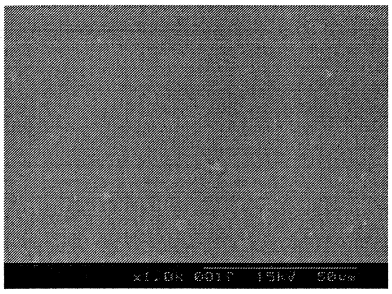

(a)

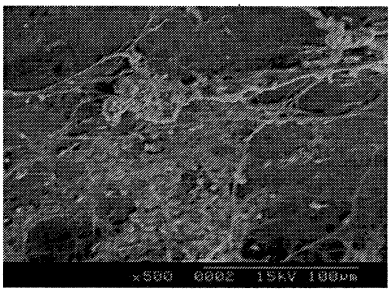

(b)

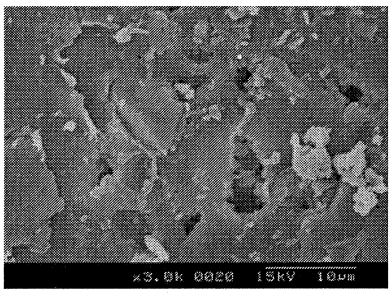

(c)

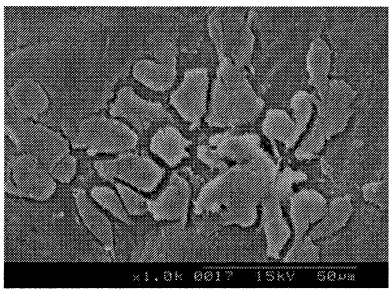

(d)

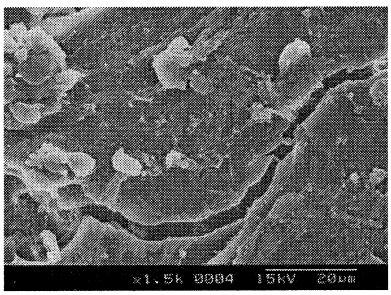

(e)

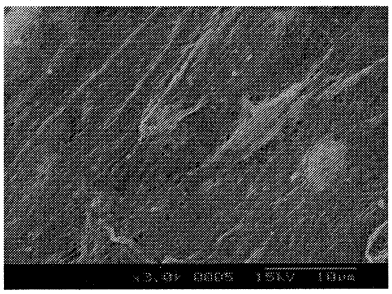

(f)

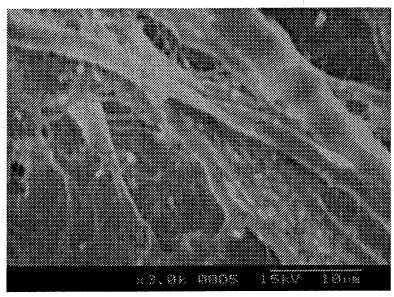

(g)

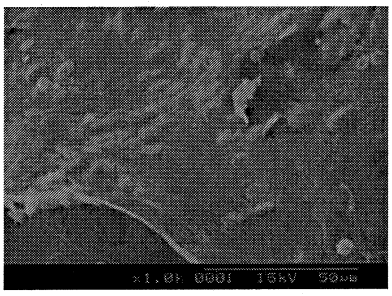

(h)

Figure 17 Scanning electron micrographs of explanted PEUU and UHMWPE at 2, 30, 60 and 90 days post-implantation. PEUU (a, c, e, g); UHMWPE (b, d, f, h).
(continued in next page)

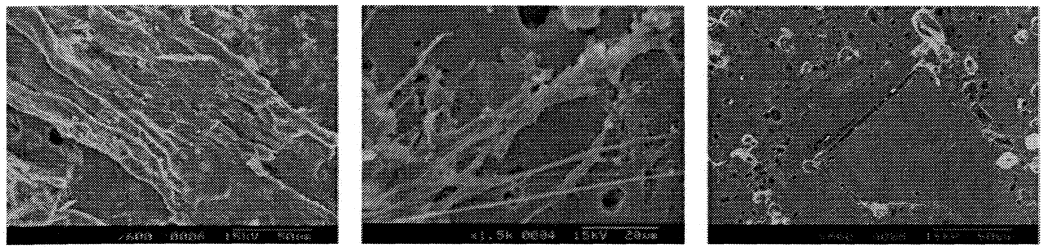

(i) (j) (k)

(Continued from previous page) Figure 17 Scanning electron micrographs of explanted PEUU at (i) 120, (j) 150, and (k) 180 days post-implantation.

4.1.6. Immunohistochemical analysis of cells and cytokines

The presence of macrophages at the implant-tissue interface was confirmed further by the positive staining for macrophage markers ED1 and ED2. Newly recruited macrophages were identified by the marker ED1 and mature resident macrophages in the tissue by the marker ED2. There was an absence of ED1 positive cells at four hours post-implantation (Figure 18 a). Positively stained cells were present at all other time periods, few at one day (Figure 18 b) and moderate at two, seven, ten and fifteen days (Figure 18 c, d, e and f). This indicates the continous recruitment of macrophages to the implant site. The presence of positive cells, though fewer in number, at the longer time periods, 120 (Figure 18 j), 150 (Figure 18 k) and 180 (Figure 18 l) days post-implantation confirms the continuous long-term recruitment of macrophages in the tissue adjacent to PEUU.

The presence of ED2 positive cells were noted at the implant adjacent tissue at all time periods examined (Figure 19). This indicates the continued presence of resident macrophages at the tissue adjacent to PEUU implant. A study by Marques *et al* (Marques *et al* 2005) showed a concentration of newly recruited macrophages at the tissue-material interface around starch based composite materials. They also reported the presence of resident macrophages in outside layers of tissues. However in our study such a difference in the distribution of ED1 and ED2 macrophages was not observed. Probably this could be due to the fact that the responses elicited by the resident as well as recruited macrophages are required to provide defense against the implanted PEUU. It has also been suggested by some earlier research groups that resident macrophages move to the site of implant and develop ED1 marker. The difference in functional aspect of ED1 and ED2 macrophages as phagocytic and regenerative respectively, has also been put forward. Since the line of demarcation

between the two is not clear it is inappropriate to elaborate on this aspect in the present context.

The functional activity of macrophages is analyzed by their cytokine profile. The cytokines secreted by macrophages signal the pace of inflammatory response (Li Y *et al* 2005). Several studies have reported that sustained or marked pro-inflammatory cytokine production in response to biomaterials is an indication of activated nature of inflammatory cells around the material. However, study of proinflammatory cytokine production at the tissue adjacent to polyetherurethane urea implants sequentially over a long time period is not reported previously. Analysis of the cytokines produced by activated macrophages around implanted PEUU is significant in the delineation of cellular mechanisms that lead to continued inflammatory response to PEUU. This was determined by the evaluation of cytokines IL-6, IL-1α, Il-1β, IFNγ and TNF α at the tissue-PEUU interface at all time periods.

Interleukin-6 was found to be positive at all the time periods studied. The expression of IL-6 was found to be intense at 15 days (Figure 20 f) and 120 days post-implantation (Figure 20 j). The transition of acute inflammation to chronic inflammation is mediated by IL-6. The progression of the inflammatory phase to one with increased recruitment and activation of macrophages was thought to be mediated by the IL-6 produced by macrophages at the implant site. The inability of macrophages to destroy the bulk PEUU implant necessitates the involvement of more cells. Hence in an attempt to sustain the inflammatory response to PEUU, IL-6 is produced. The exacerbation of macrophage response around the PEUU implant could be ascribed in part to the presence of IL-6. Earlier reports also showed that IL-6 suppresses neutrophil infiltration and concurrently increases the recruitement and activation of monocytes. It is also reported that the differentiation of monocytes to the macrophage lineage and away from the dendritic cell lineage is mediated by IL-6 (Rose-John S *et al* 2006).

The positive staining for IL-1α as early as one day post-implantation (Figure 21 b) confirmed the activation status of the macrophages present at the implant site. Positive staining continued to be seen at 10 (Figure 21 e), 15 (Figure 21 f), 30 (Figure 21 g), 90 (Figure 21 i) and 180 days (Figure 21 l). This indicates the active status of these cells at long-term and that contact with PEUU was sufficient to activate the cells.

The inflammatory phase and wound healing phase following implantation of biomaterials is mediated by macrophages through secretion of cytokines (Brodbeck *et al* 2002).

Interleukin-1β was found to be present at the implant site from seven days through 180 days post-implantation (Figure 22 1). The wound healing as well as proinflammatory roles of IL-1β are known. Hence the presence of IL-1β indicates the delicate balance between wound healing and progression of inflammatory response.

Another important pro-inflammatory cytokine secreted by macrophages is tumour necrosis factor α (TNF-α). It has been implicated as a mediator of acute as well as chronic inflammation. The presence of TNF-α was found at all time periods studied (Figure 23), particularly from seven days onwards. This highlights the potential of PEUU in eliciting the continued response by macrophages and maintenance of their functional status. Positive staining for TNF-α by macrophages adjacent to implants whenever macrophages are involved in the inflammatory response is reported in the case of other materials also (Robitaille R *et al* 2005). Monocytes and macrophages produce TNF-α in response to their contact with biomaterial surfaces. Plasma levels of TNF-α were found to be increased in patients undergoing haemodialysis. This was attributed to the direct interaction between monocytes and dialysis membrane (Anderson JM *et al* 1996). The much established roles of TNF-α in mediating inflammatory response include activation of leukocytes, adherence of neutrophils and monocytes, and increased production of pro-inflammatory cytokines (Tracey KJ *et al* 1994).

Interferon γ is produced by T cells and macrophages. The positive staining for IFN-γ obtained at different time periods in this study could be due to the production of the same by macrophages (Figure 24). Lymphocytes were significantly absent in tissue sections stained with haematoxylin and eosin. The role of IFN-γ in activating macrophages is well established (Kota RS *et al* 2006). The autocrine activation of macrophages by IFN-γ might be involved in the continued response of macrophages to implanted PEUU. Stimulation of macrophages by IFN-γ results in the secretion of more pro-inflammatory mediators such as IL-1, IL-6 and TNF-α . The positive staining for macrophages was observed as early as one and two days post-

implantation, and again at 30, 150 and 180 days post-implantation. This might be due to the stimulation of macrophages in an autocrine manner at intervals. The macrophages upon activation release inflammatory mediators which signal the recruitment of more inflammatory cells.

The lymphocyte population, especially helper T cells, was stained with the use of CD4 antibodies. The presence of CD4 positive cells were however negligible at all the time periods studied (Figure 25). This suggests an absence of adaptive immune response to the implanted PEUU.

The pro-inflammatory milieu at the PEUU adjacent tissue was reflected by the positive staining obtained for both resident and newly recruited macrophages and the pro-inflammatory mediators IL-1, IL-6 and TNF-α throughout the *in vivo* residence of the implant. A study by Robitaille R *et al* has highlighted the involvement of IL-1 and IL-6 in the primary non-specific response in inflammation, while TNF-α is considered to be involved in the change to chronic inflammation. Other reports implicate IL-6 in the changeover of acute to chronic inflammation (Rose-John S *et al* 2006). However, from the present study it can be concluded that the continued macrophage response to PEUU involves a delicate balance between the pro-inflammatory cytokines such as IL-6, IL-1α, TNF-α and the pro-wound healing effects of cytokines such as IL-1 β with both pro-wound healing and pro-inflammatory role.

ED1

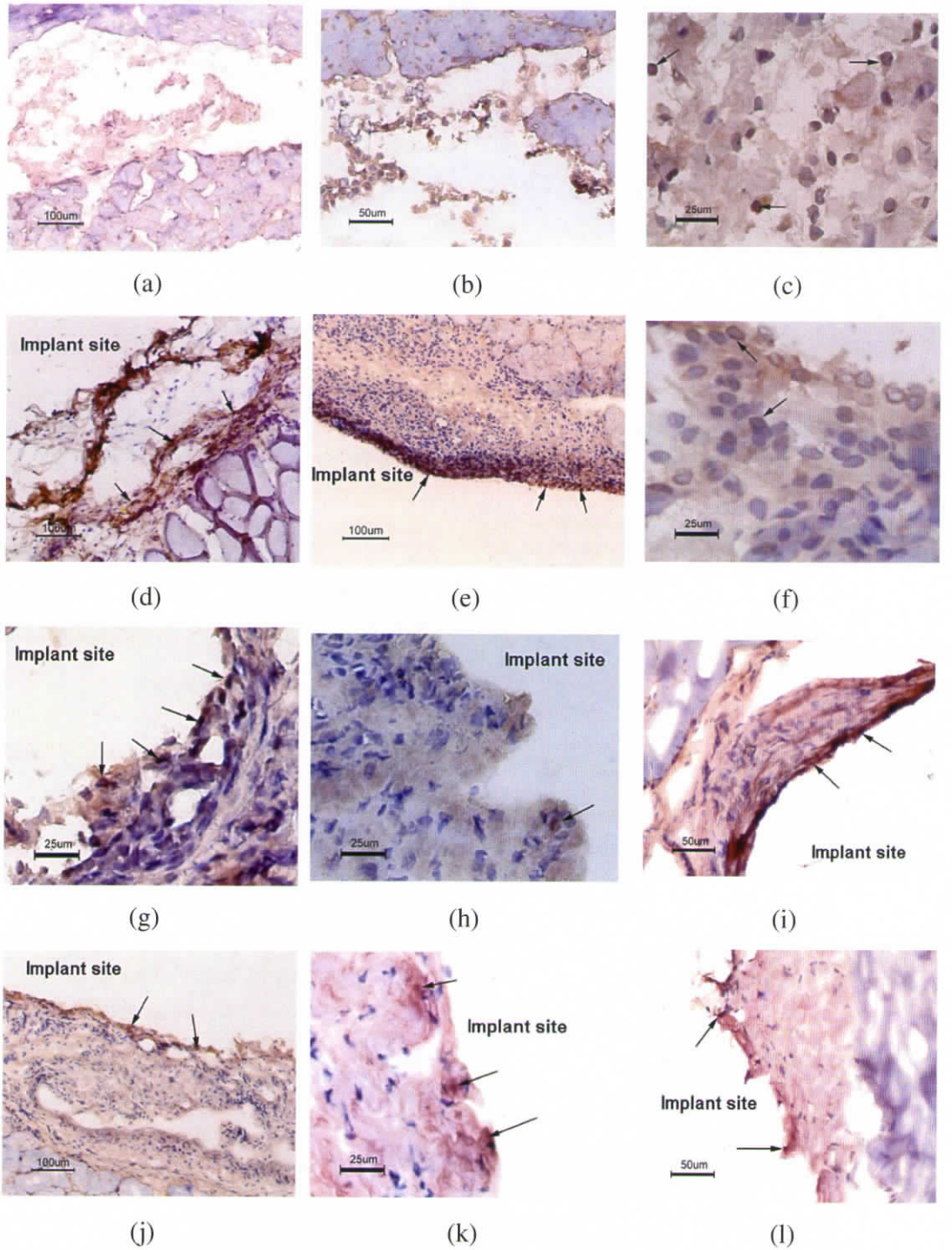

Figure 18 Light micrographs of PEUU adjacent tissue sections immunostained for ED1 at (a) 4 hours, (b) 1, (c) 2, (d) 7, (e) 10, (f) 15, (g) 30, (h) 60, (i) 90, (j) 120, (k) 150, and (l) 180 days post-implantation.
Arrows denote positive staining.

ED1

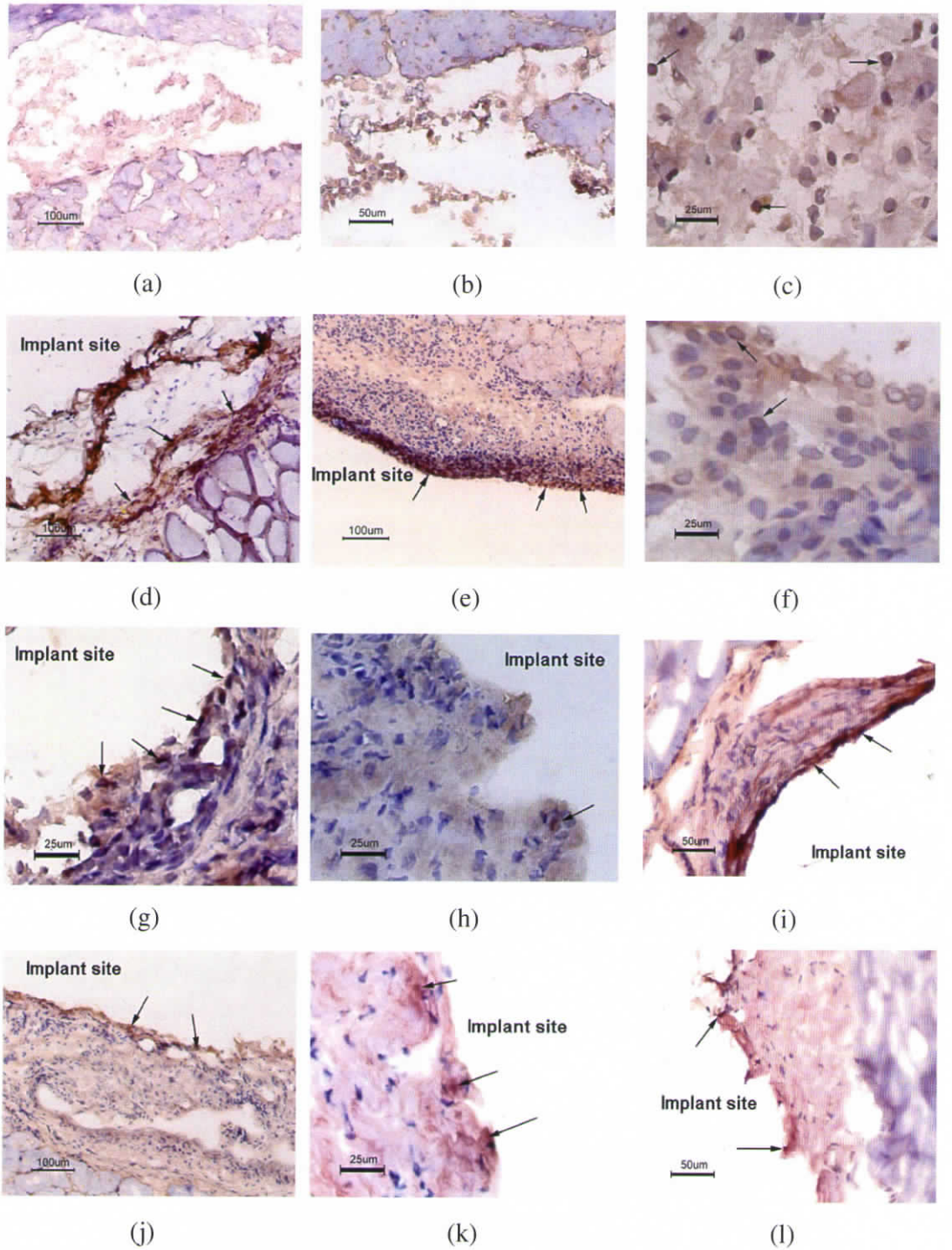

Figure 18 Light micrographs of PEUU adjacent tissue sections immunostained for ED1 at (a) 4 hours, (b) 1, (c) 2, (d) 7, (e) 10, (f) 15, (g) 30, (h) 60, (i) 90, (j) 120, (k) 150, and (l) 180 days post-implantation.
Arrows denote positive staining.

ED2

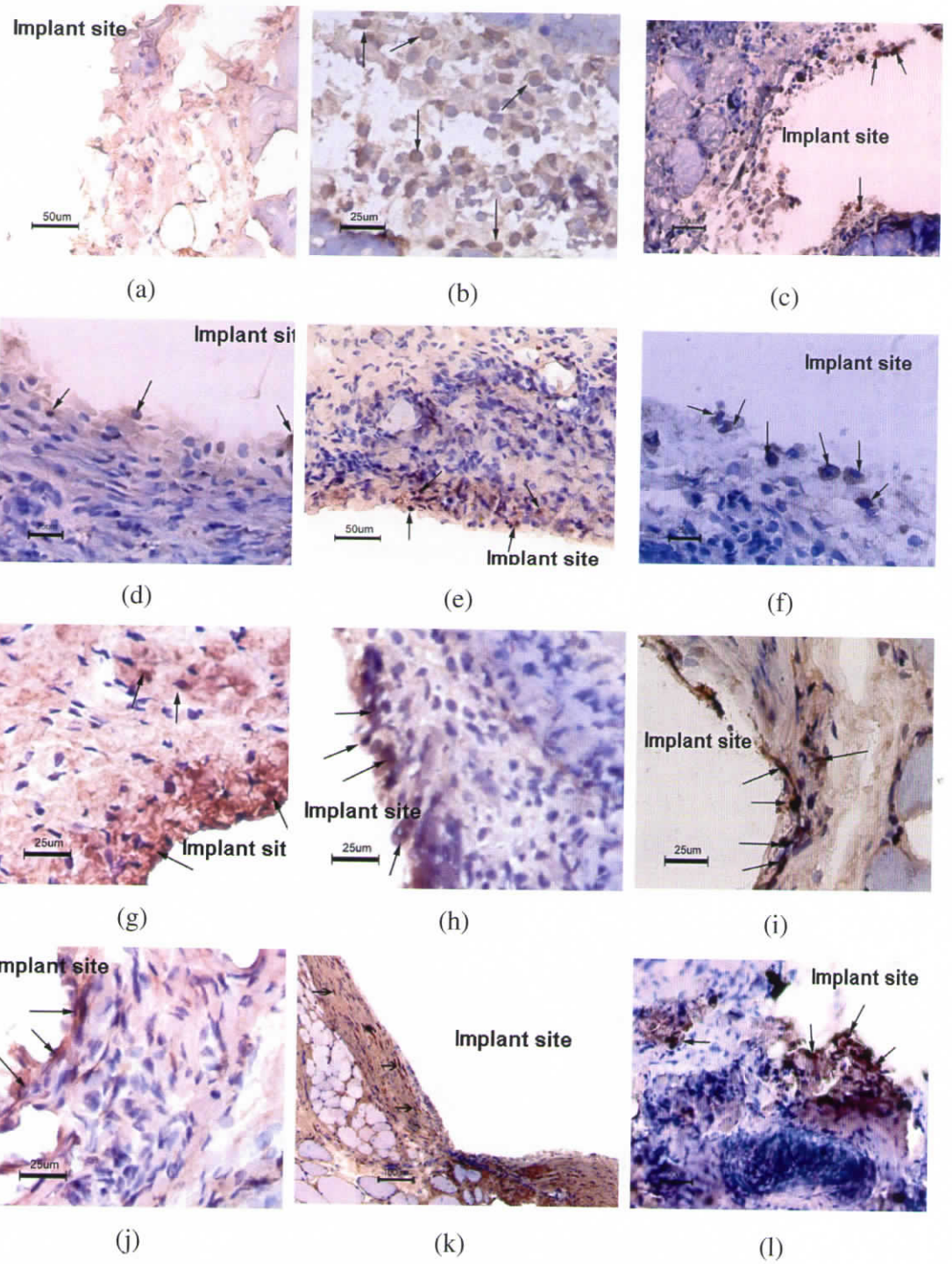

Figure 19 Light micrographs of PEUU adjacent tissue sections immunostained for ED2 at (a) 4 hours, (b) 1, (c) 2, (d) 7, (e) 10, (f) 15, (g) 30, (h) 60, (i) 90, (j) 120, (k) 150, and (l) 180 days post-implantation.
Arrows denote positive staining.

IL-6

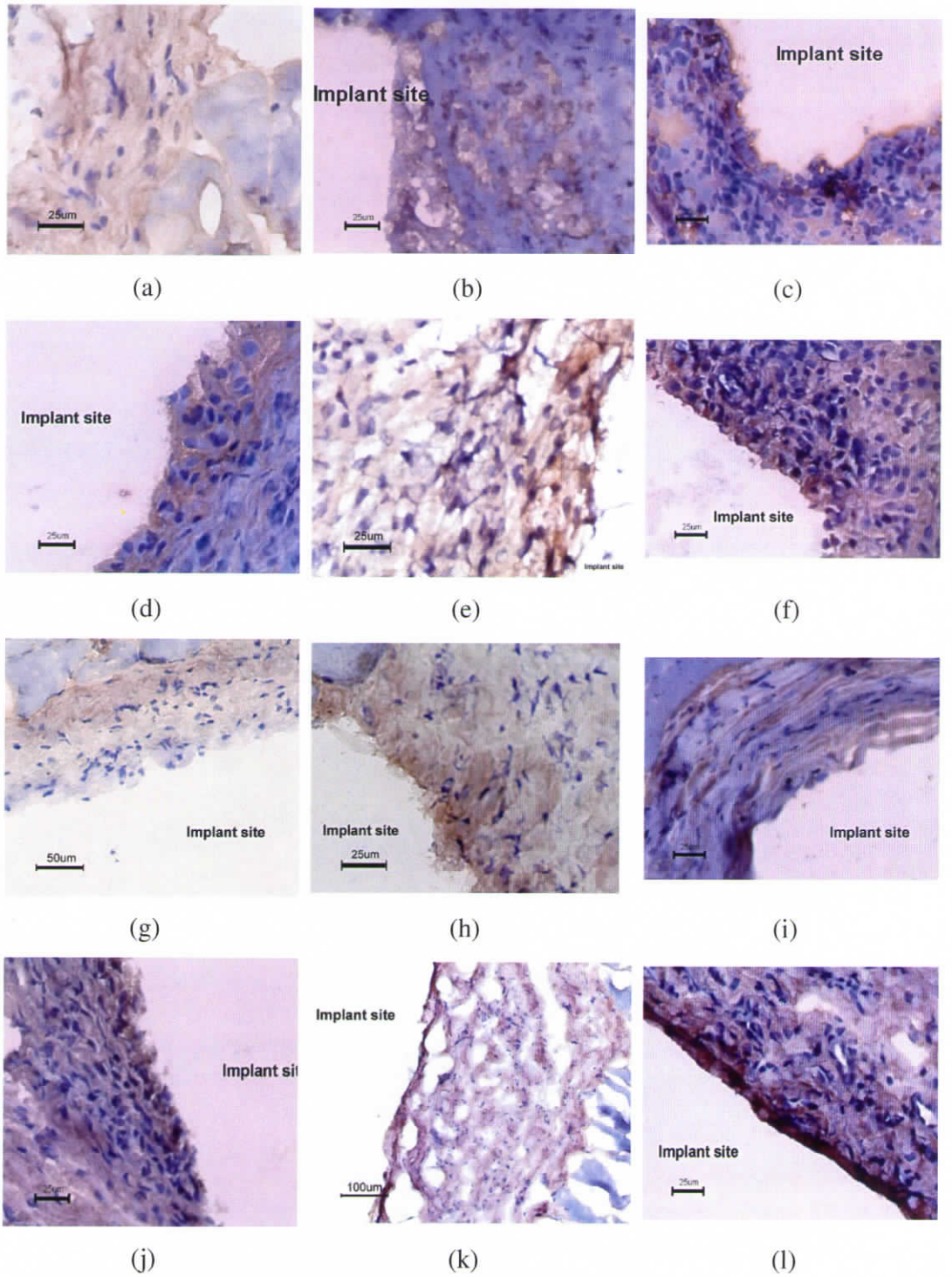

(a) (b) (c)

(d) (e) (f)

(g) (h) (i)

(j) (k) (l)

Figure 20 Light micrographs of PEUU adjacent tissue sections immunostained for IL-6 at (a) 4 hours, (b) 1, (c) 2, (d) 7, (e) 10, (f) 15, (g) 30, (h) 60, (i) 90, (j) 120, (k) 150, and (l) 180 days post-implantation.
Arrows denote positive staining.

IL-1α

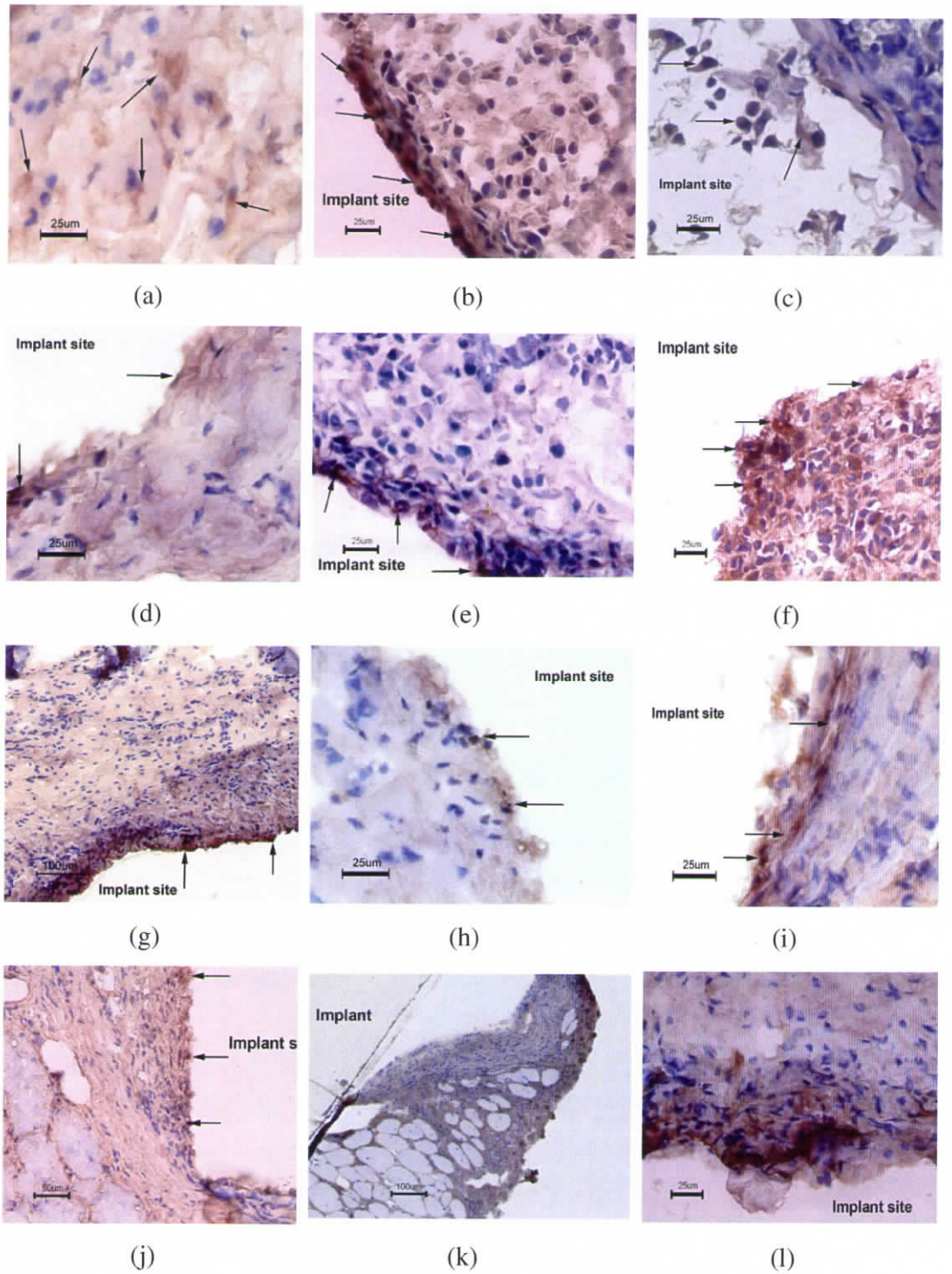

(a) (b) (c)

(d) (e) (f)

(g) (h) (i)

(j) (k) (l)

Figure 21 Light micrographs of PEUU adjacent tissue sections immunostained for IL-1α at (a) 4 hours, (b) 1, (c) 2, (d) 7, (e) 10, (f) 15, (g) 30, (h) 60, (i) 90, (j) 120, (k) 150, and (l) 180 days post-implantation.
Arrows denote positive staining.

IL-1β

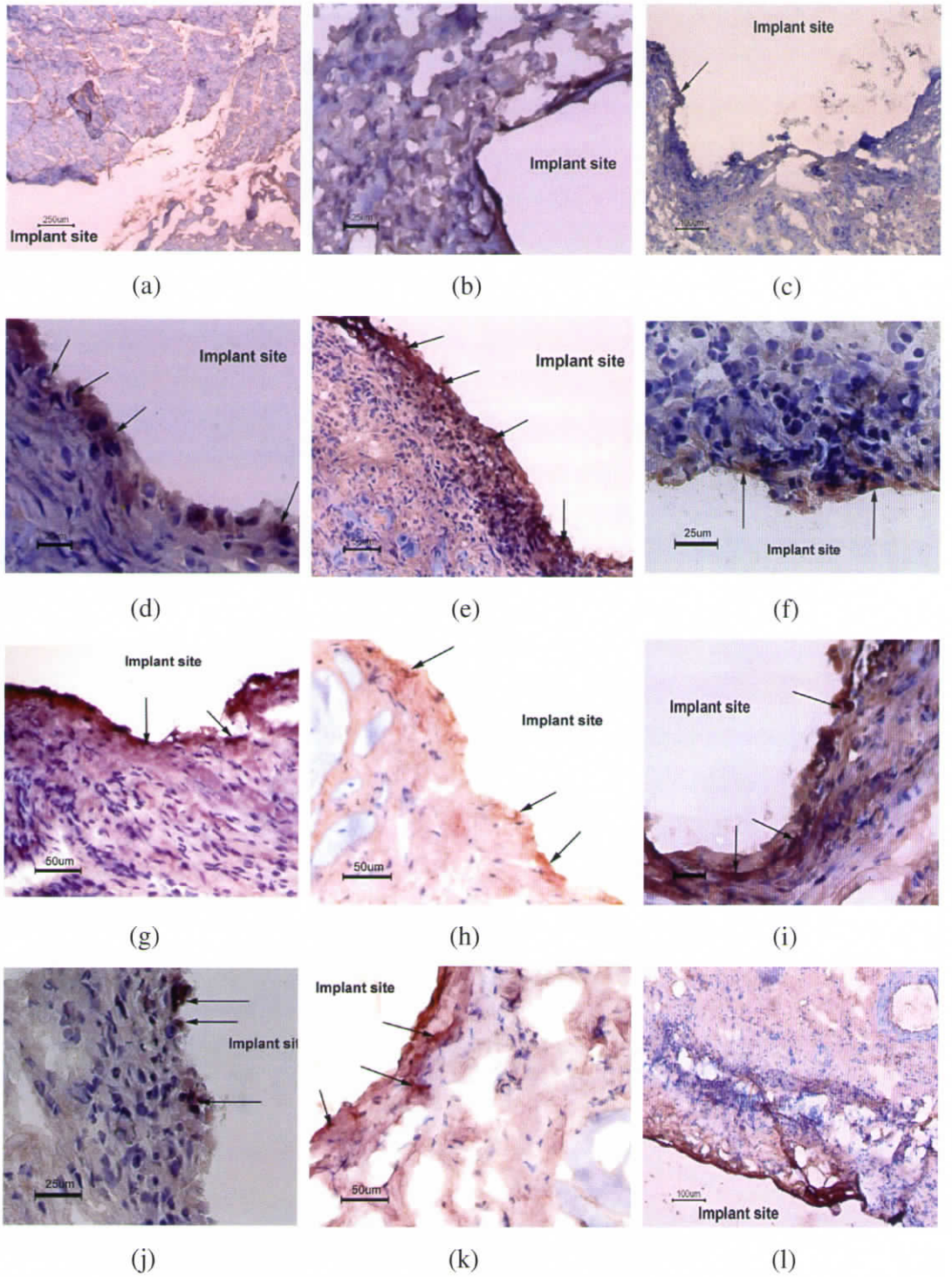

Figure 22 Light micrographs of PEUU adjacent tissue sections immunostained for IL-1β at (a) 4 hours, (b) 1, (c) 2, (d) 7, (e) 10, (f) 15, (g) 30, (h) 60, (i) 90, (j) 120, (k) 150, and (l) 180 days post-implantation.
Arrows denote positive staining.

TNF-α

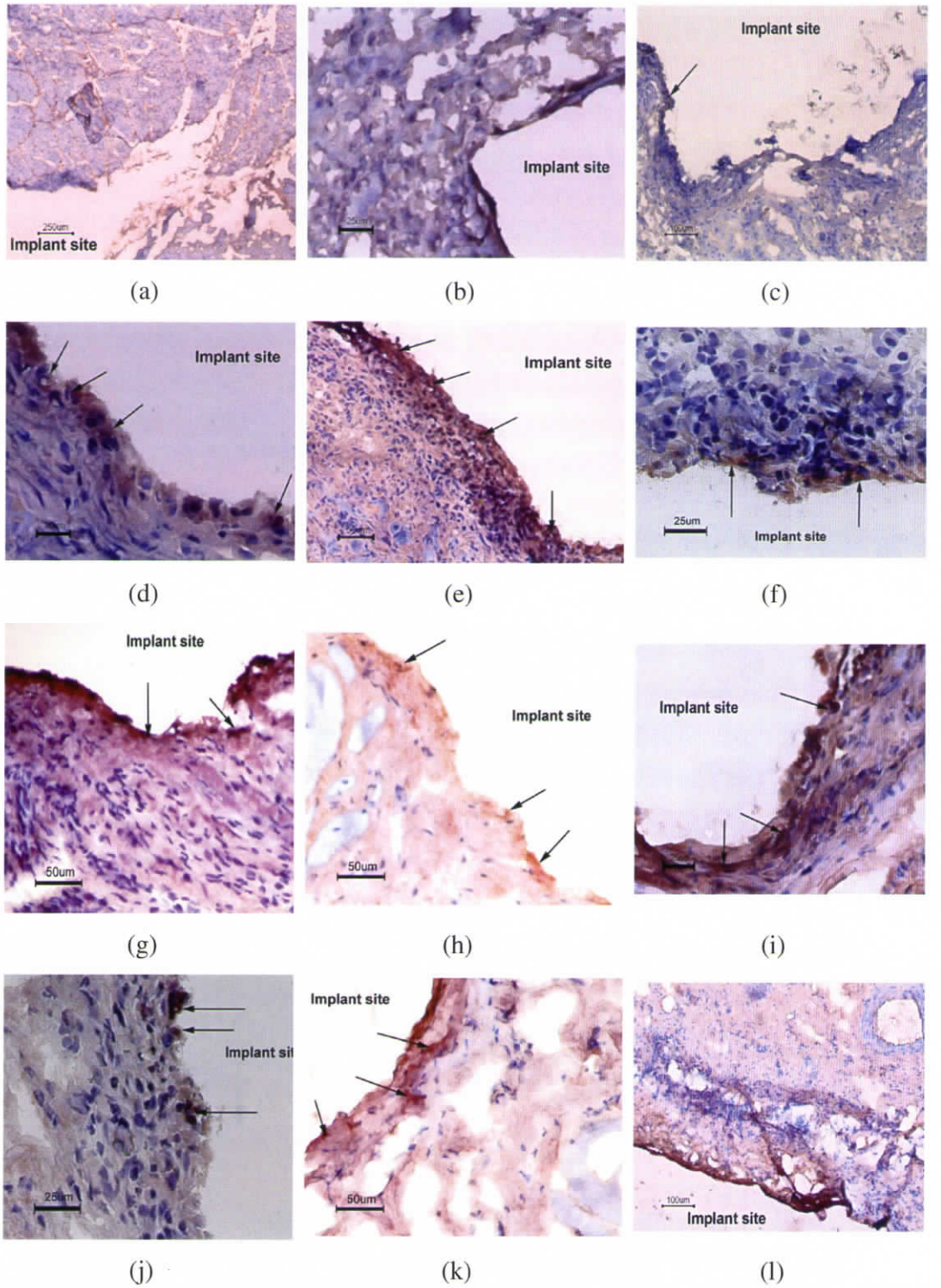

(a) (b) (c)

(d) (e) (f)

(g) (h) (i)

(j) (k) (l)

Figure 23 Light micrographs of PEUU adjacent tissue sections immunostained for TNF-α at (a) 4 hours, (b) 1, (c) 2, (d) 7, (e) 10, (f) 15, (g) 30, (h) 60, (i) 90, (j) 120, (k) 150, and (l) 180 days post-implantation.
Arrows denote positive staining.

IFN-γ

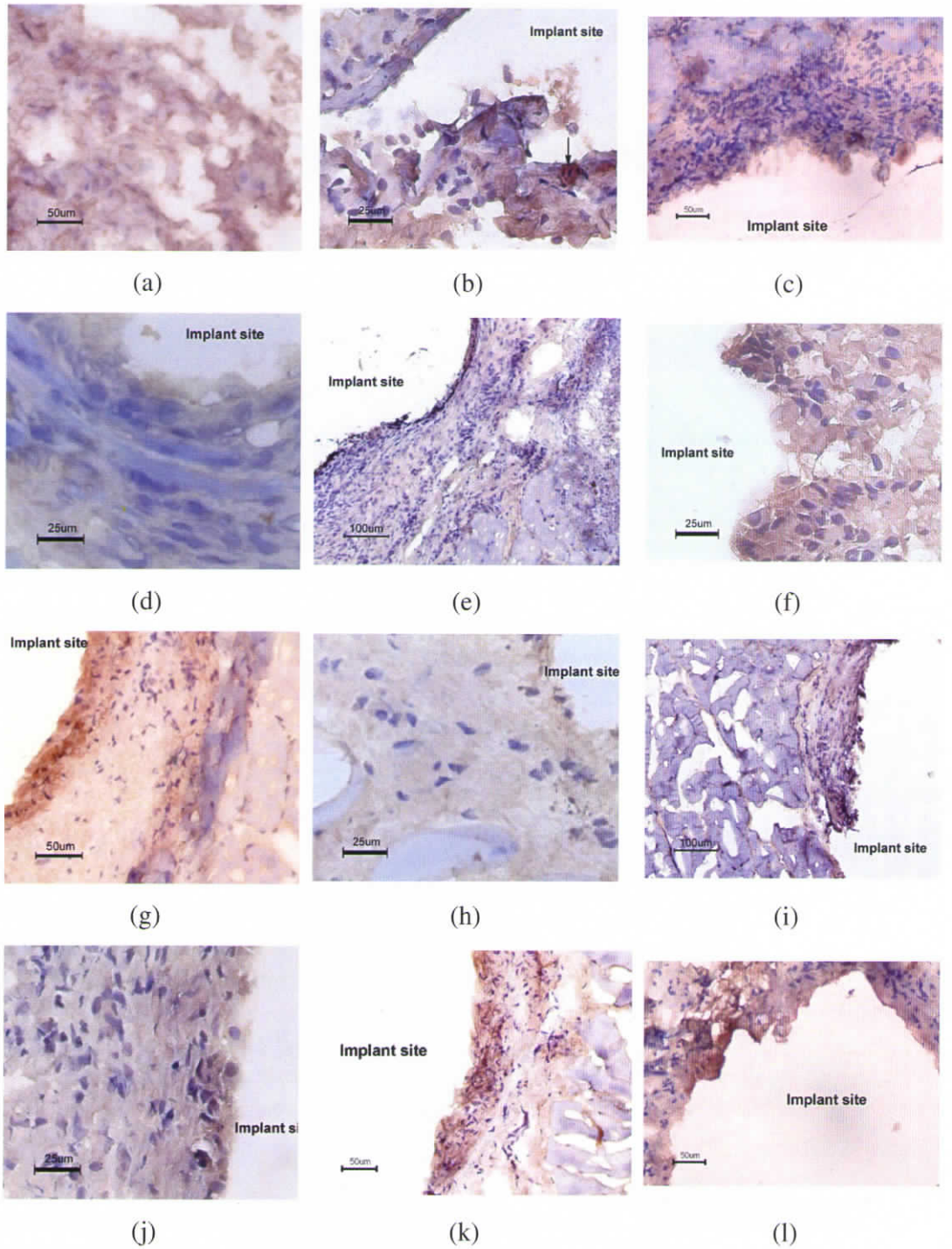

Figure 24 Light micrographs of PEUU adjacent tissue sections immunostained for IFN-γ at (a) 4 hours, (b) 1, (c) 2, (d) 7, (e) 10, (f) 15, (g) 30, (h) 60, (i) 90, (j) 120, (k) 150, and (l) 180 days post-implantation.
Arrows denote positive staining.

CD 4

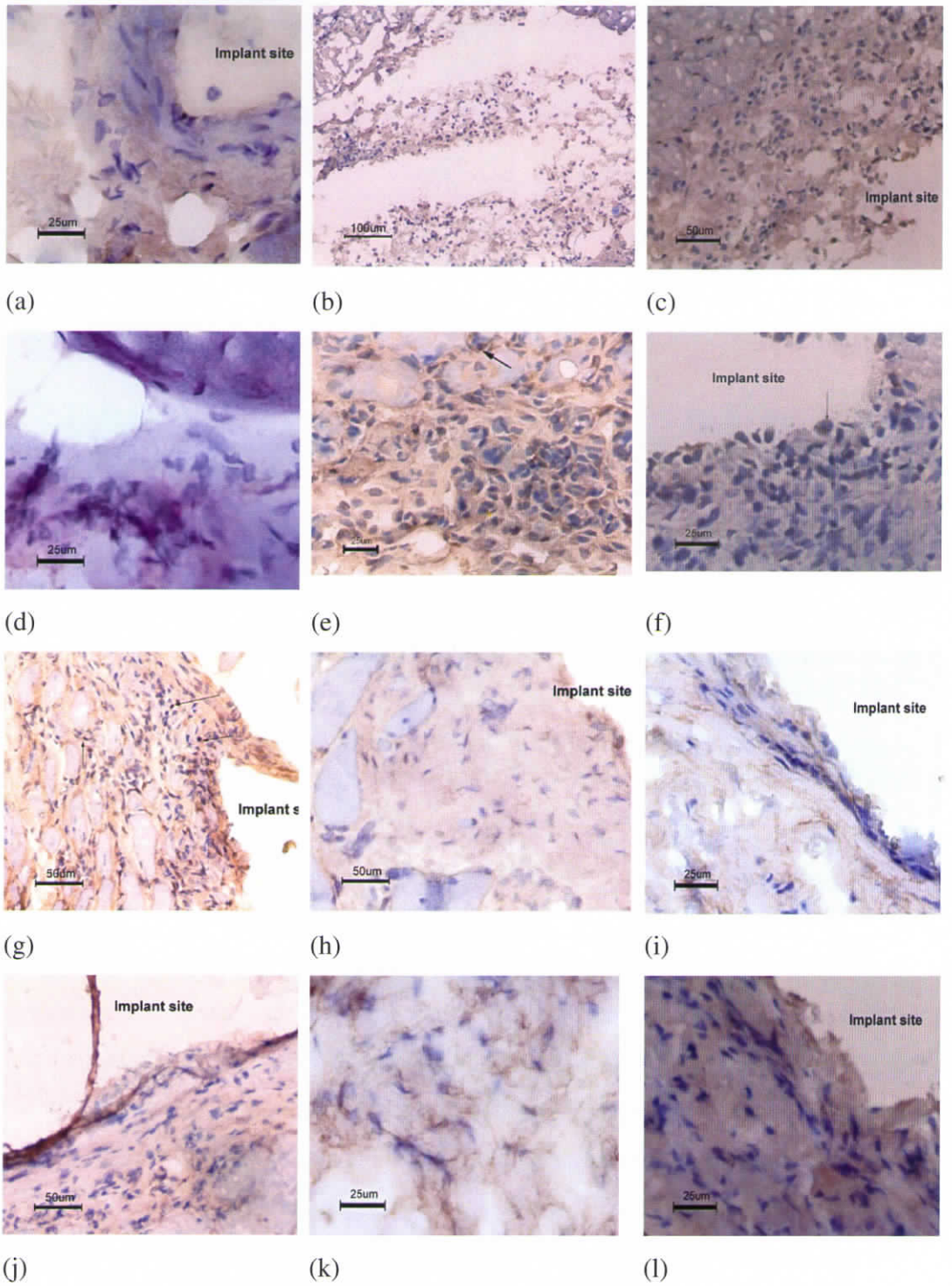

Figure 25 Light micrographs of PEUU adjacent tissue sections immunostained for CD 4 at (a) 4 hours, (b) 1, (c) 2, (d) 7, (e) 10, (f) 15, (g) 30, (h) 60, (i) 90, (j) 120, (k) 150, and (l) 180 days post-implantation.
Arrows denote positive staining.

4.1.7. Protein adsorption

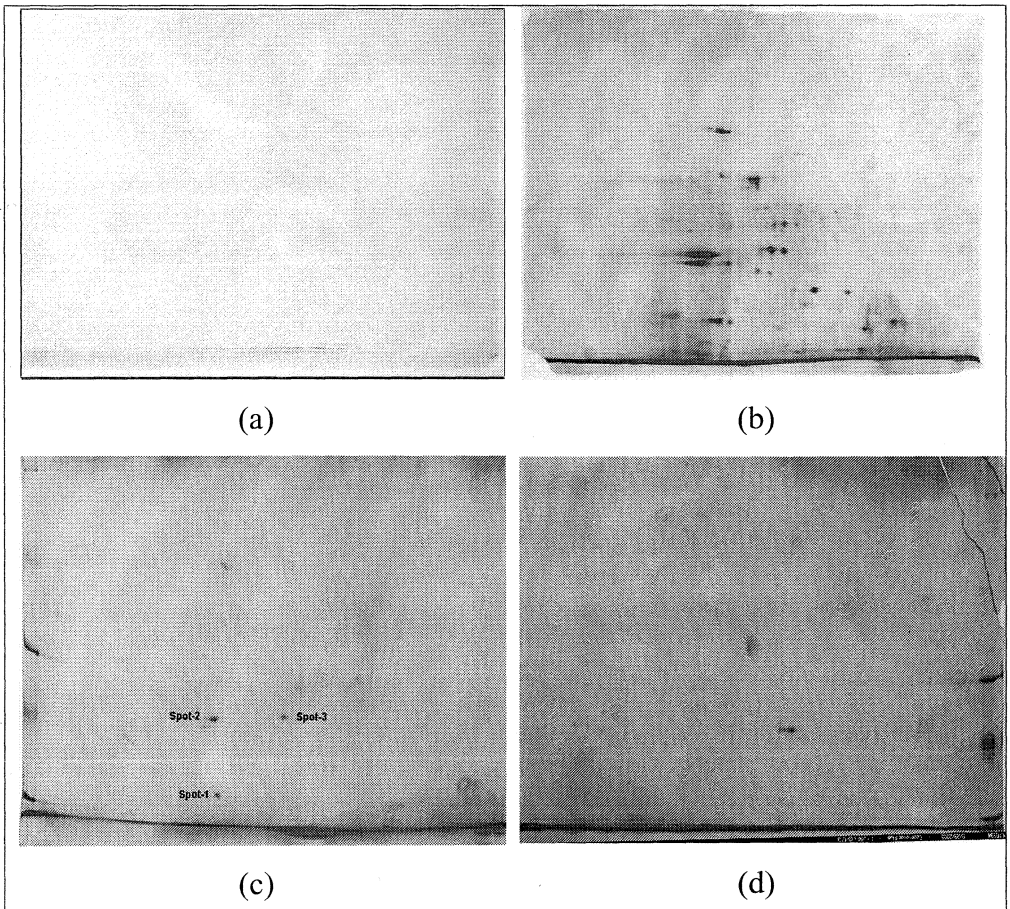

Figure 26 Representative 2D gel images of proteins eluted from (a) PEUU at 1 hour, (b) PEUU at 2 days (before wash), (c) PEUU at 2 days and (d) UHMWPE at 2 days.

Protein adsorption on implanted biomaterials varies depending upon the material surface parameters, the concentration of individual proteins in the complex biological milieu and the affinity of proteins to the surface. Protein adsorption is a dynamic event which varies with time. In this study, protein adsorption onto implanted PEUU and UHMWPE was evaluated at only a single time period that is, two days following implantation. The specific aim was to delineate any difference in the adsorption of proteins on PEUU and the known biocompatible material UHMWPE, from the complex biological tissue. The hypothesis was that the difference in tissue response elicited by PEUU and UHMWPE could be correlated with difference in early protein adsorption.

The proteins eluted at 2 days post-implantation, from PEUU revealed three protein spots (Figure 26 c) while that from UHMWPE contained only one protein spot (Figure 26 d). Since the materials were rinsed prior to elution of proteins for

electrophoresis, loosely adsorbed proteins were removed and only the strongly adsorbed proteins were separated out by electrophoresis. Representative 2D gel of proteins eluted before rinsing from a PEUU sample at two days, showed large number of protein spots (Figure 26 b). This includes both loosely adsorbed proteins as well as cellular proteins from the adhered cells.

Protein adsorption is the early event following implantation of a biomaterial. It starts even after seconds of implantation. A representative PEUU sample at one hour post-implantation did not reveal any strongly adsorbed proteins (Figure 26a). The low concentration of proteins in this study may be below the detection sensitivity of silver stain. Hence the absence of protein spots in the gel could be attributed to the low concentration of strongly adsorbed proteins at one hour post-implantation.

The MALDI-ToF MS analysis performed on the protein spots from the two day samples gave the experimental mass values of peptides. The mass spectra of protein spots are represented in figure given below (Figure 27). The spot obtained for UHMWPE had the same identity as that of spot three from PEUU.

The peptide mass values were submitted in Mass Spectra Database (MSDB) using the Mascot search engine (www.matrixscience.com) for protein identification. Even though the protein scores were low (the hits represented here are selected from the top 3 hits from each database search) they indicate probable proteins adsorbed to PEUU (Table 3). Spots 1 and 2 gave maximum scores for SCO-spondin and alpha-2 macroglobulin respectively. Spot 3 gave 24 score for TNF-stimulated gene-6 protein. The 3 proteins listed here are either secreted proteins or extracellular matrix proteins. Further confirmation of the identity of proteins is suggested by sequencing of these protein spots.

The differential protein adsorption patterns on PEUU and UHMWPE is itself a clear evidence to the difference in the initial molecular events upon implantation of different materials. Thus the present study is a step further towards the understanding of the initial molecular events associated with the biological response to PEUU, related cell adhesion and ensuing cell-mediated degradation of PEUU *in vivo*.

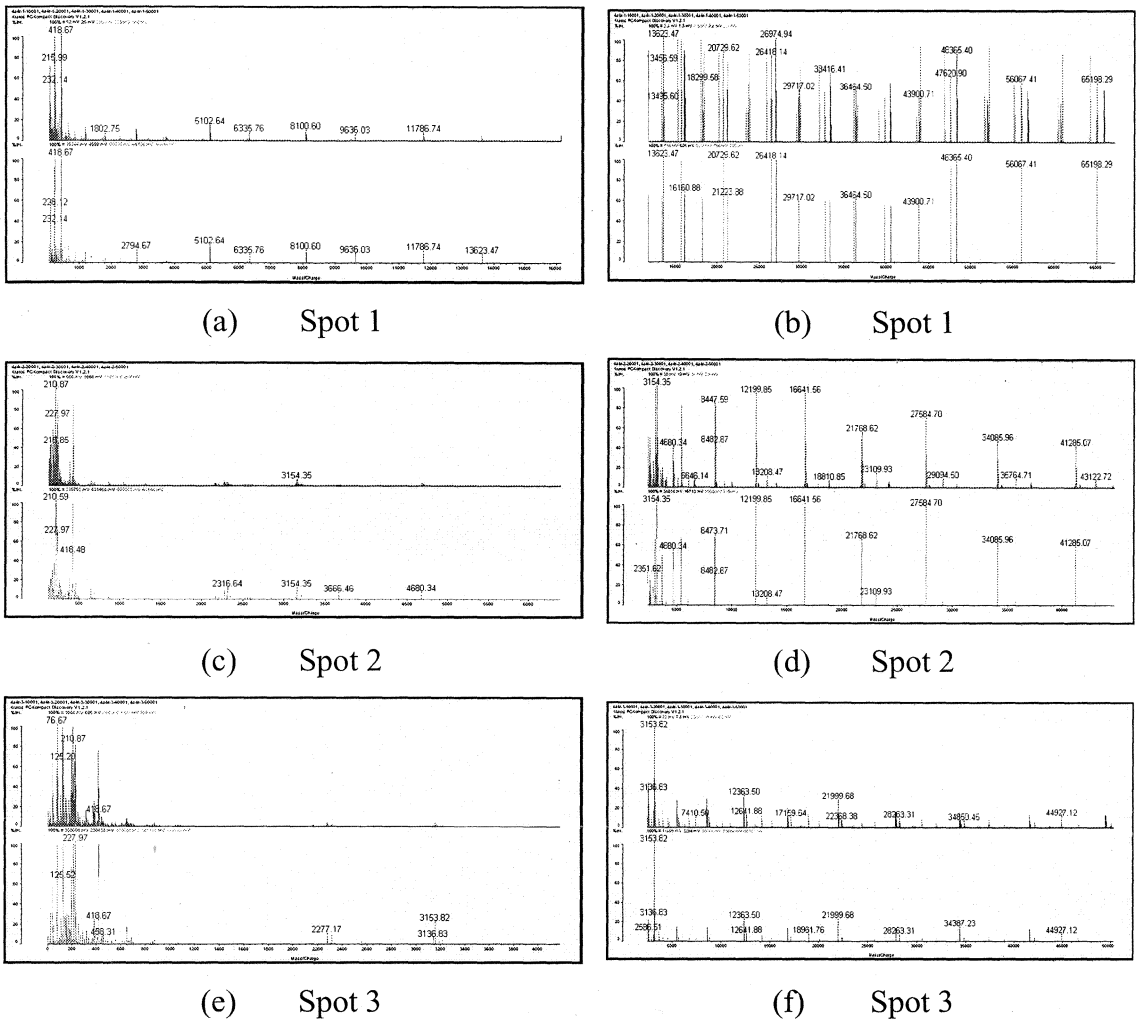

(a) Spot 1 (b) Spot 1

(c) Spot 2 (d) Spot 2

(e) Spot 3 (f) Spot 3

Figure 27 MALDI-ToF mass spectra of peptides; (a) and (b) spot 1; (c) and (d) spot 2; (e) and (f) spot 3.

Table 3 Proteins eluted from explanted materials at 2 days post-implantation identified by MALDI Tof MS followed by database matching.

Accession number (MSDB)	**Score**	**Mass value**	**Description of protein**	**Spot No.**
Q700K0_RAT	44	550275	SCO-spondin.	1
Q78E17_RAT	26	4120	Alpha-2u globulin (Fragment)	2
Q9QZV1 RAT_	24	6471	TNF-stimulated gene-6 protein (Fragment)	3

4.2. PHASE II

4.2.1. Molecular weight analysis of Commercial PUs

The molecular weight analysis of commercial PUs has revealed the molecular weight averages as indicated in Table 4. The in-house synthesized PEUU had polydispersity index and molecular weights close to that of Biospan®. This was expected because of the identical chemistry of these two materials.

Table 4 Molecular weights of polyurethanes

Material	Mn	Mw	Polydispersity
Biospan®	**98894**	**170436**	**1.7**
PurSil™ AL 80 A	**166930**	**204989**	**1.2**
PurSil™AL-20 75A	**206542**	**239055**	**1.1**
Elasthane™	**107250**	**158811**	**1.4**
CarboSil™ 20	**87495**	**142395**	**1.6**
Bionate® 80A	**116338**	**167578**	**1.4**
In-house PEUU	**94882**	**162564**	**1.7**

4.2.2. Effect of cell culture medium on polyurethane surface chemistry

The in-house synthesized PEUU, UHMWPE and the commercial PUs were analyzed for changes in material properties such as wettability and surface molecular rearrangement after incubation in cell culture medium (MEM) for 30 days at 37°C.

4.2.2.1. Contact angle analysis

The water contact angle measurement was made using a standard contact angle analysis system in air surrounding with a water drop. Contact angle values indicate the hydrophobic/hydrophilic nature of the biomaterials. The greater the water contact angle the greater the hydrophobic nature of the material. The water contact angle measurements for the materials are summarized below (Table 5). The images of

the contact angle measurement are provided in Figure 28. A water contact angle of 111.7 ± 3 for UHMWPE showed the hydrophobic nature of the material. PurSil™ AL , PurSil™AL-20 75A, Elasthane™ and CarboSil™ 20 were more hydrophobic than Biospan®, Bionate® 80A and in-house synthesized PEUU.

Table 5 Contact angle values of materials

Material	**Contact angle value**
Biospan®	86.325 ± 3.9
PurSil™ AL 80 A	104.5 ± 3.4
PurSil™AL-20 75A	98.45 ± 3.0
Elasthane™	111.42 ± 2
CarboSil™ 20	108.1 ± 0.7
Bionate® 80A	86.6 ± 3.2
In-house PEUU	81.5 ± 1.7
UHMWPE	111.7 ± 3.4

The comparable water contact angles for Biospan®, Bionate® and in-house synthesized PEUU, 86 ± 4, 86.6 ± 3 and 81.5 ± 2 respectively, denotes comparable surface energy for these materials. Surface energy is an important parameter which determines the pattern of cell adhesion on materials. Hence a similar cell response could be anticipated on the surface of these materials from a surface energy point of view.

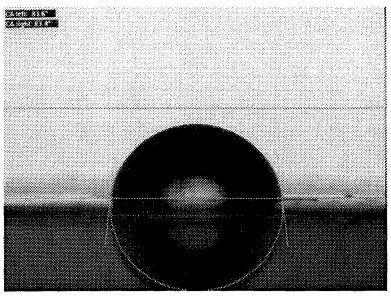

(a)

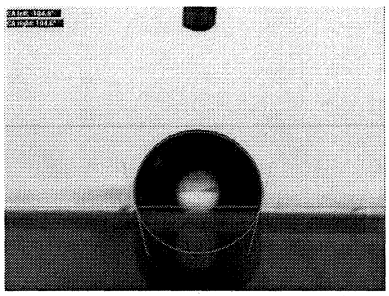

(b)

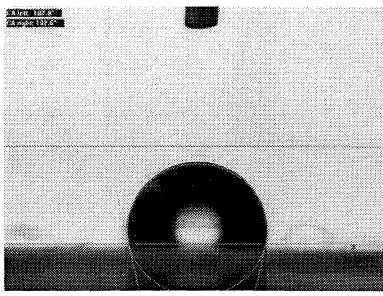

(c)

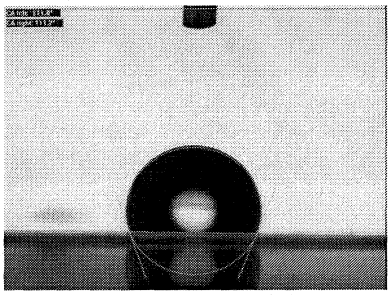

(d)

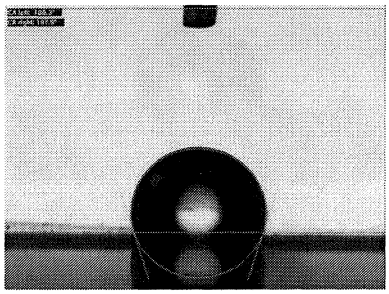

(e)

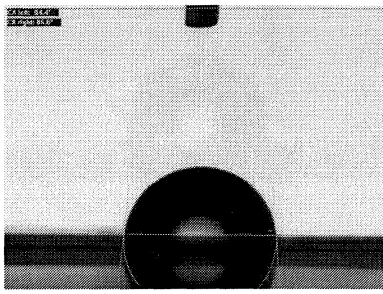

(f)

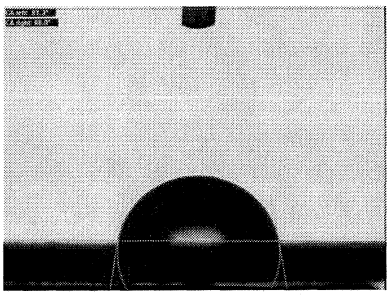

(g)

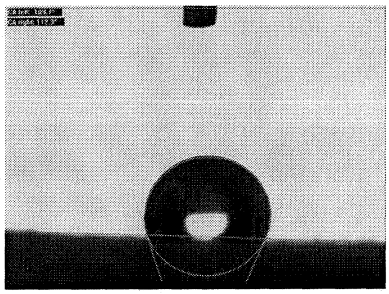

(h)

Figure 28 Images of contact angle measurement of (a) Biospan®, (b) PurSil™ AL 80 A, (c) PurSil™AL-20 75A, (d) Elasthane™, (e) CarboSil™ 20, (f) Bionate® 80A, (g) In-house PEUU, and (h) UHMWPE.

Figure 29 and Figure 30 shows the changes observed in contact angle values after 30 days incubation in MEM. The contact angle values of Biospan®, PurSil™ AL 80 A and PurSil™AL-20 75A increased after incubation in MEM for 30 days whereas for all the other materials the values decreased. The decrease in contact angle indicates a shift to hydrophilic nature. However the changes noted were non-significant ($p<0.05$) for PurSil™ AL 80A and in-house synthesized PEUU.

Table 6 Contact angle values of materials before and after 30 days of incubation in MEM

Material	Contact angle value	
	Before	After
Biospan®	86.325 ± 3.9	88.7 ± 7
PurSil™ AL 80A	104.5 ± 3.4	104.2 ± 2.5
Pursil™AL-20 75A	98.45 ± 3	102.45 ± 4.7
Elasthane™	111.42 ± 2	99.34 ± 3.7
Carbosil™ 20	108.1 ± 0.7	97.14 ± 5
Bionate® 80A	86.6 ± 3.2	83.5 ± 4.6
In-house PEUU	81.5 ± 1.7	80.025 ± 4
UHMWPE	111.7 ± 3.4	96.75 ± 6

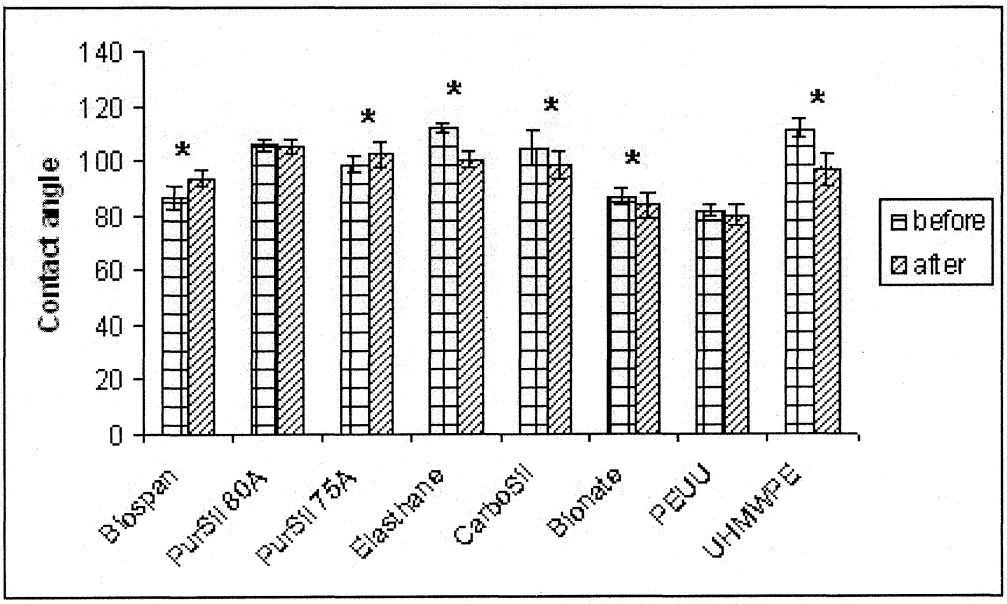

Figure 29 Contact angle values of materials before and after incubation in MEM for 30 days.
$P<0.05$.

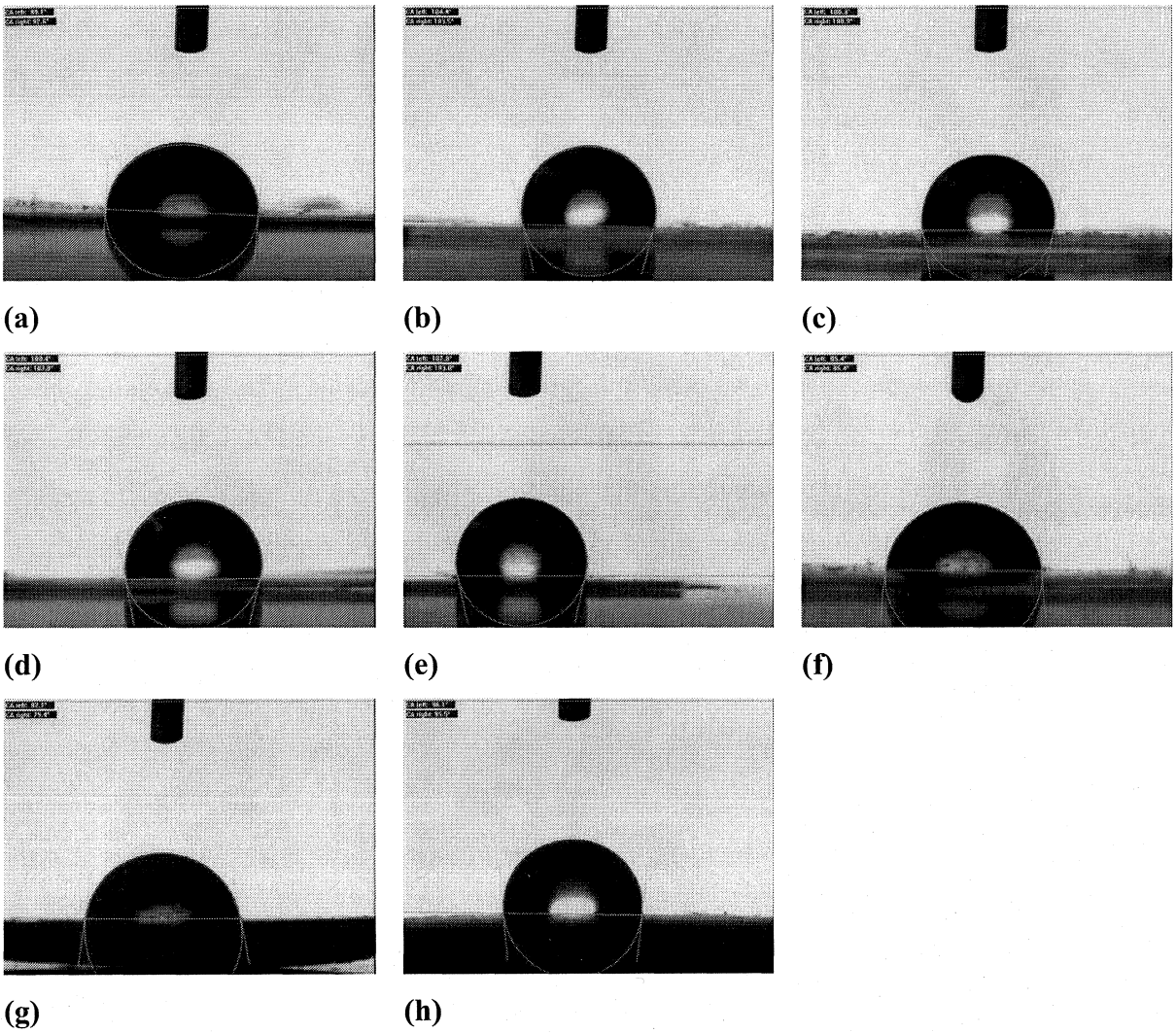

Figure 30 Images of contact angle measurement of (a) Biospan®, (b) PurSil™ AL 80 A, (c) PurSil™AL-20 75A, (d) Elasthane™, (e) CarboSil™ 20, (f) Bionate® 80A, (g) In-house PEUU, and (h) UHMWPE after 30 days of incubation in MEM.

4.2.2.2. ATR-FTIR analysis

The ATR-FTIR analysis of in-house synthesized PEUU, commercial PUs and UHMWPE before and after incubation in MEM for 30 days was carried out to evaluate any change in the functional groups present on the surface.

Biospan® did not exhibit any change in the peaks (Figure 31). The minor peak at 3319.9 cm^{-1} indicates hydrogen bonded amine, which remained intact at 3319.3 cm^{-1}. The 1730.5 cm^{-1} peak, free urethane carbonyl has shifted to 1729.4 cm^{-1}. Hydrogen bonded hard segment urea carbonyl at 1635.4 cm^{-1} remained unchanged. The 1365.5 cm^{-1}, α-methylene ether wag, has shifted to 1367.2 cm^{-1}. These minor shifts did not indicate surface changes. The 1101 cm^{-1} peak due to the soft segment ether stretch did

not change after 30 days of incubation in MEM. The aromatic C-H bend at 770.2 cm^{-1} also did not change.

The ATR-FTIR spectrum (Figure 32) of PurSil™ AL 80A showed the silicone peak C-Si at 797.2 cm^{-1}. Urethane amide at 1528.2 cm^{-1} has shifted to 1525.7 cm^{-1}. The 1366.1 cm^{-1}, α-methylene ether wag has shifted to 1365.8 cm^{-1}. The C-H in $SiCH_3$ at 1255.9 cm^{-1} has shifted to 1256.4 cm^{-1}. The 1229.6 cm^{-1} due to the amide III band remained intact. The minor shifts do not represent any surface degradation since the relative peak intensities remain unchanged. However it could be an indication of a minor surface change on exposure to biologic milieu composed of proteins and other molecules in the medium. Whether this has got any correlation with the adhesion of cells has to be probed further. The Si-C stretch observed at 797.2 cm^{-1} remained unchanged.

The spectrum (Figure 33) shows the peaks obtained for Pursil™ AL-20 75A before and after incubation in MEM. The peak at 797.1 cm^{-1} corresponding to Si-C stretch remained intact after 30 days of incubation in MEM. The 1366.1 cm^{-1}, α-methylene ether wag has shifted to 1366.48 cm^{-1}. The C-H in $SiCH_3$ at 1256.1 cm^{-1} remained intact. The 1229.6 cm^{-1} due to the amide III band remained intact.

The ATR-FTIR spectral analysis of Elasthane™ showed no significant change in peak intensities by the different functional groups (Figure 34). The hydroxyl stretching, ν (O-H) observed at 3302.5 cm^{-1} remained intact. The 2917.3 cm^{-1} and 2849.8 cm^{-1} peaks due to the antisymmetric and symmetric stretching modes of methylene groups respectively, also remained intact. The peak at 1074.6 cm^{-1} due to Si-O-Si stretch remained intact. The short aliphatic ether stretch at 1104.4 cm^{-1} also remained intact. The 1366.5 cm^{-1}, α-methylene ether wag has shifted to 1366.9 cm^{-1}. The aromatic C-H bend at 769.9 cm^{-1} remained unchanged.

Carbosil™ 20 did not show any change in the ATR-FTIR spectrum before and after incubation in MEM (Figure 35). The 1739 cm^{-1} peak of carbonyl group remained unchanged. The aromatic C-H stretch at 1596.1 cm^{-1}, the Si-O-Si stretch peaks at 1069.4 cm^{-1} and 1016.8 cm^{-1} and the aromatic C-H bend at 770.9 cm^{-1} remained intact. The hydrogen bonded carbonyl stretching at 1700.6 cm^{-1} did not change after incubation in MEM.

Characteristic ATR-FTIR spectra of Bionate® 80A, before and after incubation in MEM for 30 days were compared (Figure 36). The hydrogen bonded carbonyl stretching at 1700.9 cm^{-1} and the ether peak at 1110 cm^{-1} were found to be unchanged after incubation.

The FTIR-spectra of PEUU before and after incubation in MEM is shown in Figure 37. The peak located at 2851.7 cm^{-1} due to the symmetric stretching mode vibration of methylene group was found at 2850.5 cm^{-1}. The C=O urea peak found at 1642.4 cm^{-1} remained at 1641.9 cm^{-1}. The ether, C-O-C peak was observed at 1102.9 cm^{-1} has shifted to 1101.4 cm^{-1}. Inspite of these minor shifts the major peaks due to the various functional groups remained more or less intact. The peaks corresponding to the functional groups in UHMWPE also remained more or less the same before and after incubation in MEM for 30 days (Figure 38).

The results of ATR-FTIR analysis have further confirmed that the changes in material surface chemistry were negligible in the absence of cells. Cell culture medium alone was unable to induce any significant change in the surface chemistry. Even though contact angle measurement indicated surface changes, it could be assessed that no significant change in the arrangement of surface chemical groups had occurred during incubation in cell culture medium.

Previous studies have focused on the analysis of chemical changes on PUs *in vitro* by treating with oxidative and hydrolytic environments *in vitro*. However, the harsh conditions employed in such experiments often represented accelerated conditions which were much different from the actual *in vivo* conditions. But in this study the use of cell culture medium for analyzing surface changes mimics a condition which is more biologically relevant.

The ATR-FTIR spectra obtained for all the PUs did not show any significant difference in intensities. However minor shifts were observed in some of the peaks. This did not reflect any surface degradation. Loss of soft segment was observed in an *in vitro* study where polyether and polycarbonate urethanes were incubated in cholesterol esterase solution for 36 days, in comparison to incubation in phosphate buffer control (Christenson EM *et al* 2006). Christenson *et al* has in fact used an enzyme concentration much above physiological range in order to accelerate

degradation. In the present study the use of cell culture medium was adopted to study the *in vitro* surface degradation. Here the absence of active enzymes released by cells was a notable feature. This denotes the fact that the phenomenon of surface degradation was not evidenced in the absence of cellular activity.

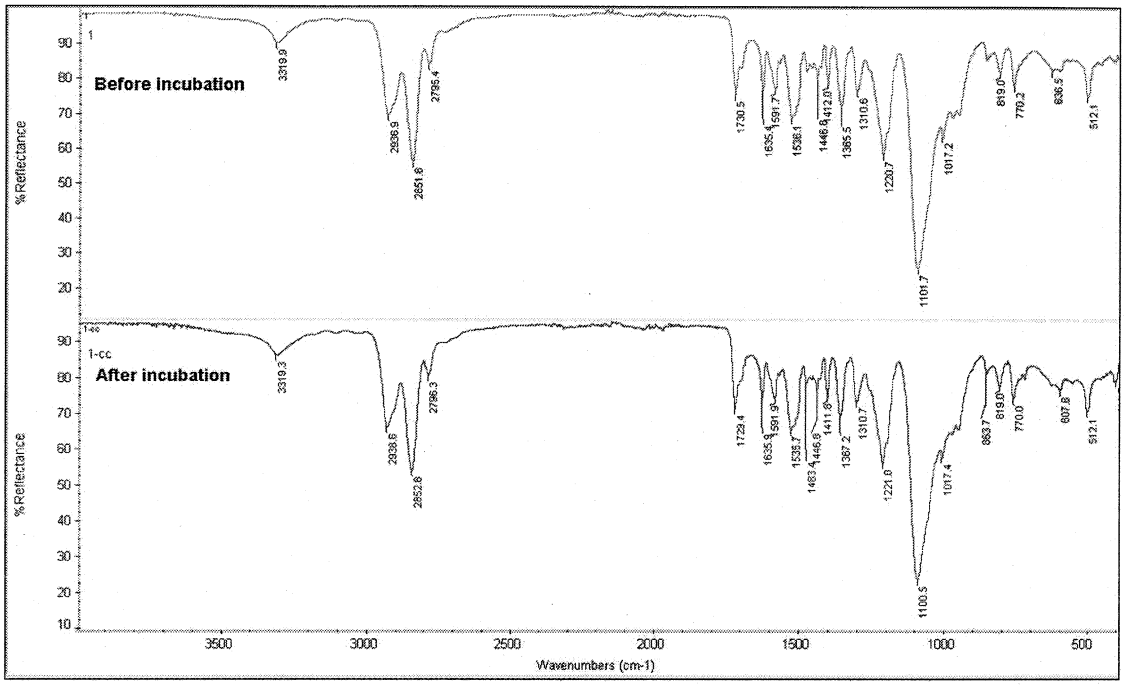

Figure 31 ATR-FTIR spectra of Biospan® before and after incubation in MEM for 30 days

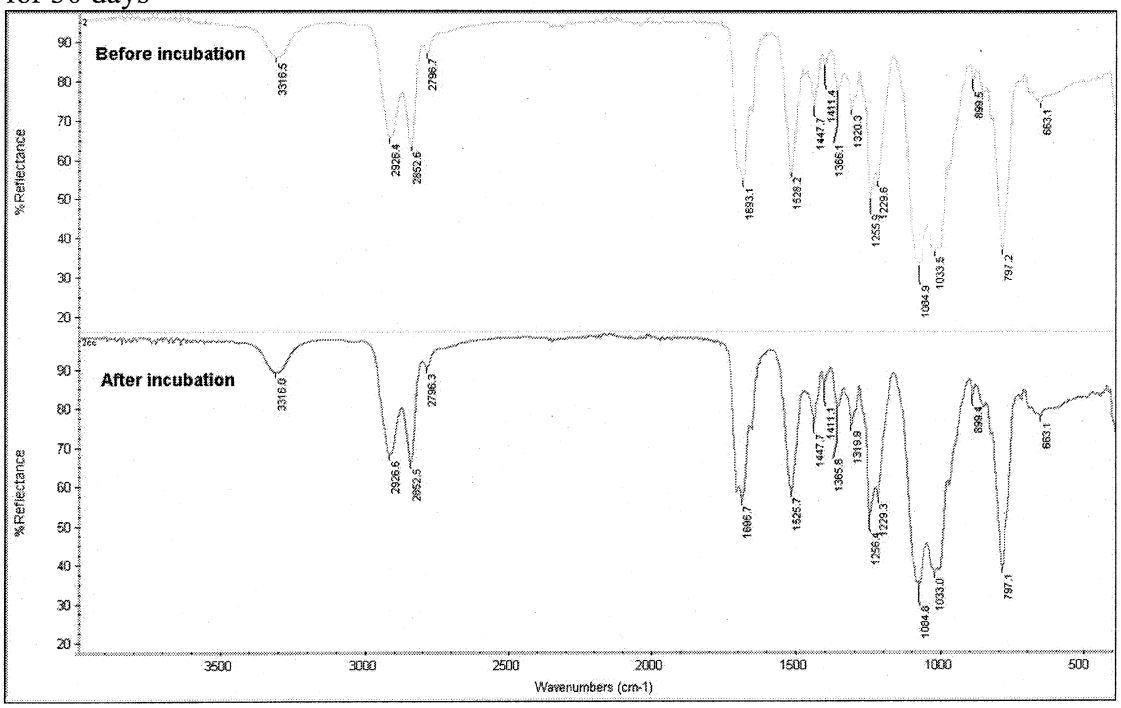

Figure 32 ATR-FTIR spectra of PurSil™ AL 80A before and after incubation in MEM for 30 days.

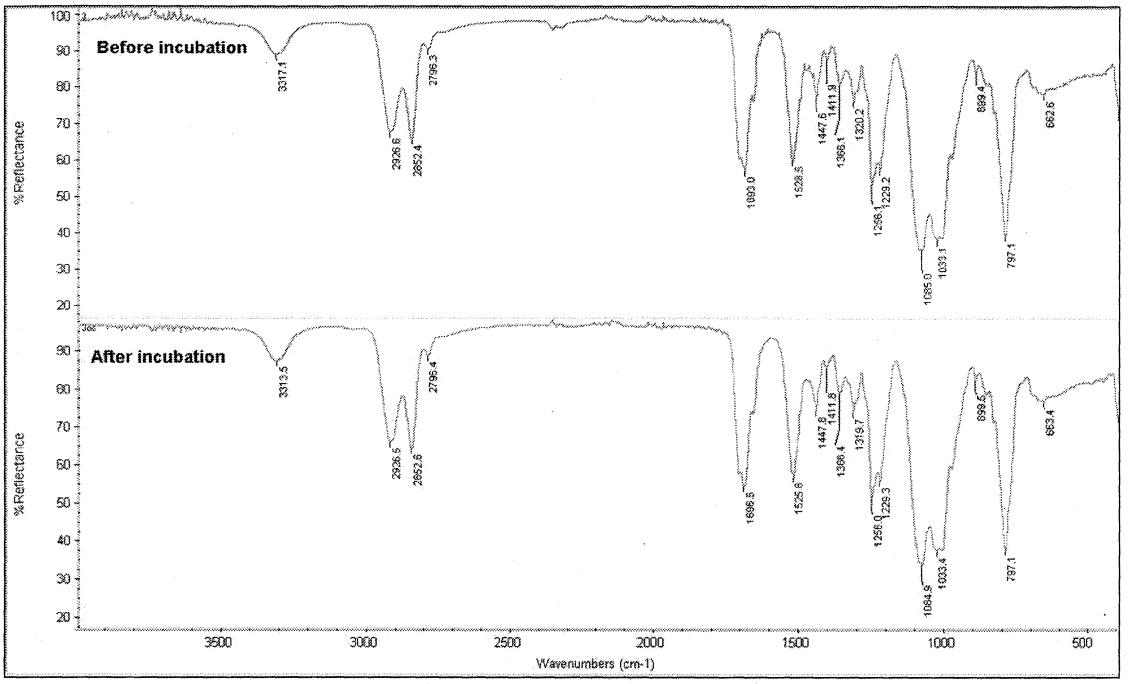

Figure 33 ATR-FTIR spectra of Pursil™ AL-20 75A before and after incubation in MEM for 30 days.

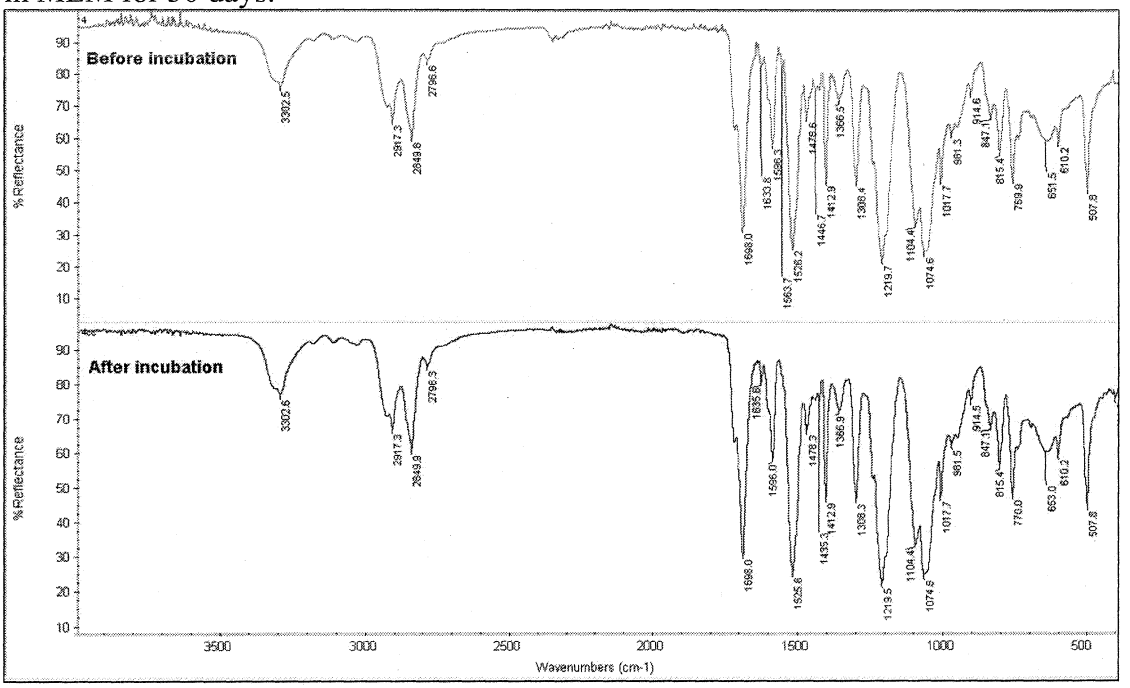

Figure 34 ATR-FTIR spectra of Elasthane™ before and after incubation in MEM for 30 days.

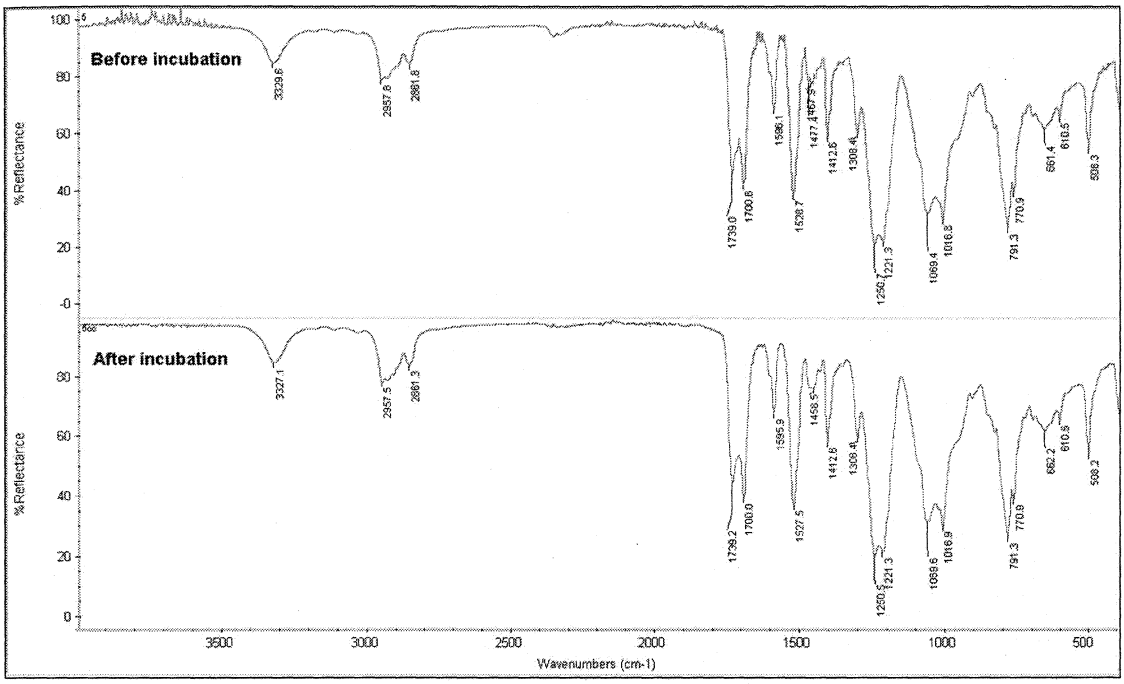

Figure 35 ATR-FTIR spectra of Carbosil™ 20 before and after incubation in MEM for 30 days.

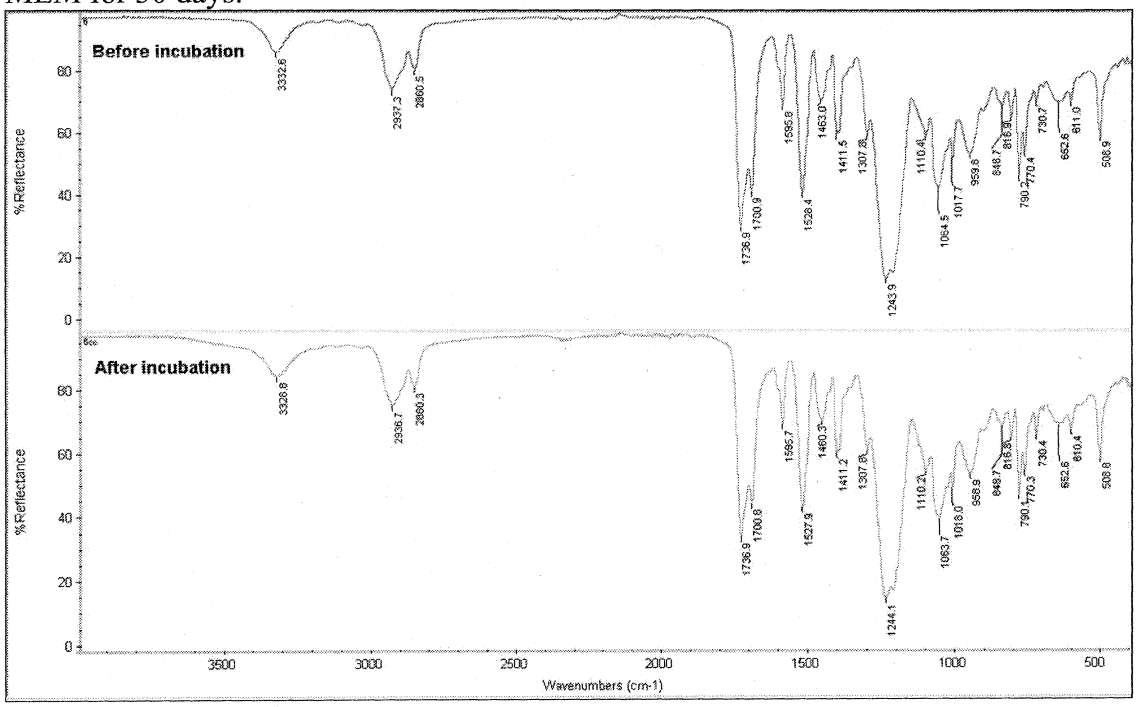

Figure 36 ATR-FTIR spectra of Bionate® 80A before and after incubation in MEM for 30 days.

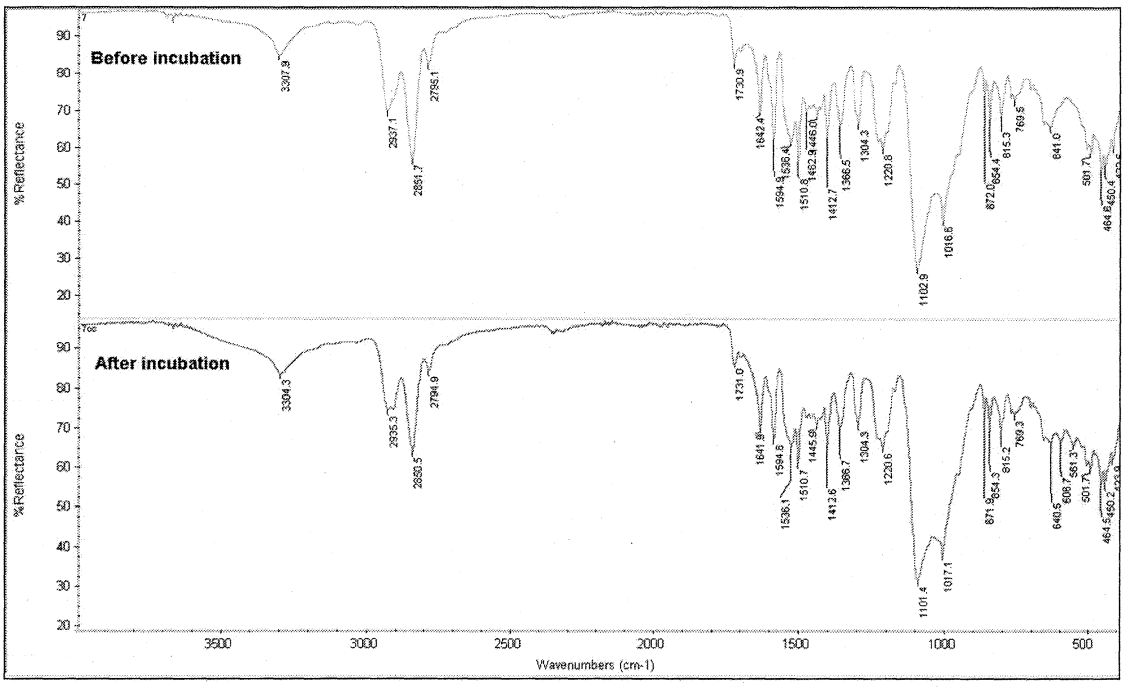

Figure 37 ATR-FTIR spectra of in-house synthesized PEUU before and after incubation in MEM for 30 days

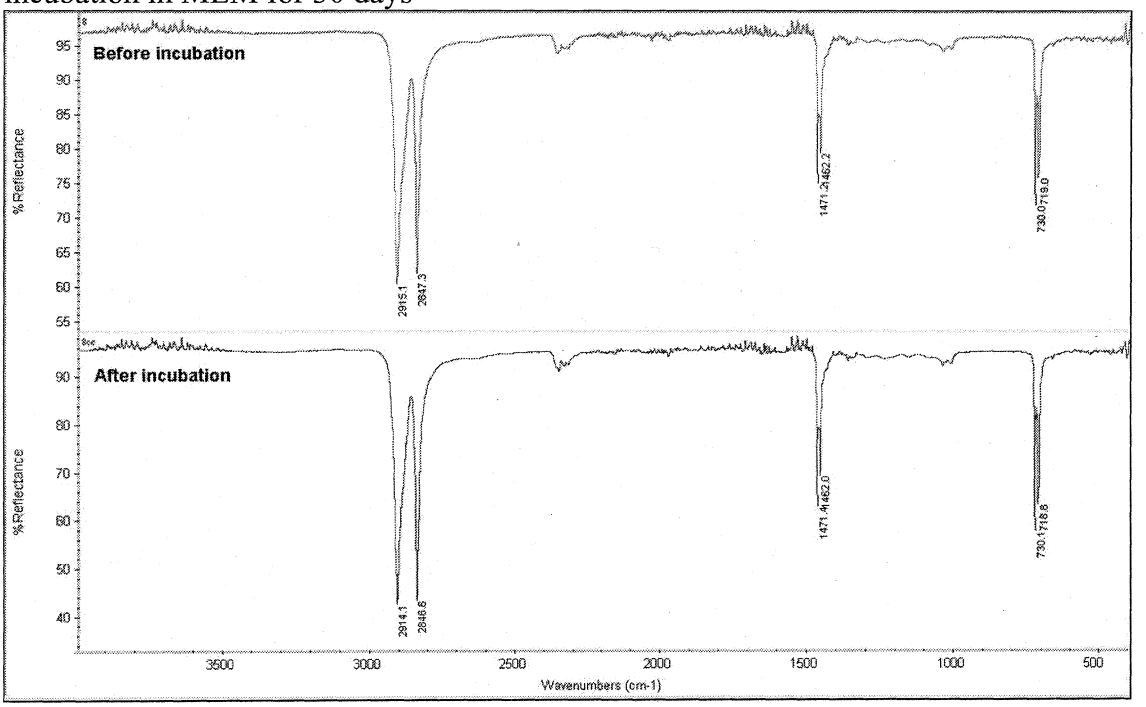

Figure 38 ATR-FTIR spectra of UHMWPE before and after incubation in MEM for 30 days.

4.2.3. Analysis of cell adhesion

Macrophage adhesion on biomaterials is an important event which decides the response elicited towards the biomaterials. Hence the study of macrophage adhesion assumes great importance. It was difficult to view the adherent cells on in-house synthesized PEUU under phase contrast microscope, because of the relative thickness and opaqueness of the material. Cell adhesion on all the commercial PUs was analysed in comparison to that of control, glass coverslip by phase contrast microscopy. Whereas in the case of in-house synthesized PEUU the analysis was performed by ESEM. For comparison Biospan® and control glass coverslip were also examined under ESEM.

4.2.3.1. Analysis of macrophage adhesion on material surfaces by phase contrast microscopy

Phase contrast microscopy was used to assess the morphological changes of cells adherent on PUs over time. The morphology of RAW 264.7 macrophages was similar on commercial PUs and the control, glass coverslip surfaces at four hours after seeding (Figure 39).

After 24 hours of seeding, the cell morphology has changed. On Elasthane™, (Figure 40 d) the cells appeared to be rounded, whereas in the case of other materials including glass coverslip the cells has started extending outgrowths in the form of filopodia. At 48 hours after seeding the cytoplasmic extensions of macrophages has increased on all materials except Elasthane™ (Figure 41 d). Elasthane™, did not contain any PDMS. Also this material did not contain urea linkages, since the chain extender used was butane diol.

The cytoplasmic extensions were prominent at 72 hours after seeding, especially on PurSil™ -80A (Figure 42 b), PurSil™ -75A (Figure 42 c) and CarboSil™ 20 (Figure 42 e). By 72 hours cells grown on Elasthane™ have also started putting forth cytoplasmic extensions (Figure 42 d).

(a)

(b)

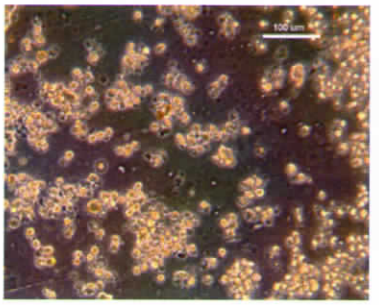

(c)

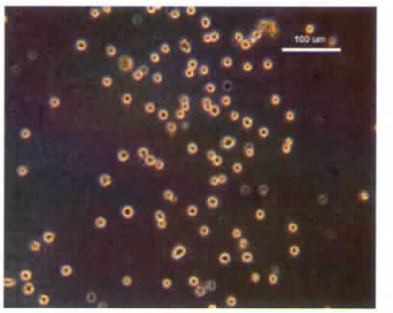

(d)

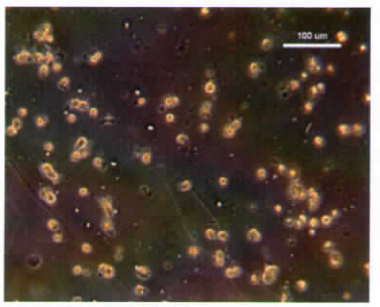

(e)

(f)

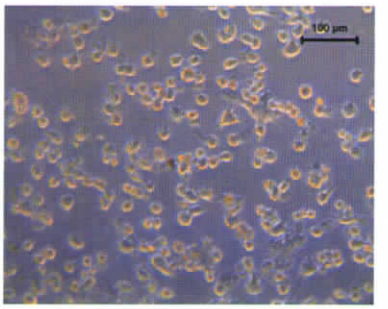

(g)

Figure 39 Phase contrast micrographs of RAW 264.7 cells seeded on (a) Biospan®, (b) PurSil™ -80A, (c) PurSil™ -75A, (d) Elasthane™, (e) CarboSil™ 20, (f) Bionate® 80A, and (g) glass coverslip following 4 hours of culture.

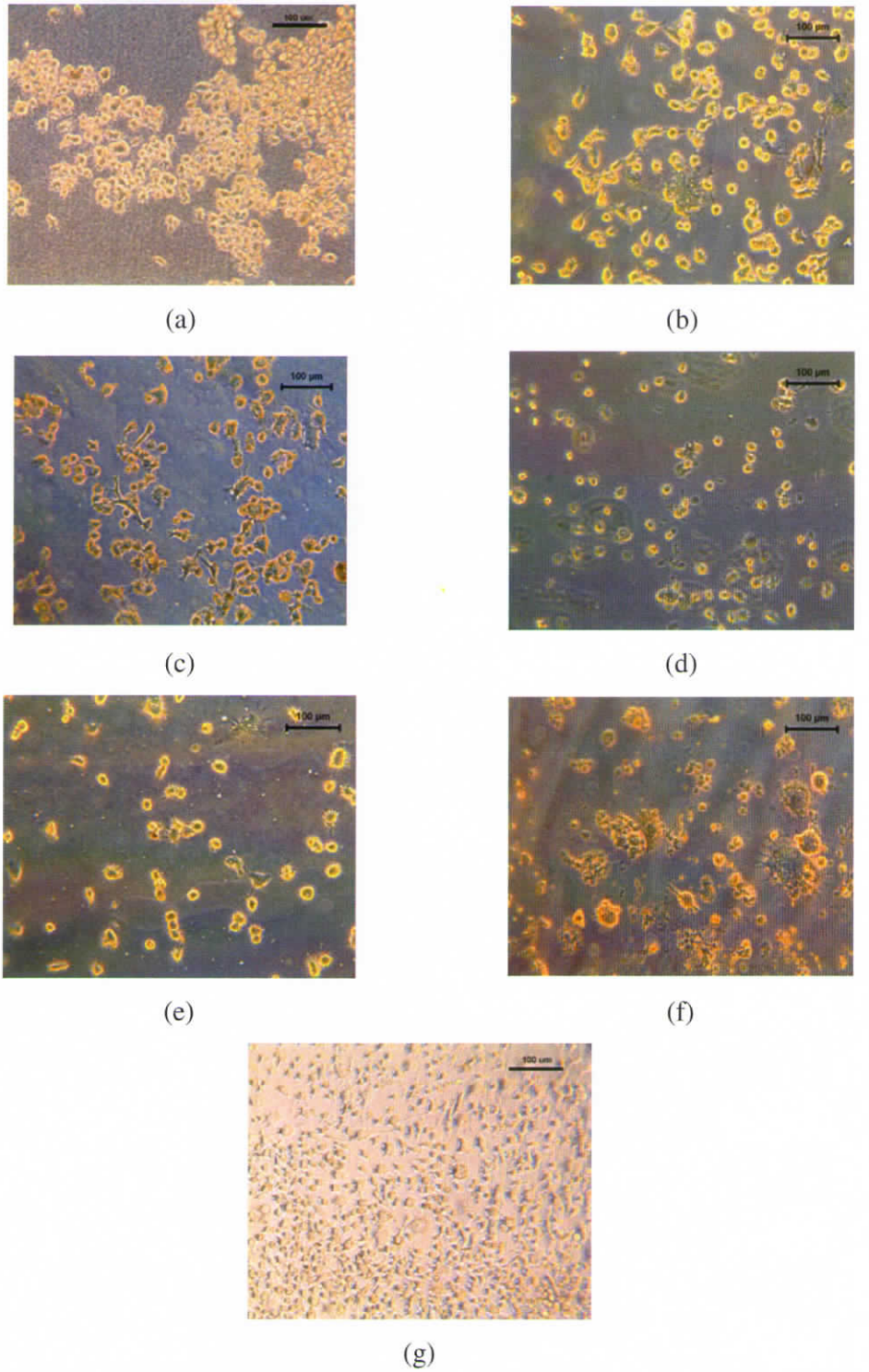

Figure 40 Phase contrast micrographs of RAW 264.7 cells seeded on (a) Biospan®, (b) PurSil™ -80A, (c) PurSil™ -75A, (d) Elasthane™, (e) CarboSil™ 20, (f) Bionate® 80A, and (g) glass coverslip following 24 hours of culture.

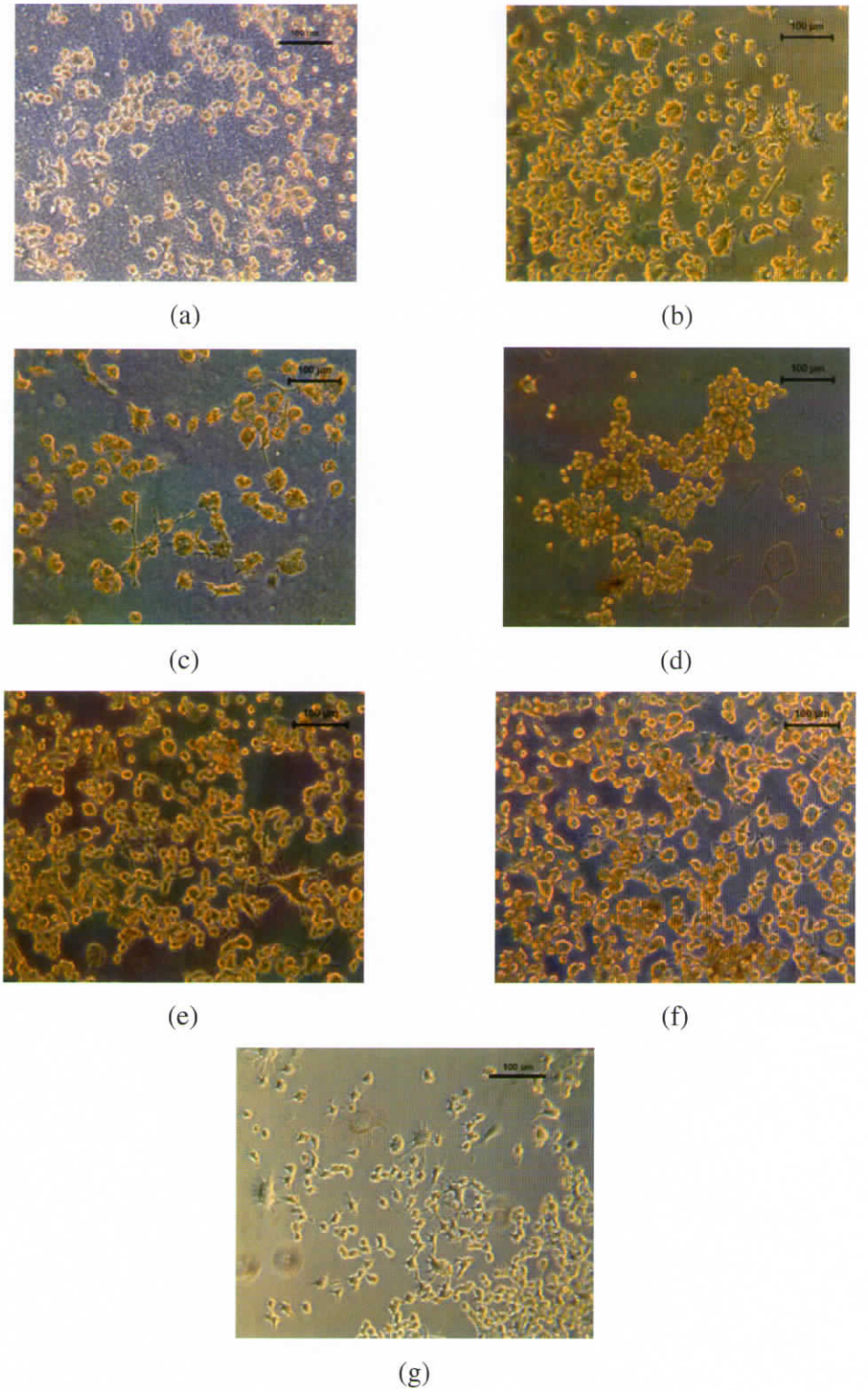

Figure 41 Phase contrast micrographs of RAW 264.7 cells seeded on (a) Biospan®, (b) PurSil™ -80A, (c) PurSil™ -75A, (d) Elasthane™, (e) CarboSil™ 20, (f) Bionate® 80A, and (g) glass coverslip following 48 hours of culture.

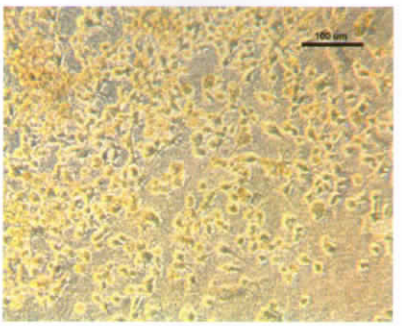

(a)

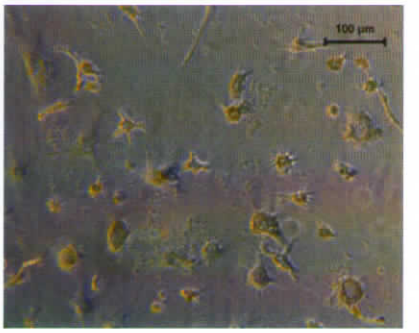

(b)

(c)

(d)

(e)

(f)

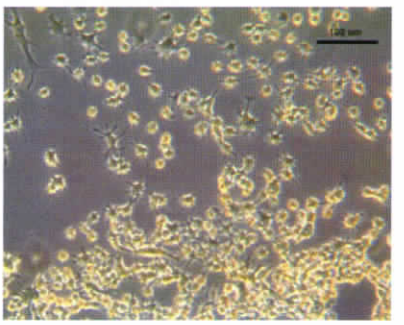

(g)

Figure 42 Phase contrast micrographs of RAW 264.7 cells seeded on (a) Biospan®, (b) PurSil™ -80A, (c) PurSil™ -75A, (d) Elasthane™, (e) CarboSil™ 20, (f) Bionate® 80A, and (g) glass coverslip following 72 hours of culture.

PurSil™ -80A, PurSil™ -75A and Carbosil™ 20 had polydimethyl siloxane endgroups on the surface which confer hydrophibicity to the materials. The

puttingforth of cytoplasmic extensions by macrophages on these materials could hence be attributed to an attempt made by the cells to get adhered on the surface. Elasthane™ also had a higher water contact angle indicating the hydrophobic nature of the material. Eventhough this material induced rounded morphology of cells at earlier time periods, by 72 hours the cells exhibited same morphology as that on the other hydrophobic materials. PurSil PUs and Elasthane had the same chemical composition, with an aromatic hard segment of MDI chain extended with butane diol and a PTMO soft segment. However PurSils had 20% PDMS co-soft segment and 0.2 wt% PDMS surface modifying end (SME) groups. CarboSil also had silicone SME groups.

In a study by Jones JA *et al* it was found that modification of PUs with PDMS, polyethylene oxide (PEO) and fluorocarbon groups did not change macrophage adhesion on PUs (Jones JA *et al* 2004). They suggested that in cell culture medium the fluorocarbon SMEs migrate away from the surface in order to evade the energetically unfavorable aqueous medium. In the case of PEO modification the mass of PEO was insufficient to induce significant difference in cell adhesion. However PDMS modification promoted macrophage fusion and apoptosis in the absence of IL-4. Jones *et al* investigated macrophage adhesion at two hours, three and seven days. However, the changes in macrophage adhesion pattern on material surface vary at earlier time periods, before they attain a rather uniform adhesion at a later time. This may be the reason why the study by Jones *et al* did not reveal subtle changes in macrophage adhesion overtime.

The present study, evaluated the adhesion pattern of macrophages at earlier and smaller time intervals of 4, 24, 48 and 72 hours. The difference between macrophage adhesion pattern on PUs with different surface chemistry, at earlier time periods was delineated. At 72 hours (3 days) the similar adhesion pattern observed on different materials was in agreement with the findings of Jones *et al* at (three days) the same time period. Phase contrast microscopic examination of macrophages (RAW 264.7, J774A.1 and IC-21 cell lines) cultured on tissue culture polystyrene, polystyrene, poly L-lactide and Teflon® AF surfaces indicated difference in morphology on different surfaces (Godek ML *et al* 2006).

Adhesion of cells to foreign surfaces is through cell surface receptor interaction with proteins adsorbed on the material. In the present study, proteins present in the medium (serum proteins) will adsorb on the material surfaces depending upon the material surface energy and surface chemistry. The difference in cell adhesion observed in the different materials can hence be attributed to the difference in material chemistry.

4.2.3.2. Analysis of macrophage adhesion on material surfaces by environmental scanning electron microscopy (ESEM)

The cell adhesion pattern on in-house synthesized PEUU could not be visualized by phase contrast microscopy. Environmental scanning electron microscopy is a powerful microscopic technique which allows visualization of morphological features without any processing steps. Figure 43 shows the morphological features of macrophages adherent on in-house synthesized PEUU in comparison to that of the commercial PU, Biospan® and glass coverslip. Biospan® had chemical composition similar to in-house synthesized PEUU. Hence it is appropriate to select Biospan® from among other commercial PUs used in this study for further detailed comparisons.

The macrophages exhibited spread morphology on glass coverslip at four hours (Figure 43 c). The morphology of adherent macrophages indicated spreading on the glass coverslip at 24 hours (Figure 43 f) and 48 hours (Figure 43 i) as well. The cytoplasmic protrusions and intercellular contacts were evident at 72 hours (Figure 43 l). The cells adherent on in-house synthesized PEUU did not exhibit spread morphology as that was observed on glass coverslips. At 4 hours (Figure 43 b) and 24 hours (Figure 43 e) the cells were round in shape. The adherent macrophages exhibited ruffled morphology at 48 hours (Figure 43 h) and 72 hours (Figure 43 k). The morphology of macrophages adherent on Biospan® was also similar to that on in-house synthesized PEUU. At 4 hours (Figure 43a) the cells were not spread. The cellular morphology at 24 hours (Figure 43 d) and 48 hours (Figure 43 g) remained the same. At 72 hours (Figure 43 j) intercellular connections between the round cells were evident.

The rounded morphology and ruffled appearance of macrophages adherent on the in-house synthesized PEUU denoted the frustrated and active nature of these cells.

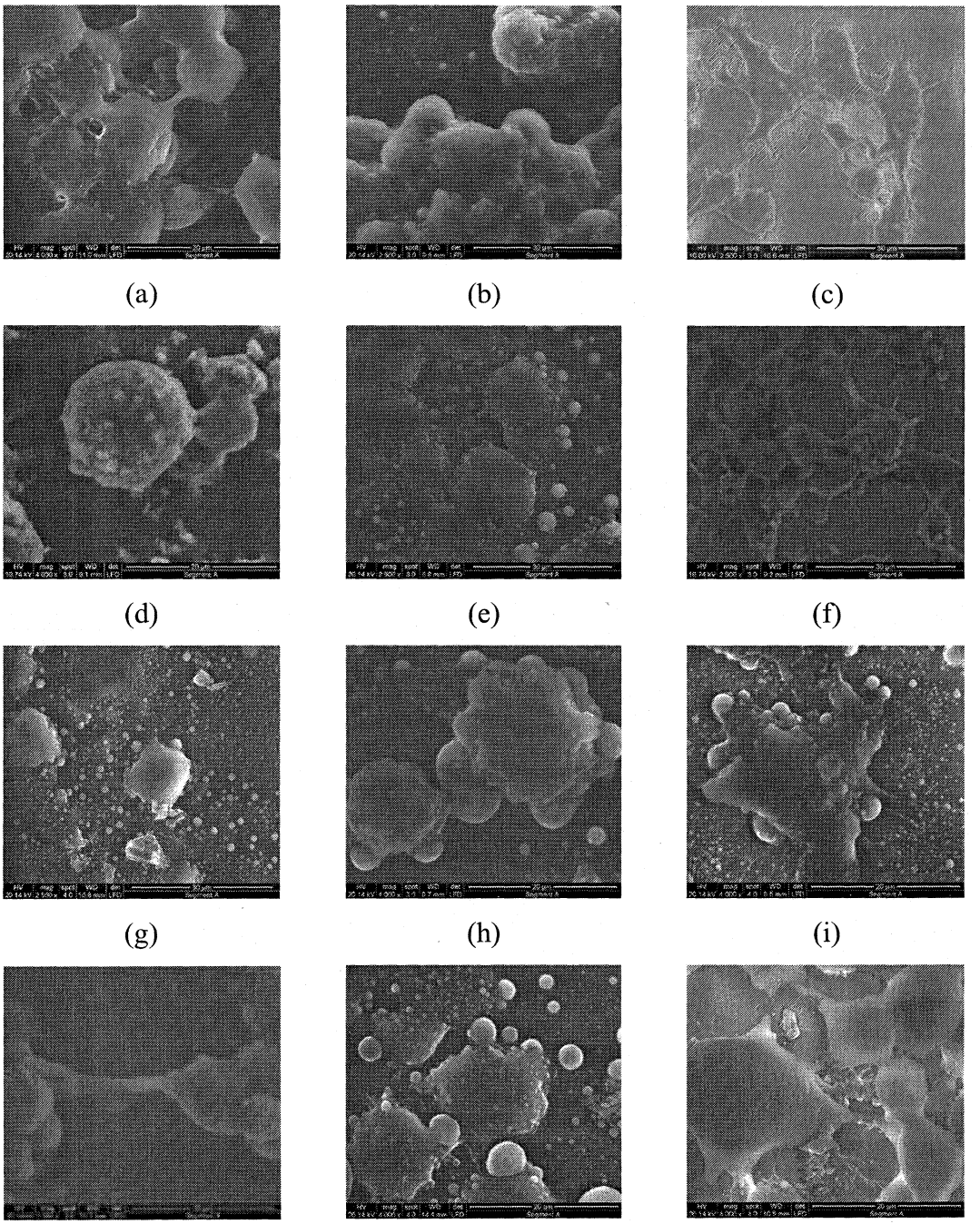

Figure 43 Environmental scanning electron micrographs of RAW 264.7 macrophages seeded on materials. (a) Biospan® - 4 hours, (b) in-house synthesized PEUU - 4 hours, (c) glass coverslip - 4 hours, (d) Biospan® - 24 hours, (e) in-house synthesized PEUU - 24 hours, (f) glass coverslip - 24 hours, (g) Biospan® - 48 hours, (h) in-house synthesized PEUU - 48 hours, (i) glass coverslip - 48 hours, (j) Biospan® - 72 hours, (k) in-house synthesized PEUU – 72 hours, and (l) glass coverslip -72 hours.

4.2.4. Analysis of actin cytoskeletal arrangement

The difference in adhesion pattern between the different commercial PUs and the in-house PEUU prompted further detailed investigations. The spreading and adhesion behaviour of macrophages is mediated by reorganization of cytoskeleton. Cytoskeletal architecture is important in cell adhesion and maintenance of cell shape. Arrangement of cytoskeletal components is considered as a marker of monocyte activation status and as an early indicator of potential inflammatory signaling (Linder S *et al* 2002). In the present study, actin cytoskeletal arrangement in adherent macrophages was examined by laser scanning confocal microscopy.

The involvement of actin filaments in polarization, protrusion and contraction of eukaryotic cells is well established. Arrangement of actin filaments vary in these different processes (Evangelista M *et al* 2003). In a migrating cell, polymerized actin is arranged in three major types. They are lamellipodia, filopodia and actin-myosin filament bundles as in stress fibres. Lamellipodia are sheet-like structures composed of cross-linked meshwork of actin filaments. Filopodia are fingerlike structures composed of thin parallel bundles of actin filaments. These two are found at the leading edge of cells. The third type, stress fibres are associated with focal adhesion complexes (Nobes CD and Hall A 1999). Cortical actin polymerization and extension of pseudopodia are important events in the host defense system of immune cells (Howard TH 1994 *et al*).

Adhesion of macrophages on biomaterial surfaces initiates a series of events which determines the ultimate fate of the material in the biological milieu. The dynamic rearrangements of actin cytoskeleton during the initial stages of macrophage adhesion is investigated in this study to delineate the different phases of adhesion. The initial events in macrophage adhesion serve as deciding factors in the response elicited by macrophages at a longer time period.

4.2.4.1. Laser Scanning Confocal microscopy

Actin cytoskeletal arrangement in adherent macrophages on materials after 4 hours of culture

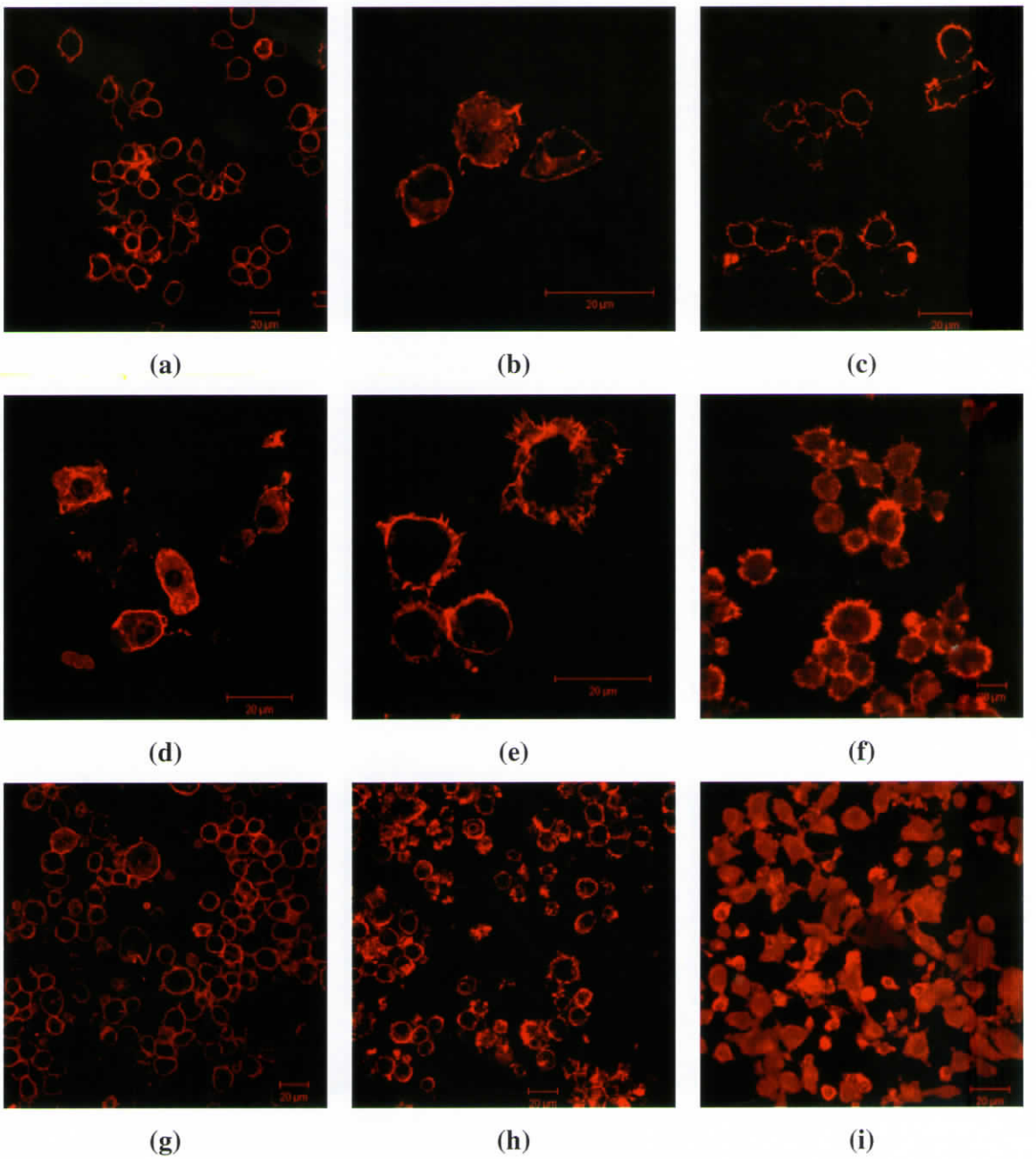

Figure 44 Confocal micrographs of RAW 264.7 macrophages, stained for F-actin, after 4 hours. Macrophages were seeded on (a) Biospan®, (b) PurSil™ -80A, (c) PurSil™ -75A, (d) Elasthane™, (e) CarboSil™ 20, (f) Bionate® 80A, (g) in-house synthesized PEUU, (h) UHMWPE, and (i) glass coverslip.

Actin cytoskeletal arrangement in adherent macrophages on materials after 24 hours of culture

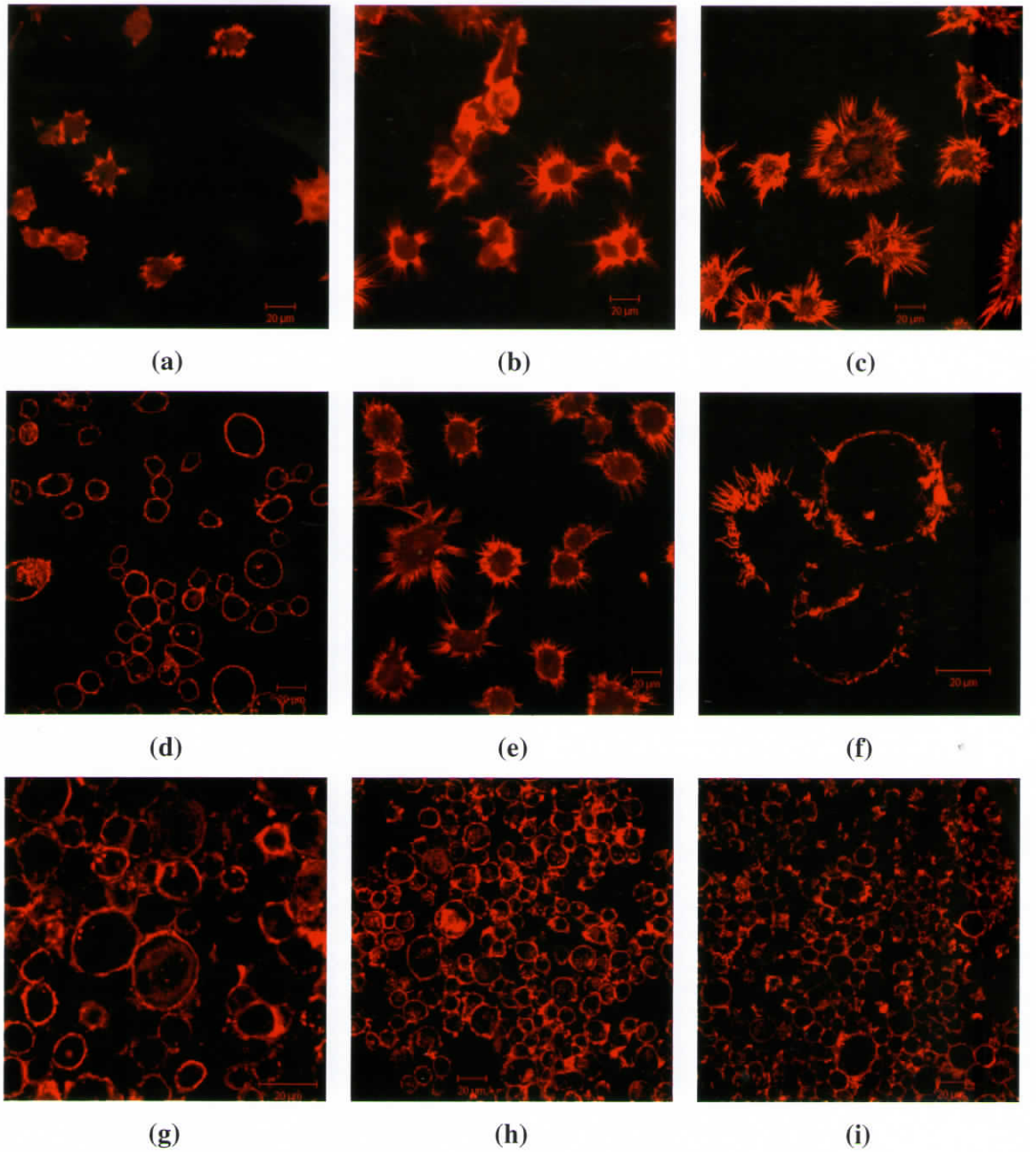

Figure 45 Confocal micrographs of RAW 264.7 macrophages, stained for F-actin, after 24 hours. Macrophages were seeded on (a) Biospan®, (b) PurSil™ -80A, (c) PurSil™ -75A, (d) Elasthane™, (e) CarboSil™ 20, (f) Bionate® 80A, (g) in-house synthesized PEUU, (h) UHMWPE, and (i) glass coverslip.

Actin cytoskeletal arrangement in adherent macrophages on materials after 48 hours of culture

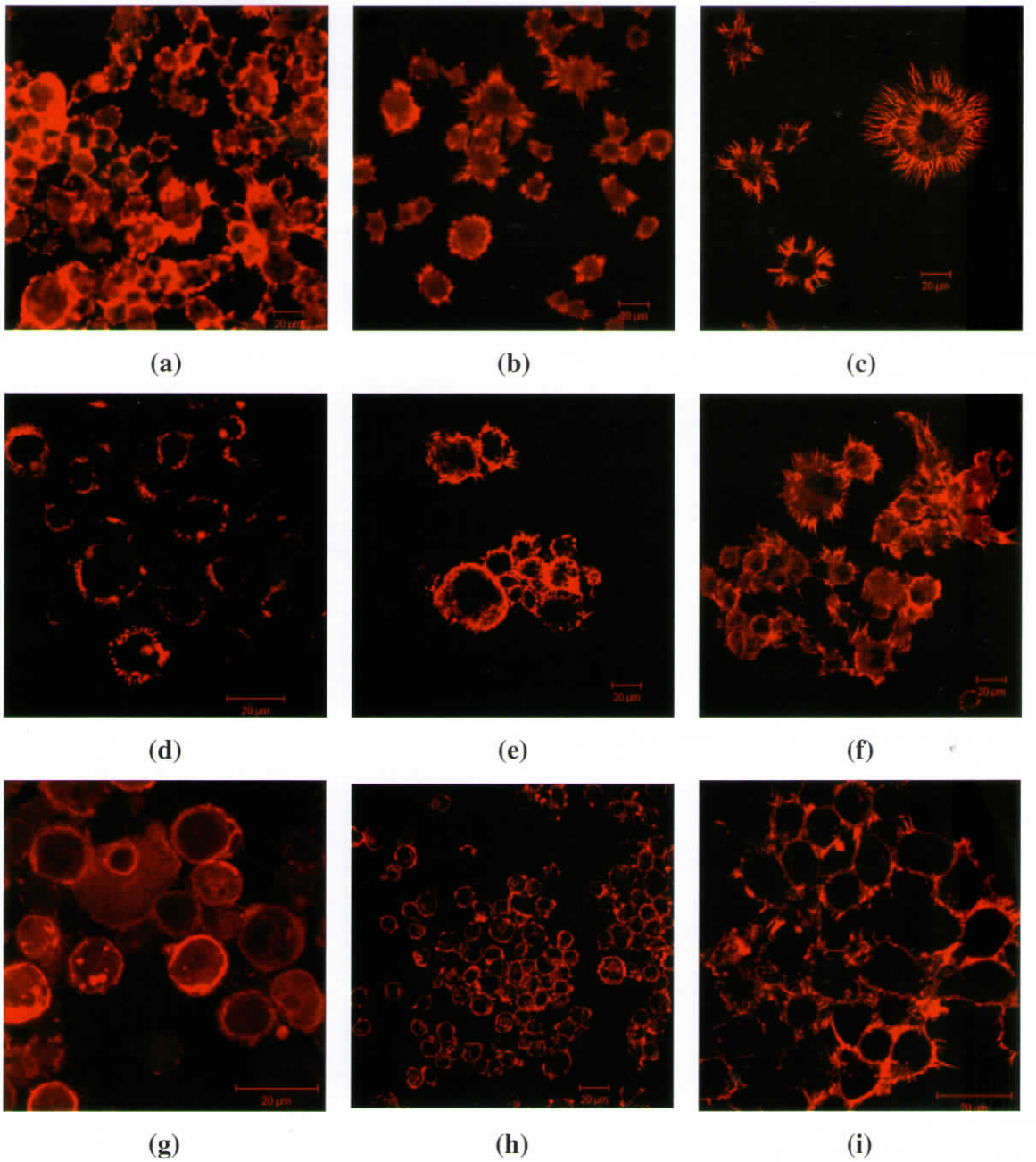

Figure 46 Confocal micrographs of RAW 264.7 macrophages, stained for F-actin, after 48 hours. Macrophages were seeded on (a) Biospan®, (b) PurSil™ -80A, (c) PurSil™ -75A, (d) Elasthane™, (e) CarboSil™ 20, (f) Bionate® 80A, (g) in-house synthesized PEUU, (h) UHMWPE, and (i) glass coverslip.

Actin cytoskeletal arrangement in adherent macrophages on materials after 72 hours of culture

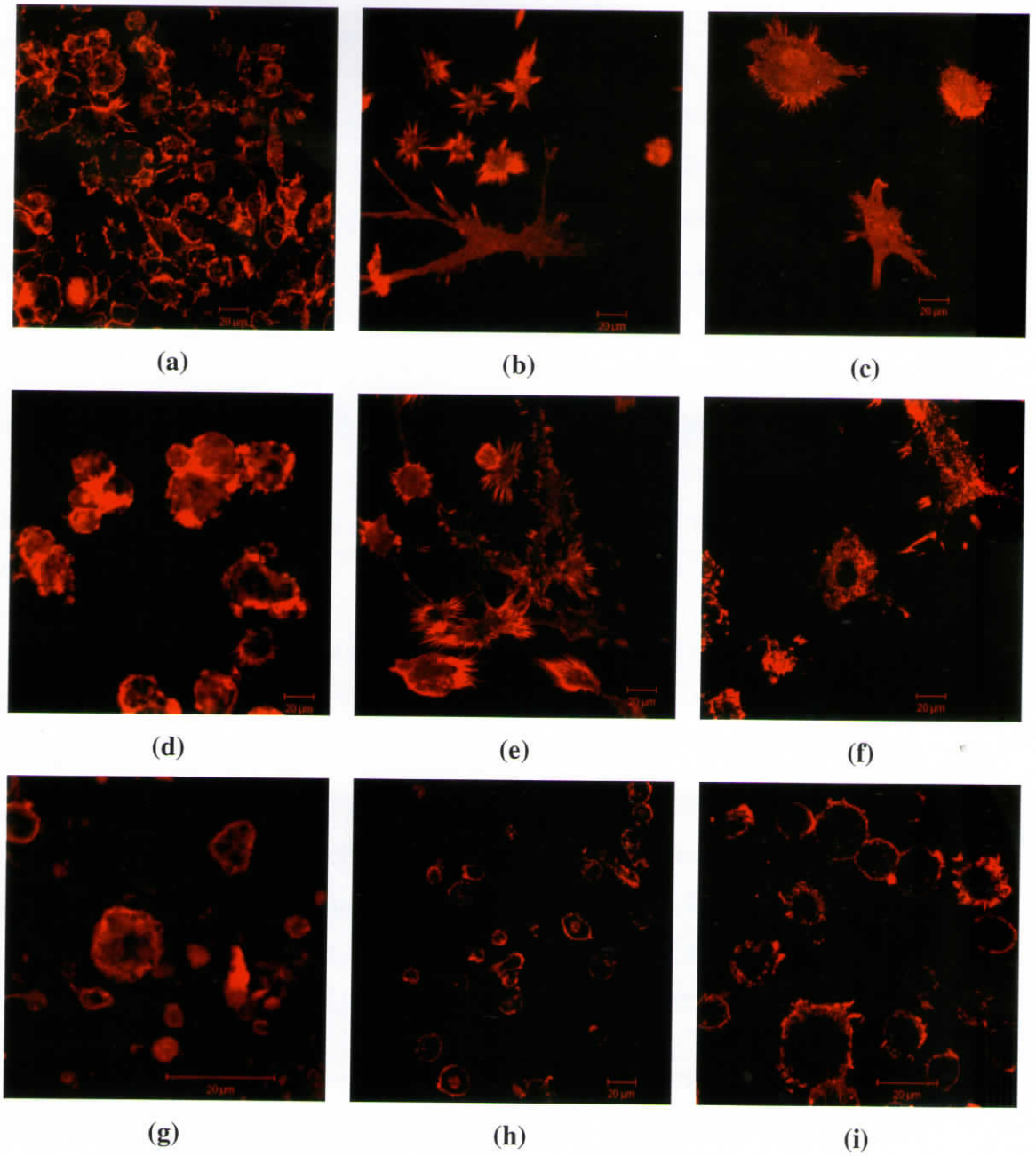

Figure 47 Confocal micrographs of RAW 264.7 macrophages, stained for F-actin, after 72 hours. Macrophages were seeded on (a) Biospan®, (b) PurSil™ -80A, (c) PurSil™ -75A, (d) Elasthane™, (e) CarboSil™ 20, (f) Bionate® 80A, (g) in-house synthesized PEUU, (h) UHMWPE, and (i) glass coverslip.

The arrangement of actin filaments in macrophages adherent on the commercial PUs as well as in-house synthesized PEUU and UHMWPE was similar at 4 hours (Figure 44). It was observed at the periphery of the cell in the form of a smooth boundary lining the cell. In the case of glass coverslip, (Figure 44i) the spreading of actin cytoskeleton was more obvious.

At 24 hours, filopodial extensions were seen on the adherent macrophages. This was more pronounced in the case of PurSil™ -80A (Figure 45b), PurSil™ -75A (Figure 45c) and CarboSil™ 20 (Figure 45e). The cells adherent on Biospan® (Figure 45a), Bionate® 80A (Figure 45f) and UHMWPE (Figure 45h) had also filopodial extensions but to a lesser extent than on the PurSils and CarboSil. However, the adherent macrophages on Elasthane™ exhibited a smooth actin cytoskeletal morphology around the cell periphery (Figure 45d). In the case of in-house synthesized PEUU filopodial extensions were less evident. The cytoskeletal arrangement in cells grown on glass coverslip indicates a spread morphology (Figure 45i).

At 48 hours the actin cytoskeletal morphology of macrophages adherent on Biospan® (Figure 46a), PurSil™ -80A (Figure 46b), PurSil™ -75A (Figure 46c), CarboSil™ 20 (Figure 46e), and Bionate® 80A (Figure 46f) exhibited extensive filopodia. However the cells adherent on Elasthane™ (Figure 46d) and UHMWPE (Figure 46h) appeared rounded. The actin cytoskeleton extended neither filopodia nor lamellipodia. The actin cytoskeletal morphology of cells adherent on in-house synthesized PEUU remained rather round in the form of a ring at the periphery of cells (Figure 46g). On glass coverslips the cells were uniformly spreading (Figure 46i).

At 72 hours the adherent macrophages were found to have extended long filopodia on PurSil™ -80A (Figure 47b), PurSil™ -75A (Figure 47c), CarboSil™ 20 (Figure 47e) and Bionate® 80A (Figure 47f). The adherent cells on Elasthane™ (Figure 47d) had not extended filopodia, however the cells had spread on the material surface. The surface of UHMWPE did not favour cell spreading as observed on other materials even by 72 hours (Figure 47h). On the surface of glass coverslip, the cells had spread with minor filopodial extensions (Figure 47i). On the other hand, on Biospan and in-house synthesized PEUU, the adherent macrophages were not found

to put filopodia. But the cells were spread to certain extent, the actin cytoskeleton was rather concentrated around the cell nucleus extending toward the periphery of cell.

The putting forth of filopodial extensions is considered as a method by which cells sample the surroundings in different directions in order to find a 'desirable' region to adhere or to move into (Godek ML *et al* 2006). The near absence of filopodial extensions in cells adherent on in-house PEUU needed further investigation to probe the activity status of the cells.

4.2.4.2. Z-sectioning of confocal images

The representative images of z-sectioned micrographs of cells adherent on Biospan® (Figure 48) and on in-house synthesized PEUU (Figure 49) further revealed the ruffled morphology of the actin cytoskeleton in a three dimensional arrangement.

It could be suggested that the reorganization of actin filaments in response to the stimuli from the material surface is mediated by the small GTPases.

Membrane ruffling is associated with phagocytic activity of macrophages. Pseudopodial extension is concomitant with engagement of cell membrane with particles to be engulfed (Araki N *et al* 1996). In the present study, the formation of membrane ruffles observed in the case of RAW 264.7 cells adhered on PEUU surfaces could be considered as an early attempt for phagocytosis. It is well known that macrophages adherent on biomaterial surfaces exhibit frustrated phagocytosis, because of its inability to engulf the bulk material. Hence it is appropriate to extend these findings to the investigation of activation of macrophages on these biomaterial surfaces.

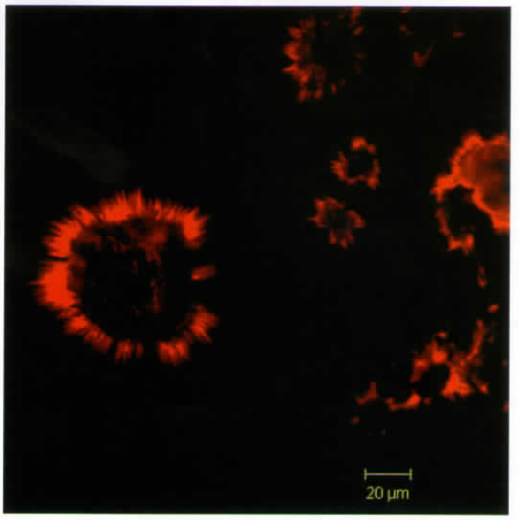

(a)

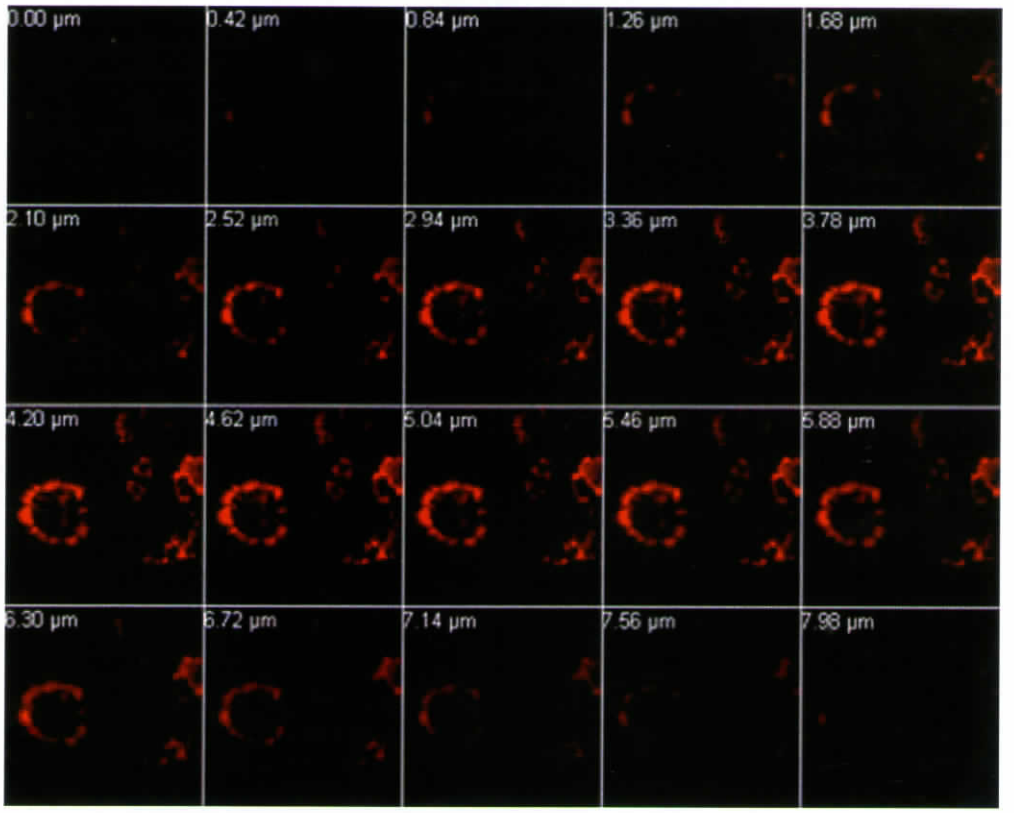

(b)

Figure 48 (a) Confocal micrograph of RAW 264.7 macrophages on Biospan® stained for F-actin following 48 hours culture and (b) Z-stack image of RAW 264.7 macrophages grown on Biospan® following 48 hours of culture.

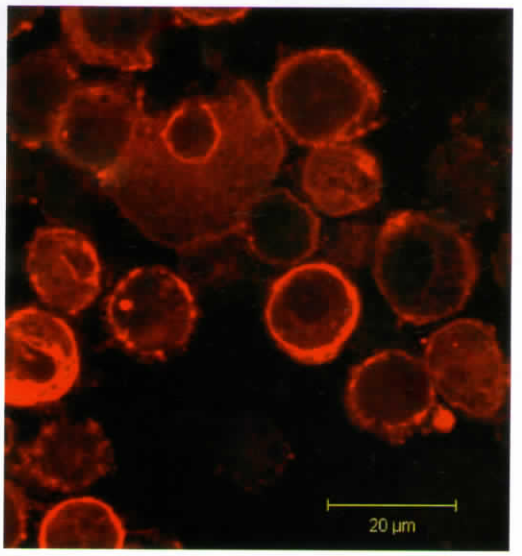

(a)

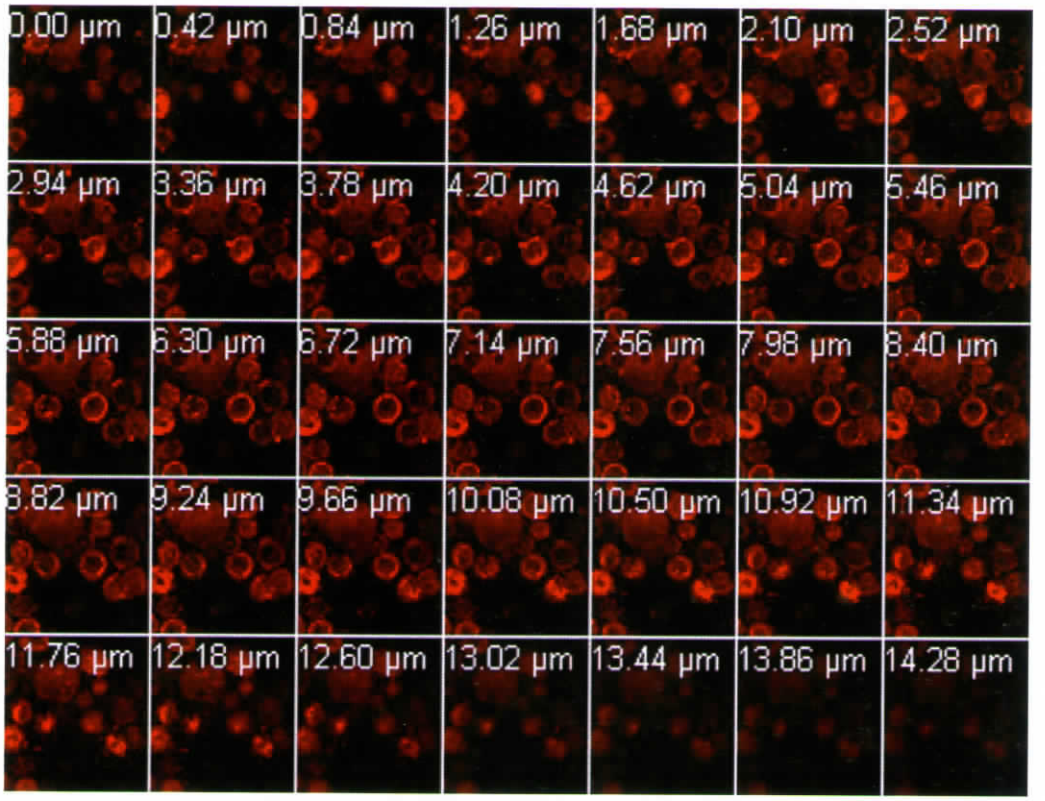

(b)

Figure 49 (a) Confocal micrograph of RAW 264.7 macrophages on PEUU stained for F-actin following 48 hours culture and (b) Z-stack image of RAW 264.7 macrophages grown on PEUU following 48 hours of culture.

4.2.4.3. Fluorescence microscopy

Representative photographs showing punctate actin in macrophages is shown in Figure 50. Punctate accumulation of actin is indicated by the arrows. Podosomes were also noted in the commercial PUs studied (Figure 50). These structures were visualized by fluorescence microscopy. Normal development of podosomes was reported in the case of primary macrophages adherent on diamond-like carbon coated surfaces (Linder S *et al* 2002).

Actin filaments are linked with the extracellular matrix through cell surface receptors. These are involved in the signal transduction events and hence determine the cellular activity to a great extent. The actin cytoskeletal arrangement observed in the case of Biospan® and the in-house synthesized PEUU showed the concentration of the filaments around the nucleus at the later time periods. These could be the sites of contact with the substratum. The substratum in the *in vitro* culture conditions is composed of adsorbed proteins on the material surface. Hence the actin cytoskeleton is found to be involved in the transduction of signal imparted by the adsorbed proteins.

Actin filaments in the form of lamellipodia and filopodia are dynamic structures and they detach from the substratum to fold upon themselves to form membrane ruffles. The membrane ruffles are nothing but the accumulation of actin filaments at the plasma membrane. In swiss 3T3 fibroblasts, the formation of actin stress fibres, lamellipodia and filopodia are regulated by small GTPases rho, rac and cdc42 respectively, (Nobes CD and Hall A 1995). However, macrophages are not known to form stress fibres, rather the actin cables observed in macrophages are the macrophage counterpart to fibroblast stress fibres. Actin filaments in Bac1, murine macrophage cell line were found as fine network at the level of substratum, parallel cables running through the cytoplasm, and as membrane ruffles on the dorsal surface of the cell. They were not found beneath the nucleus or and above the nucleus (Allen WE *et al* 1997). The present study also showed the same pattern of distribution of actin filaments around the nucleus. Figure 50 a is a representative image of an adherent macrophage on PurSil at 72 hours. The presence of actin fibres around the nucleus is clearly seen. Parallel bundles of actin running through the cytoplasm (arrow) and filopodia (*) in macrophages adherent on Bionate® are seen in Figure 50 b.

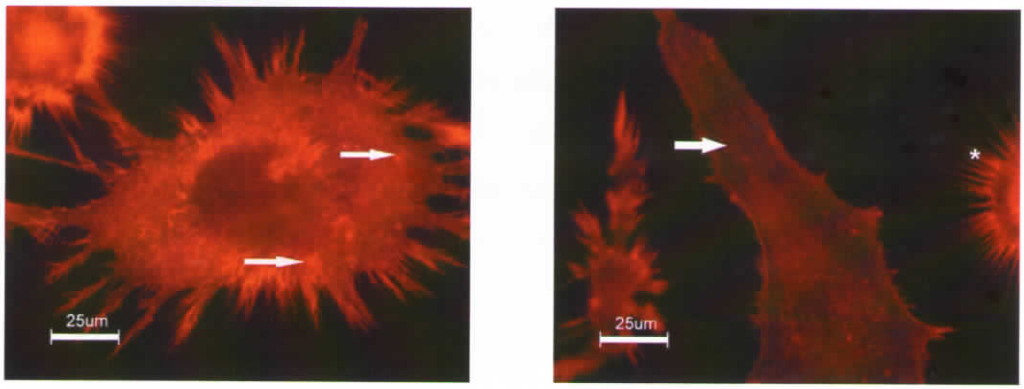

(a) (b)

Figure 50 Fluorescence micrographs of RAW 264.7 macrophages stained for F-actin (a) PurSil™ -80A (b) Bionate® 80A following 72 hours of culture. (Arrows (a) indicate punctate actin ; (b) parallel bundles of actin)

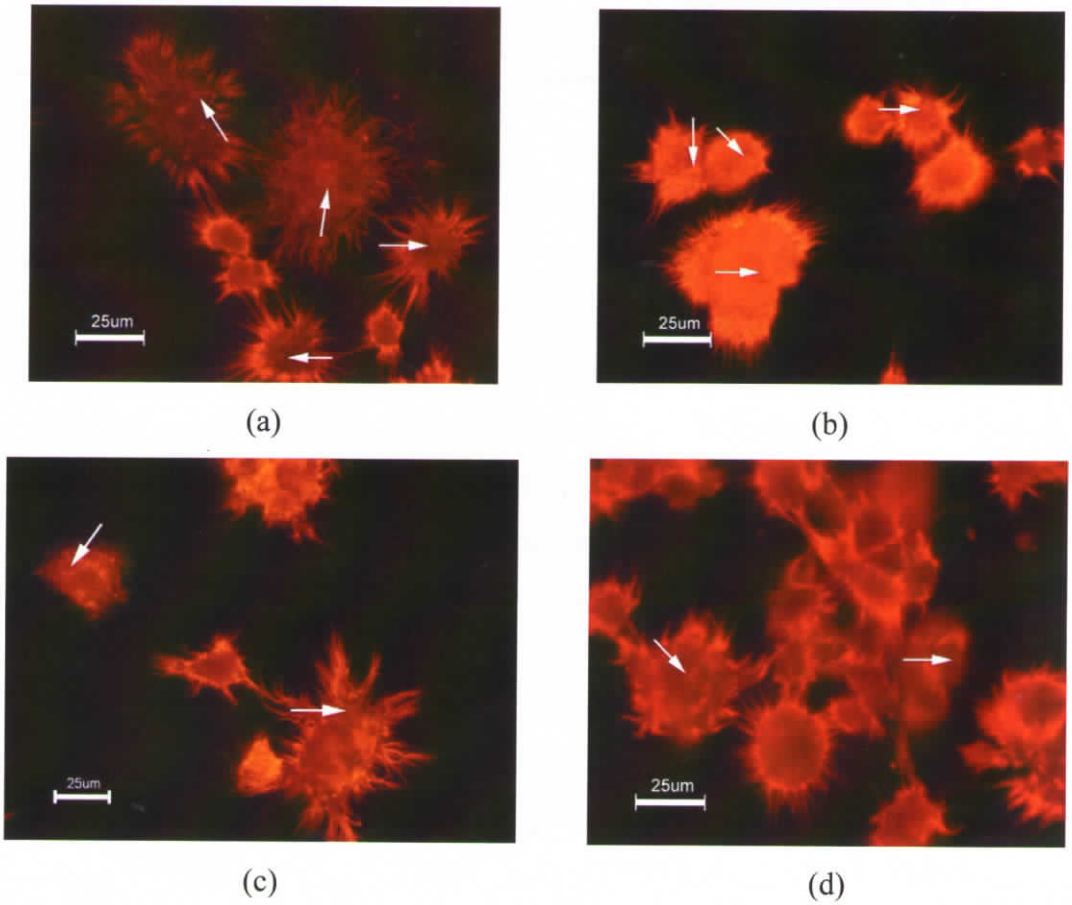

(a) (b)

(c) (d)

Figure 51 Fluorescence micrographs of podosomal structures in adherent RAW 264.7 macrophages following 72 hours of culture, on (a) Biospan®, (b) PurSil™ -80A, (c) PurSil™ -75A, and (d) Bionate® 80A.
(Arrows indicate punctate actin)

The Rho GTPases are involved in the cytoskeletal reorganization and cell adhesion by mediating the signal transduction events following activation of the cell by external stimuli. They are also implicated in the response elicited by cell adhesion on surfaces. A recent *in vitro* study revealed that the active GTP bound form of Cdc-42 was detected in macrophages cultured on polar surfaces. However, differences in surface chemistry were insufficient to differentially regulate the activation of GTPases (Godek ML *et al* 2006).

4.2.5. Measurement of IL-1α and IL-6 by ELISA

In this study, the production of pro-inflammatory cytokines such as IL-6 and IL-1α by RAW 264.7 cells on contact with polyurethanes was quantified. In-house synthesized PEUU and commercial PU (Biospan®) were assessed for induction of cytokine secretion by macrophages. Glass coverslips were assessed for the same, as a control.

The production of IL-1α was found to be higher at 24 hours in all the three materials tested (Figure 52). At 48 hours the secretion of IL-1α was found to be decreased than at 24 hours, however the decrease was significant only in the case of glass coverslip. IL-1α secretion was highest on Biospan® at both the time periods tested (25.53 pg/ml at 24 hours and 24.10 pg/ml at 48 hours). In the case of cells adherent on in-house synthesized PEUU, (22.33 pg/ml at 24 hours and 20.61 pg/ml at 48 hours) the secretion was lesser than that on Biospan®, but higher than on glass coverslip (21.89 pg/ml at 24 hours and 17.89 pg/ml at 48 hours).

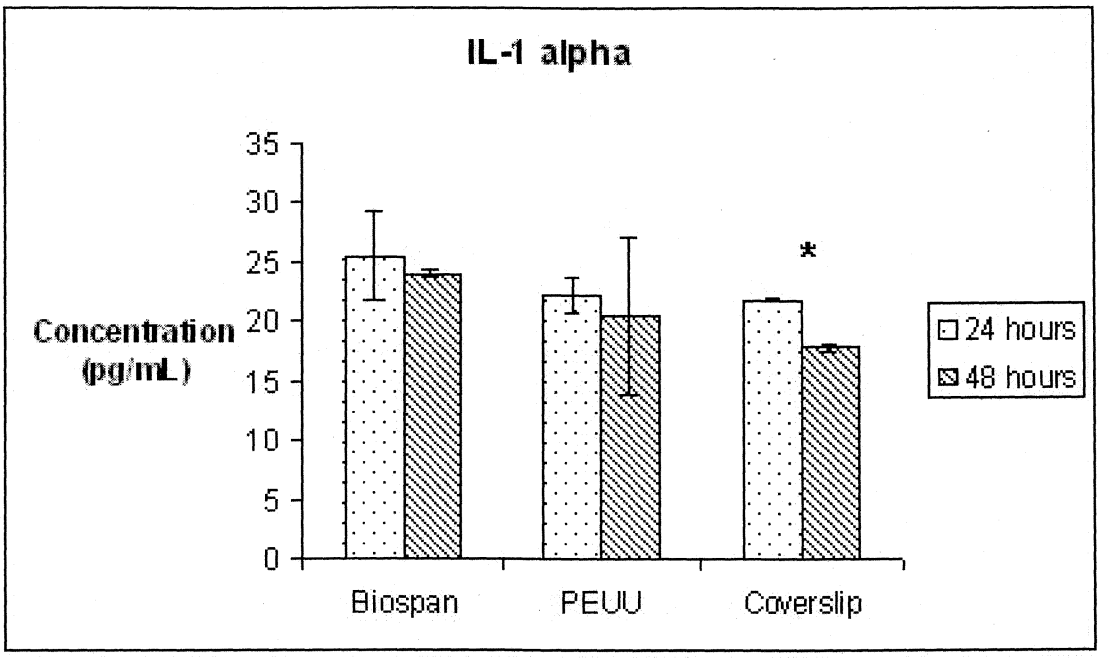

Figure 52 IL-1α production in RAW 264.7 macrophages seeded on Biospan®, in-house synthesized PEUU and glass coverslip. IL-1 α production was assessed by ELISA using cell culture medium collected at 24 and 48 hours.
Significant difference between 24 hours and 48 hours was obtained in the case of glass coverslip alone (* $P<0.05$)

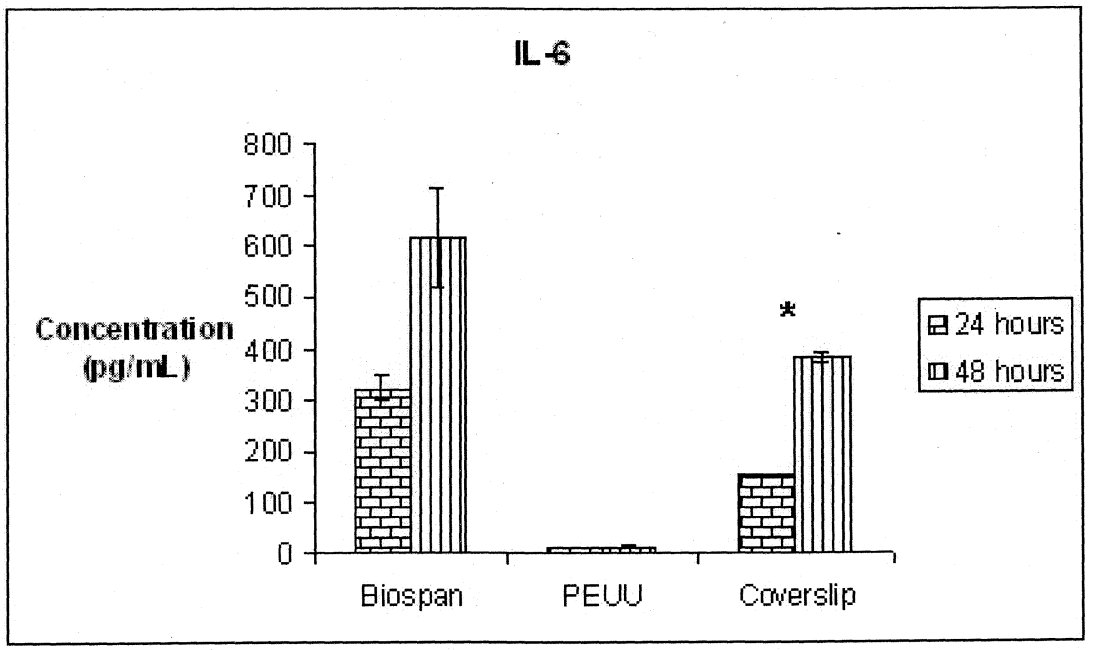

Figure 53 IL-6 production in RAW 264.7 cells seeded on Biospan®, in-house synthesized PEUU and glass coverslip. IL-6 production was assessed by ELISA using cell culture medium collected at 24 and 48 hours.
Significant difference between 24 hours and 48 hours was obtained in the case of glass coverslip alone (* $P<0.05$)

The secretion of IL-6 was found to increase with time in all the materials tested (Figure 53). However the increase was significant only in the case of cells seeded on glass coverslip. IL-6 secretion was highest on Biospan® at both the time periods tested (321.72 pg/ml at 24 hours and 618.11 pg/ml at 48 hours). In the case of cells adhered on in-house synthesized PEUU, the secretion was lesser (11.92 pg/ml at 24 hours and 13.33 pg/ml at 48 hours) than that on glass coverslip (150.83 pg/ml at 24 hours and 381.55 pg/ml at 48 hours).

The release of cytokines by the macrophages adherent on PUs indicated the active nature of these cells. The secretion of IL-6 was found to be low in the case of PEUU. This may be due to the fact that the PEUU was synthesized in-house without the icorporation of any additives. The presence of additives in the commercial PU may be responsible for the higher release in the case of Biospan®.

4.3. PHASE III

4.3.1. The role of JNK in macrophage response to PU

Macrophages are believed to mediate the response to biomaterials (Anderson (JM *et al* 1999). However comparatively little is known about the signal transduction events and involvement of signaling molecules in the activation of macrophages by biomaterials, specifically by PUs.

Members of JNK (c-Jun NH2-terminal kinase) family includes, JNK1, JNK2 and JNK3, each of which has several isoforms. JNK phosphorylates transcription factors such as c-Jun, ATF-2 and Jun D which partake in the formation of AP-1 complex (Karin M and Gallagher E 2005). Activation of AP-1 complex leads to induction of inflammatory mediators (Chang L and Karin M 2001). However, the role of JNK in activation of macrophages adherent on PU has not been investigated. In this study the role of JNK in activation of macrophages adhered on PU, was investigated.

4.3.2. CASE assay for JNK activation

In order to elucidate whether JNK is involved in signal transduction initiated by adhesion on PUs, we detected the dually phosphorylated (Thr/Tyr) form of JNK by a method following the commercial CASE kit.

A higher level of phosphorylation of JNK was found in the case of both PUs in comparison to the control, being more with in-house PEUU than with Biospan (Figure 54). This indicated that phosphorylation of JNK has occurred to a greater extent on adhesion to the materials tested.

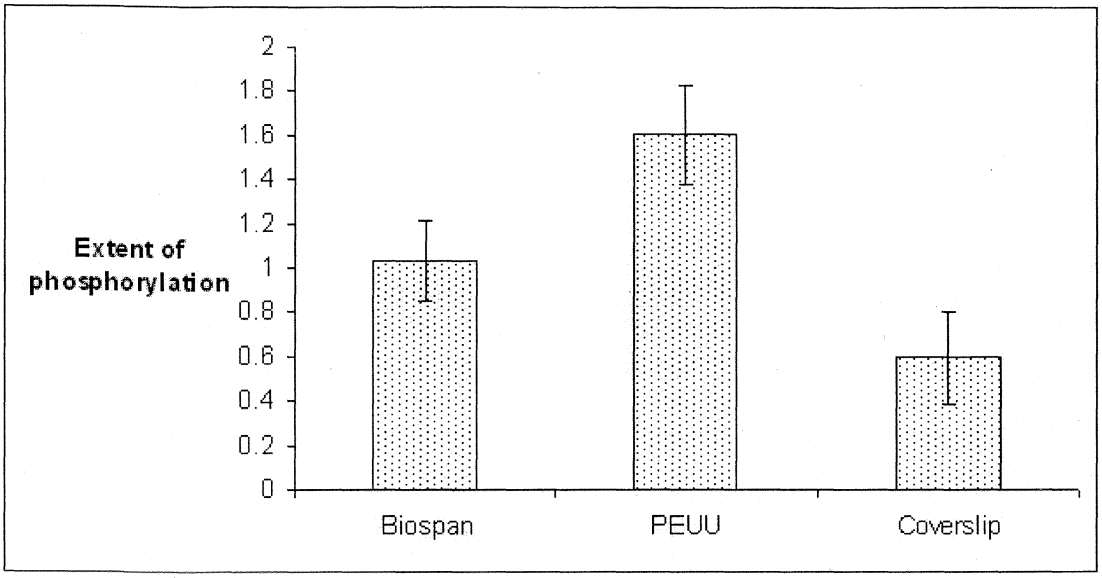

Figure 54 JNK activation in RAW 264.7 macrophages adherent on materials after 24 hours of culture.

4.3.3. Effect of SP600125 on JNK activation

To further study the role of JNK activation in macrophages adherent to PUs, the extent of JNK phosphorylation was measured after pretreatment with JNK inhibitor SP600125. It has been reported that SP600125, anthrax[1,9-cd]pyrazol-6(2H)-one is a reversible ATP-competitive inhibitor of JNK (Bennet BL *et al* 2001). In this study it was observed that pretreatment with inhibitor has decreased the levels of phosphorylation of JNK (Figure 55). However, the phosphorylation was not completely inhibited by SP600125. Even though the inhibitor specifically blocks the activity of JNK, this study has not looked into the phosphorylation of downstream signaling molecules phosphorylated by JNK. Rather the activation of JNK was studied by measuring the extent of JNK phosphorylation itself.

The extent of phosphorylation has decreased, but was not significant, in the case of in-house synthesized PEUU. While in the case of commercial PU, Biospan®, the extent of JNK phosphorylation is significantly reduced (Figure 56). This indicates that the macrophage response to in-house synthesized PEUU may be mediated by

other MAPKs also. In a study by Lu Z *et al*, it was observed that the inhibitor SP600125, caused a partial inhibition of JNK phosphorylation in RAW 264.7 cells activated by P. falciparum glycosylphosphatidylinositol (pf GPI) anchor. They suggested cross-talk between different MAPKs during pf GPI induced signaling in macrophages. A probable lack of specificity of the inhibitor was also suggested (Lu Z *et al* 2006).

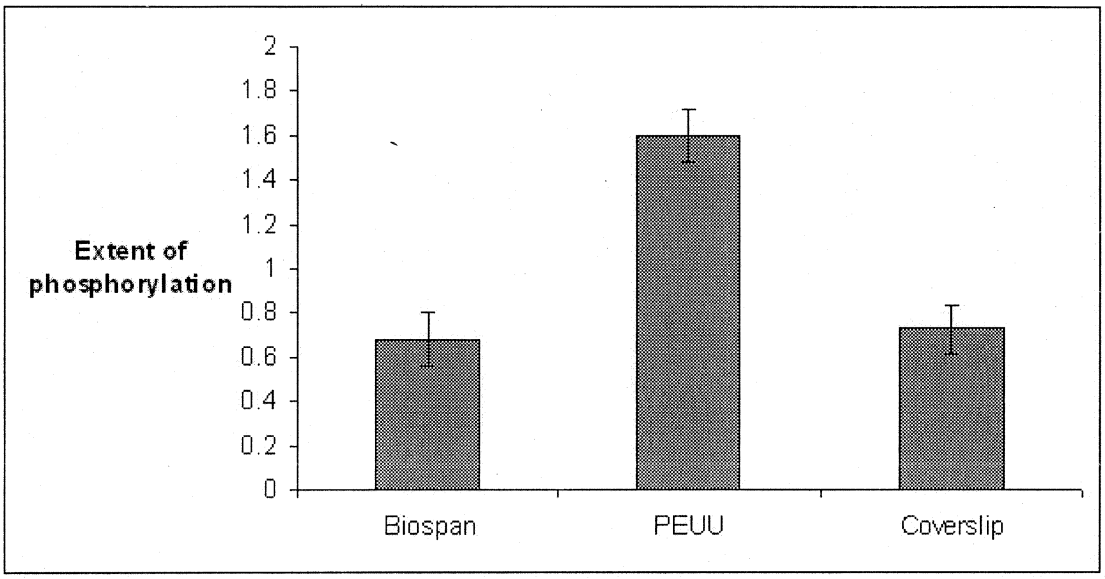

Figure 55 JNK activation in RAW 264.7 macrophages adherent on materials after 24 hours of culture, measured after treatment with SP600125.

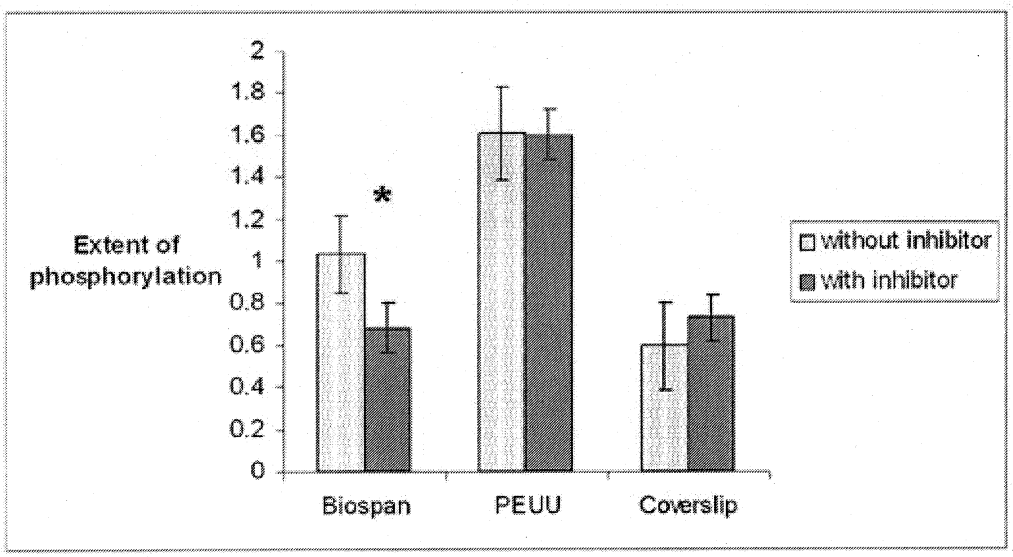

Figure 56 Comparison of JNK phosphorylation before and after treatment with SP600125.
($p<0.05$)

In the case of glass coverslip the phosphorylation increased after SP600125 treatment. This indicates that macrophage adhesion on glass coverslip is rather non-specific and is not directly related to JNK activation led inflammatory cytokine response. This further indicates that responses elicited by different materials differ at the molecular level.

This study did not further confirm the downstream effect of phosphorylated JNK on molecules such as c-Jun, ATF-2 and Jun D. Nonetheless the activation of JNK in macrophages adherent on PUs was investigated. This study is the first one to report the involvement of JNK in mediating the macrophage response to PUs. The role of JNK in activation of macrophages could be further confirmed by looking at the immediate downstream events such as c-Jun phosphorylation and also by quantitating cytokine production after inhibitor treatement. Since the present study aimed only at elucidating the involvement of JNK in macrophage response to PU, delineation of downstream signaling falls beyond the immediate objective.

The role of JNK in mediating cytokine expression is well studied (Swantek JL *et al* 1997, Tuyt L *et al* 1999, Lu H *et al* 1999). JNK signal transduction is reported to be involved in the secretion of pro-inflammatory cytokine, TNF-α in macrophages (Lu Z *et al* 2006). Hirasawa N *et al* have reported that JNK is involved in the production of histamine by RAW 264 cells by lipopolysaccharide induction (Hirasawa N *et al* 2006). In the present study the activation of JNK is evidenced, hence a possible correlation between increased cytokine production and JNK activation could be drawn out. This can be further confirmed by quantitating the cytokine production after treatment with inhibitor.

From the *in vivo* experiments it was evidenced that continued cytokine expression and macrophage mediated surface degradation of PEUU are interrelated. In other words it is now evident that the modulation of signaling mechanisms that result in proinflammatory cytokine production is central to the continued response elicited against implanted PEUU. The involvement of JNK in survival of macrophages is reported earlier. JNK activation was an important event in the transition through G_2/M checkpoint in cell cycle and hence is significant for proliferation, differentiation and survival of murine macrophages (Himes SR *et al*

2006). However this study for the first time relates the activation of JNK and survival of macrophages on PUs.

Taken together, these results point to the positive correlation between JNK activation and macrophage response to PEUU. The therapeutic potential of JNK inhibition has been implicated in pathological conditions such as Parkinson's disease, Alzheimer's disease, and multiple sclerosis (Manning AM and Davis RJ 2003). JNK could be suggested as a potential target for therapeutic intervention of macrophage mediated host response to PEUU. The findings of the present study reveal the possibility of developing methods to reduce/prevent JNK activation in macrophages adherent on PUs.

Chapter 5

SUMMARY, CONCLUSIONS AND FUTURE DIRECTIONS

5.1. Summary

An understanding of the events following the interaction of PUs with the biological environment is of importance in formulating methods to prevent degradation of PU in the biological environment. The use of PUs in implantable devices intended for long-term residence in human body was limited due to the lack of stability in biological conditions. Several mechanisms such as hydrolysis, oxidation and environmental stress cracking have been put forward. Of late the significance of cellular contribution to the observed biodegradation has been highlighted. However despite the current awareness of cell-material interactions, less is known about the cell-PU interactions. In this context the present study was formulated with the specific aim to understand the molecular mechanisms of cell-PEUU interaction. The present study is an approach towards delineating the sequential events following implantation of (polyether urethane) urea in rat animal model. In order to further understand the mechanisms of cellular interaction with PEUU, *in vitro* cell culture method was employed.

The study was performed in 3 phases. In the **first phase** a poly(ether urethane) urea, referred to as PEUU, was synthesized, characterized, tested for *in vitro* cytotoxicity and evaluated *in vivo*. The ATR-FTIR spectrum for the PEUU indicated peaks which are characteristic of polyurethanes, thus confirming the chemistry of the

in-house synthesized PEUU. The glass transition temperature of the material was found to be at -2.9°C. Contact angle measurement proved the hydrophobic nature of PEUU as evidenced by the observed contact angle value of 81.5. Molecular weight analysis by gel permeation chromatography has shown that the material had a polydispersity index of 1.7. Assessment of *in vitro* cytotoxic potential by a direct contact method using L929 mouse fibroblast cells revealed the non-cytotoxic nature of the PEUU. Histological analysis of tissue response to the sham operated site revealed that the sequence of events had followed a normal wound healing process. Neutrophils and monocytes were present at the site of injury at the initial time periods following injury. Macrophages which are the tissue counterparts were later involved in the removal of cell and tissue debri. This was followed by the remodeling phase, in which fibroblasts were predominant. By the end of 15 days, a completely remodeled tissue has formed. The tissue response to PEUU and UHMWPE also followed a similar reaction pattern at the initial stages. In the case of UHMWPE, a thin fibrous capsule had formed by 60 days. However the tissue response to PEUU did not follow a similar pattern as that of the control. Even at 180 days post-implantation, macrophages persisted in the fibrous capsule. A critical finding was this continued presence of macrophages adjacent to the implant site. Ultrastructural details of the implant sites as well as sham operated site observed by transmission electron microscopy further substantiated the histological findings.

Further, the analysis of surface morphology of the explanted materials by SEM indicated that surface degradation has occurred on PEUU surface at 30 days post-implantation. With increase in time the degradation had progressed to extensive pitting and cracking. This was in contrast to the absence of surface degradation in explanted UHMWPE, which was covered by a fibrous capsule at the end of 60 days post-implantation.

In the **second phase** of the study cell-material interactions were analysed by an *in vitro* method using the murine monocyte/macrophage cell line RAW 264.7. The cell adhesion pattern at four hours after seeding remained similar on all the materials studied including the in-house synthesized PEUU, UHMWPE, control glass coverslip, and a series of six commercial biomedical grade PUs as observed with phase contrast microscope and scanning electron microscope. At 24 hours, filopodial extensions

were putforth by the commercial PUs with PDMS content. Filopodial extensions were evident in other materials except in-house synthesized PEUU by 48 hours. At the end of 72 hours filopodia became more evident in all materials except PEUU. The difference in adhesion pattern was due to the reorganization of actin cytoskeleton in the adherent macrophages to different extents. From this it could be concluded that difference in the chemistry of polyurethanes definitely influence the cell adhesion pattern accordingly. Analysis of cytokine secretion at 24 and 48 hours by the cells adherent on in-house synthesized PEUU and a commercial PU, Biospan having the same chemistry indicated that IL-1α production follows a similar pattern in both cases. However, IL-6 secretion was significantly low in the case of in-house synthesized PEUU. This could be attributed to the fact that other additives present in the commercial PU is responsible for the early induction of IL-6 by adherent cells.

In the **final phase** of study, the role of a cell signaling molecule, JNK in macrophage activation on PU was investigated by a cell based assay. The activation of JNK as indicated by the extent of phosphorylation was higher in cells adherent on in-house synthesized PEUU. Earlier research groups have proved the involvement of JNK in the transition through G2/M checkpoint in cell cycle and hence relates JNK activation necessary for cell survival. Taken together, the findings of the present study also denotes the fact that the prolonged presence of macrophages in PEUU adjacent tissue may be due to an early survival signal passed onto the cells.

5.2. Conclusions

The results of this study indicate the persistence of macrophages adjacent to PEUU at long-term residence in biological tissue with concomitant surface degradation in the implant. The study delineates the active nature of these cells and implicates the role of JNK phosphorylation in activation and survival of macrophages adhered on PEUU. The investigation into the role of a signaling molecule in survival and activation of macrophages on PU surface has not been carried out earlier. The differential protein adsorption on PEUU and the control UHMWPE at an early time period post-implantation indicates the differential signal transmitted to the cells by these adsorbed proteins.

This study assumes significance in that it provides insights into the molecular mechanisms of macrophage activation on PEUU which will be useful to devise methods to prevent the survival of macrophages on PEUU. Selective inhibition of signaling molecules to prevent persistence and activation of macrophages on PUs could be effected to ensure long-term *in vivo* stability of material. This in turn will aid in designing better PUs which could resist degradation in the biological milieu.

5.3. Future Directions

On the basis of the findings of the present study, investigations in different lines could be further extended in future. Analysis of protein adsorption pattern could be carried out over time at short intervals in the initial time frame following implantation. This will provide valuable information on the dynamic nature of protein adsorption and how it is related to the cellular responses. Another aspect which needs further investigations is to confirm the role of JNK in macrophage activation *in vivo*, as well as their persistence at long-term at the implant adjacent tissue. This could be effected by the use of knock-out animals. Methods could be devised to prevent JNK activation and thus limit macrophage survival and activation, which will definitely improve the *in vivo* life of PU implants. Moreover, with the advent of high throughput techniques in molecular biology, the entire intracellular signaling network behind macrophage activation could be delineated so as to gain a better understanding of cell-material interactions which aid in designing of better and safe biomaterials.

BIBLIOGRAPHY

Abramson S, Alexander H, Cooper SL, Hoffman AS, Langer R, and Yannas IV. Classes of materials used in medicine. In: Biomaterials science An introduction to materials in medicine 2nd edition. Ratner BD, Hoffman AS, Schoen FJ and Lemons JE. Elsevier academic press. California. **2004**. pg.67.

Ademovic Z, Holst B, Kahn RA, Jorring L, Brevig T, Wei J, Hou X, Winter-Jensen B, Kingshott P. The method of surface PEGylation influences leukocyte adhesion and activation. *J Mater Sci Mater Med* **2006**;17:203-211.

Alano CC, Swanson RA. Players in the PARP-1 cell-death pathway: JNK-1 joins the cast. *TRENDS in biochemical sciences* **2006**;31(6):309-311.

Allen LT, Tosetto M, Miller IS, O'Connor DP, Penney SC, Lynch I, Keenan AK, Pennington SR, Dawson KA, Gallagher WM. Surface-induced changes in protein adsorption and implications for cellular phenotypic responses to surface interaction. *Biomaterials* **2006**;27:3096-3108.

Allen WE, Jones GE, Pollard JW, Ridley AJ. Rho, Rac and Cdc42 regulate actin organization and cell adhesion in macrophages. *Journal of Cell Science* **1997**;110:707-720.

Ambrosio L, Netti PA, Nicolais L. Soft tisuue. In: Integrated Biomaterials Science Ed. Rolando Barbucci. Kluwer Academic/ Plenum publishers Newyork **2002**. pg.347.

Anderson JM, Christina AG, Hanson SR, Harker LA, Johnson RJ, Merritt K, Naylor PT, Schoen FJ. Host reactions to biomaterials and their evaluation. In: Biomaterials Science. An introduction to materials in medicine. Eds.Ratner BD, Hoffman AS, Schoen FJ, Lemons JE, editors. New York. Academic press, **1996**.p.165-214.

Anderson JM, Defife K, Mcnally A, Collier T, Jenney C. Monocyte, macrophage and foreign body giant cell interactions with molecularly engineered surfaces. *J Mater Sci Mater Med* **1999**;10:579-588.

Araki N, Johnson MT, Swanson JA. A role for phosphoinositide 3-Kinase in the completion of macropinicytosis and phagocytosis by macrophages. *The journal of cell biology* **1996**;135:1249-1260.

Bennett BL, Sasaki DT, Murray BW, O'Leary EC, Sakata ST, Xu W, Leisten JC, Motiwala A, Pierce S, Satoh Y, Bhagwat SS, Manning AM, Anderson DW. SP600125, an anthraprazolone inhibitor of Jun N-terminal kinase. *PNAS* **2001**;98(24):13681-13686.

Bernacca GM, Straub I, Wheatley DJ. Mechanical and morphological study of biostable polyurethane heart valve leaflets explanted from sheep. *J Biomed Mater Res* **2002**;61:138-145.

Bernatchez SF, Atkinson MR, Parks PJ. Expression of intercellular adhesion molecule-1 on macrophages *in vitro* as a marker of activation. *Biomaterials* **1997**;18:1371-1378.

Boretos JW, Pierce WS. Segmented polyurethane: a new elastomer for biomedical applications. *Science* **1967**;1481-1482.

Brodbeck WG, Nakayama Y, Matsuda T, Colton E, Ziats NP, Anderson JM. Biomaterial surface chemistry dictates adherent monocyte/macrophage cytokine expression *in vitro*. *Cytokine* **2002**;18(6):311-319.

Brodbeck WG, Shive MS, Colton E, Nakayama Y, Matsuda T, Anderson JM. Influence of biomaterial surface chemistry on the apoptosis of adherent cells. *J Biomed Mater Res* **2001**;55:661-668.

Brodbeck WG, Voskerician G, Ziats NP, Anderson JM. *In vivo* leukocyte cytokine mRNA responses to biomaterials are dependent on surface chemistry. *J Biomed Mater Res* **2003**;64A:320-329.

Cassa J, Donovan M, Schroeder P, Stokes K, Untereker D. *In vitro* modulation of macrophage phenotype and inhibition of polymer degradation by dexamethasone in a human macrophage/Fe/stress system. *J Biomed Mater Res* **1999**;46:475-484.

Chang L and Karin M. Mammalian MAP kinase signaling cascades. *Nature* **2001**;410:37-40.

Chapekar MS, Zaremba TG, Kuester RK, Hitchins VM. Synergistic induction of tumor necrosis factor α by bacteraial lipopolysaccharide and lipotechoic

acid in combination with polytetrafluoroethylene particles in a murine macrophage cell line RAW 264.7. *J Biomed Mater Res* **1996**;31:251-256.

Chawla AS, Blais P. Degradation of explanted polyurethane cardiac pacing leads and of polyurethane. *Biomat Art Cells Art Org* **1988**;16(4):785-800.

Christenson EM, Anderson JM, Hiltner A. Oxidative mechanisms of poly(carbonate urethane) and poly(ether urethane) biodegradation: *In vivo* and *in vitro* correlations. *J Biomed Mater Res* **2004**[a];70A: 245-255.

Christenson EM, Dadsetan M, Wiggins M, Anderson JM, Hiltner A. Poly(carbonate urethane) and poly(ether urethane) biodegradation: *In vivo* studies. *J Biomed Mater Res* **2004**[b];69A:407-416.

Christenson EM, Patel S, Anderson JM, Hiltner A. Enzymatic degradation of poly(ether urethane) and poly(carbonate urethane) by cholesterol esterase. *Biomaterials* **2006**;27:3920-3926.

Collier T, Tan J, Shive M, Hasan S, Hiltner A, Anderson J. Biocompatibility of poly(etherurethane urea) containing dehydroepiandrosterone. *J Biomed Mater Res* **1998**;41:192-201.

Collier TO, Anderson JM, Brodbeck WG, Barber T, Healy KE. Inhibition of macrophage development and foreign body giant cell formation by hydrophilic interpenetrating polymer network. *J Biomed Mater Res* **2004**; 69A: 644-650.

Collier TO, Anderson JM. Protein and surface effects on monocyte and macrophage adhesion, maturation and survival. *J Biomed Mater Res* **2002**;60:487-496.

Crowley MT, Costello PS, Fitzer-Attas CJ, Turner M, Meng F, Lowell C, Tybulewicz VLJ, Defranco AL. A critical role for Syk in signal transduction and phagocytosis mediated by Fcγ receptors on macrophages. *J Exp. Med* **1997**;186(7):1027-1039.

Defife KM, Jenney CR, Colton E, Anderson JM. Cytoskeletal and adhesive structural polarizations accompany IL-13 induced human macrophage fusion. *The journal of histochemisty and cytochemistry* **1999**;47(1):65-74.

Derhami K, Zheng J, Li L, Wolfaardt JF, Scott PG. Proteomic analysis of human skin fibroblasts grown on titanium: novel approach to study molecular biocompatibility. *J Biomed Mater Res* **2001**;56:234-244.

Ernsting MJ, Labow RS, Santerre JP. Surface modification of a polycarbonate-urethane using a vitamin-E-derivatized fluoroalkyl surface modifier. *J Biomater Sci Polymer Edn* **2003**;14(12):1411-1426.

Evangelista M, Zigmond S, Boone C. Formins: signaling effectors for assembly and polarization of actin filaments. *Journal of Cell Science* **2003**;116:2603-2611.

Falck P. Characterization of human neutrophils adherent to organic polymers. *Biomaterials* **1995**;16(1):61-66.

Fare S, Petrini P, Motta A, Cigada A, Tanzi MC. Synergistic effects of oxidative environments and mechanical stress on *in vitro* stability of polyetherurethanes and polycarbonateurethanes. *J Biomed Mater Res* **1998**;45:62-74.

Gallagher WM, Lynch I, Allen LT, Miller I, Penney SC, O'Connor DP, Pennington S, Keenan AK, Dawson KA. Molecular basis of cell-biomaterial interaction: Insights gained from transcriptomic and proteomic studies. *Biomaterials* **2006**;(27):5871-5882.

Ghadially FN. Ultrastructural pathology of the cell and matrix. Butterworths, London. second edition **1982**.

Godek ML, Sampson JA, Duchsherer NL, McElwee Q, Grainger DW. Rho GTPase protein expression and activation in murine monocytes/macrophages are not modulated by model biomaterial surfaces in serum-containing *in vitro* cultures. *J Biomater Sci. Polymer Edn.* **2006**;17(10):1141-1158.

Goldstein AS, DiMilla PA. Effect of adsorbed fibronectin concentration on cell adhesion and deformation under shear on hydrophobic surfaces. *J Biomed Mater Res* **2002**;59:665-675.

Gretzer C, Gisselfalt K, Liljensten E, Ryden L, Thomsen P. Adhesion, apoptosis and cytokine release of human mononuclear cells cultured on degradable poly(urethane urea), polystyrene and titanium *in vitro*. *Biomaterials* **2003**;24(17):2843-2852.

Griesser HJ, Kingshott P, McArthur SL, McLean KM, Kinsel GR, Timmons RB. Surface-MALDI mass spectrometry in biomaterials research. *Biomaterials* **2004**;25:4861-4875.

Hergenrother RW, Waber HD, Cooper SL. Effect of hard segment chemistry and strain on the stability of polyurethanes: *in vivo* stability. *Biomaterials* **1993**;14(6):449-458.

Himes SR, Sester DP, Ravasi T, Cronau SL, Sasmono T, Hume DA. The JNK are important for development and survival of macrophages. *The journal of immunology* **2006**;176:2219-2228.

Hirasawa N, Torigoe M, Ohgawara R, Murakami A, Ohuchi K. Involvement of MAP kinases in lipopolysaccharide-induced histamine production in RAW 264 cells. *Life Sciences* **2006**;80:36-42.

Howard TH and Watts RG. Actin polymerization and leukocyte function. Curr. Opin. Hematol. **1994**;1:61-68.

Hunt JA, Flanagan BF, McLaughlin PJ, Strickland I, Williams DF. Effect of biomaterial surface charge on the inflammatory response: Evaluation of cellular infiltration and TNF-∝ production. *J Biomed Mater Res* **1996**;31:139-144.

Jahangir R, McCloskey CB, Mc Clung WG, Labow RS, Brash JL, Santerre JP. The influence of protein adsorption and surface modifying macromolecules on the hydrolytic degradation of a poly(ether-urethane) by cholesterol esterase. *Biomaterials* **2003**;24:121-130.

Jenney CR, Anderson JM. Adsorbed IgG: A potent adhesive substrate for human macrophages. J Biomed Mater Res **2000**[a];50:281-290.

Jenney CR, Anderson JM. Adsorbed serum proteins responsible for surface dependent human macrophage behaviour. *J Biomed Mater Res* **2000**[b];49:435-447.

Jones JA, Dadsetan M, Collier TO, Ebert M, Stokes KS, Ward RS, Hiltner PA, Anderson JM. Macrophage behaviour on surface-modified polyurethanes. *J Biomater. Sci. Polymer Edn.* **2004**;15(5):567-584.

Kao WJ, Liu Y. Intracellular protein tyrosine phosphorylation of adherent human macrophages on adsorbed fibronectin. Biomaterials **2003**;24:1183-1191.

Kao WJ, McNally AK, Hiltner A, Anderson JM. Role for interleukin-4 in foreign-body giant cell formation on a poly(etherurethane urea) *in vivo*. *J Biomed Mater Res* **1995**;29:1267-1275.

Kao WJ. Evaluation of leukocyte adhesion on polyurethanes: the effects of shear stress and blood proteins. *Biomaterials* **2000**;21:2295-2303.

Kaplan SS, Heine RP, Simmons RL Defensins impair phagocytic killing by neutrophils in biomaterial-related infection. *Infection and immunity* **1999**;67(4):640-1645.

Karin M., and Gallagher E. From JNK to pay dirt: jun kinases, their biochemistry, physiology and clinical importance. *IUBMB Life* **2005**;57:283-295.

Keselowsky BG, Collard DM, Garcia AJ. Surface chemistry modulates fibronectin conformation and directs integrin binding and specificity to control cell adhesion. *J Biomed Mater Res* **2003**;66A:247-259.

Kharazmi A, Nielson H, Bendtzen K. Recombinant interleukin 1α and β prime human monocyte superoxide production but have no effect on chemotaxis and oxidative burst response of neutrophils. *Immunobiology* **1988**;177:32-39.

Kota RS, Rutledge JC, Gohil K, Kumar A, Enelow RI, Ramana CV. Regulation of gene expression in RAW 264.7 macrophage cell line by interferon -γ. *Biochemical and Biophysical and Biophysical Research Communications* **2006**;342:1137-1146.

Kowalczynska HM, Nowak-Wyrzykowska M, Dokowski J, Kolos R, Kaminski J, Makowska-Cynka A, Marciniak E. Adsorption characteristics of human plasma fibronectin in relationship to cell adhesion. *J Biomed Mater Res* **2002**;61:260-269.

Krishnan A, Liu Y-H, Allara D, Vogler EA. Scaled interfacial activity of proteins at a hydrophobic solid/aqueous-buffer interface. *J Biomed Mater Res* **2005**;75A:445-457.

Labow RS, Erin M, Loren AM, Santerre JP. Human macrophage mediated biodegradation of polyurethanes: assessment of candidate enzyme activities. *Biomaterials* **2002**[a];23:3969-3975.

Labow RS, Meek E, Santerre JP. Differential synthesis of cholesterol esterase by monocyte-derived macrophages cultured on poly(ether or ester)-based poly(urethane)s. *J Biomed Mater Res* **1998**;39:469-477.

Labow RS, Meek E, Santerre JP. Hydrolytic degradation of poly(carbonate)-urethanes by monocyte-derived macrophages. *Biomaterials* **2001**[a];22:3025-3033.

Labow RS, Meek E, Santerre JP. Model systems to assess the destructive potential of human neutrophils and monocyte-derived macrophages during the acute and chronic phases of inflammation. *J Biomed Mater Res* **2001**[b];54:189-197.

Labow RS, Meek E, Santerre JP. The biodegradation of poly(urethane)s by the esterolytic activity of serine proteases and oxidative enzyme systems. *J Biomater. Sci. Polymer Edn.* **1999**;10(7):699-713.

Labow RS, Santerre JP, Waghray G. The effect of phospholipids on the biodegradation of polyurethanes by lysosomal enzymes. *J Biomater. Sci. Polymer Edn.* **1997**;8(10):779-795.

Labow RS, Tang Y, Mccloskey CB, Santerre JP. The effect of oxidation on the enzyme-catalyzed hydrolytic biodegradation of poly(urethane)s. *J Biomater. Sci. Polymer Edn.* **2002**[b];13(6):651-665.

Leibovich SJ, Polverini PJ, Shepard HM, Wiseman DM, Shively V, Nuseir N. Macrophage-induced angiogenesis is mediated by tumour necrosis factor-α. *Nature* **1987**;329(15):630-632.

Li Y, Schutte RJ, Abu-Shakra A, Reichert WM. Protein array method for assessing *in vitro* biomaterial-induced cytokine expression. *Biomaterials* **2005**;26:1081-1085.

Lin CQ and Bissell MJ. Multi-faceted regulation of cell differentiation via extracellular matrix. *FASEB J.* **1993**;7:737-743.

Linder S, Pinkowski W, Apfelbacher M. Adhesion, cytoskeletal architecture and activation status of primary human macrophages on a diamond-like carbon coated surface. *Biomaterials* **2002**;23:767-773.

Lu H, Yang DD, Wysk M, Gatti E, Mellman I, Davis RJ, Flavell RA. Defective IL-12 production in mitogen activated protein (MAP) kinase kinase3 (Mkk3)-deficient mice. *EMBO Journal* **1999**;18:1845.

Lu Z, Serghides L, Patel SN, Degousee N, Rubin BB, Krishnegowda G, Channe Gowda D, Karin M, Kain KC. Disruption of JNK2 decreases the cytokine response to Plasmodium falciparum glycosylphosphatidylinositol *in vitro*

and confers protection in a cerebral malaria model. *The journal of immunology* **2006**;177:6344-6352.

Luttikhuizen DT, van Amerongen MJ, de Feijter PC, Petersen AH, Harmsen MC, van Luyn MJA. The correlation between difference in foreign body reaction between implant locations and cytokine and MMP expression. *Biomaterials* **2006**;27:5763-5770.

Ma N, Petit A, Yahia L, Huk OL, Tabrizian M. Cytotoxic reaction and TNF-α response of macrophages to polyurethane particles. *J Biomater. Sci. Polymer Edn.* **2002**;13(3):257-272.

MacEwan MR, Brodbeck WG, Matsuda T, Anderson JM. Monocyte/lymphocyte interactions and the foreign body response: *in vitro* effects of biomaterial surface chemistry. *J Biomed Mater Res* **2005**;74A:285-293.

Maguire JK, Cosca MF, Lynch MH. Foreign body reaction to polymeric debris following total hip arthroplasty. *Clin Orthop* **1987**;216:213-223.

Manning AM and Davis RJ. Targeting JNK for therapeutic benefit: from junk to gold. *Nature reviews, Drug Discovery* **2003**;2:554-565.

Marques AP, Reis RL, Hunt JA. An *in vivo* study of the host response to starch-based polymers and composites subcutaneously implanted in rats. *Macromol. Biosci.* **2005**;5:775-785.

Matheson LA, Labow RS, Santerre JP. Biodegradation of polycarbonate- based polyurethanes by the human monocyte derived macrophage and U937 cell systems. *J Biomed Mater Res.* **2002**;61:505-513.

Mathur AB, Collier TO, Kao WJ, Schubert MA, Hiltner A, Anderson JM. *In vivo* biocompatibility and biostability of modified polyurethanes. *J Biomed Mater Res* **1997**;36:246-257.

Maurin N, Daty N, Guernier C, Dahmen K, Richter H. An *in vivo* study of the biodegradation of the hydrophilic Mitrathane. *J Biomed Mater Res* **1997**;34:73-78.

Nobes CD and Hall A. Rho, Rac and Cdc42 GTPases regulate the assembly of multimolecular focal complexes associated with actin stress fibres, lamellipodia and filopodia. *Cell* **1995**;81:53-62.

Nobes CD, Hall A. Rho GTPases control polarity, protrusion, and adhesion during cell movement. *The Journal of Cell Biology* **1999**;144(6):1235-1244.

Nobes CD, Hall A. Rho, Rac and Cdc42 GTPases regulate the assembly of multimolecular focal complexes associated with actin stress fibres, lamellipodia and filopodia. *Cell* **1995**;81:53-62.

Ochsenhirt SE, Kokkoli E, McCarthy JB, Tirrell M. Effect of RGD secondary structure and the synergy site PHSRN on cell adhesion, spreading and specific integrin engagement. *Biomaterials* **2006**;27:3863-3874.

Petillo O, Peluso G, Ambrosio L, Nicolais L, Kao WJ, Anderson JM. *In vivo* induction of macrophage Ia antigen (MHC classII) expression by biomedical polymers in the cage implant system. *J Biomed Mater Res* **1994**;28:635-646.

Petrie TA, Capadoma JR, Reyes CD, Garcia AJ. Integrin specificity and enhanced cellular activities associated with surfaces presenting a recombinant fibronectin fragment compared to RGD supports. *Biomaterials* **2006**;27:5459-5470.

Rao KM. MAP kinase activation in macrophages. *J Leukoc Biol* **2001**;69(1):3-10.

Robitaille R, Dusseault J, Henley N, Desbiens K, Labrecque N, Halle J-P. Inflammatory response to peritoneal implantation of alginate-Poly-L-lysine microcapsules. *Biomaterials* **2005**;26:4119-4127.

Rose-John S, Scheller J, Elson G, Jones S A. Interleukin-6 biology is coordinated by membrane-bound and soluble receptors: role in inflammation and cancer. *Journal of leukocyte biology* **2006**;80:1-10.

Rosengart MR, Arbabi S, Garcia I, Maier RV. Interactions of calcium/calmodulin-dependent protein kinases (CaMK) and extracellular – regulated kinase (ERK) in monocyte adherence and TNF-α production. *Shock* **2000**;13(3):183-189.

Ruoslahti E and Reed JC. Anchorage dependence, integrins and apoptosis. *Cell* **1994**;77:477-478.

Saad B, Casotti M, Huber T, Schmutz P, Welti M, Uhlschmid GK, Neuenschwander P, Suter UW. *In vitro* evaluation of the biofunctionality

of osteoblasts cultured on DegraPol-foam. *J Biomater Sci Polym Edn.* **2000**;11(8):787-800.

Salacinski HJ, Odlyha M, Hamilton G, Seifalian AM. Thermo-mechanical analysis of a compliant poly(carbonate-urea) urethane after exposure to hydrolytic, oxidative, peroxidative and biological solutions. *Biomaterials* **2002**[a];23:2231-2240.

Salacinski HJ, Tai NR, Carson RJ, Edawards A, Hamilton G, Seifalian AM. *In vitro* stability of a novel compliant poly(carbonate-urea)urethane to oxidative and hydrolytic stress. *J Biomed Mater Res* **2002**[b];59:207-218.

Santerre JP, Labow RS, Adams GA. Enzyme–biomaterial interactions: effect of biosystems on degradation of polyurethanes. *J Biomed Mater Res.***1993**;27:97-109.

Santerre JP, Labow RS, Duguay DG, Adams GA. Biodegradation evaluation of polyether and polyester-urethanes with oxidative and hydrolytic enzymes. *J Biomed Mater Res* **1994**;28:1187-1199.

Schlosser M, Wilhelm L, Urban G, Ziegler B, Ziegler M, Zippel R. Immunogenicity of polymeric implants: long term antibody response against polyester (Dacron) following the implantation of vascular prostheses into LEW. IA rats. *J Biomed Mater Res* **2002**;61:450-457.

Schubert MA, Wiggins MJ, Anderson JM, Hiltner A. Role of oxygen in biodegradation of poly(etherurethane urea) elastomers. *J Biomed Mater Res* **1997**[a];34:519-530.

Schubert MA, Wiggins MJ, Anderson JM, Hiltner A. The effect of strain state on the biostability of a poly(etherurethane urea) elastomer. *J Biomed Mater Res* **1997**[b];35:319-328.

Schubert MA, Wiggins MJ, DeFife KM, Hiltner A, Anderson JM. Vitamin E as an antioxidant for poly(etherurethane urea): *In vivo* studies. *J Biomed Mater Res* **1996**;32:493-504.

Schubert MA, Wiggins MJ, Schaefer MP, Hiltner A, Anderson JM. Oxidative biodegradation mechanisms of biaxially strained poly(etherurethane urea) elastomers. *J Biomed Mater Res* **1995**;29:337-347.

Sevilla L, Aperlo C, Dulie V, Chambard JC, Butonnet C, Pasquier O, Pognonec P, Boulukos KE. The Ets2 transcription factor inhibits apoptosis induced by

colony-stimulating factor 1 deprivation of macrophages through a Bcl-xL-dependent mechanism. *Mol. Cell Biol.* **1999**;19:2624-2634.

Simmons A, Hyvarinen J, Odell RA, Martin DJ, Gunatillake, Noble KR, Poole-Warren LA. Long-term *in vivo* biostability of poly(dimethylsiloxane)/poly(hexamethylene oxide) mixed macrodiol-based polyurethane elastomers. *Biomaterials* **2004**;25:4887-4900.

Simonovsky FI, Porter SC, Ratner BD. Synthesis of segmented poly(ether urethane)s incorporating various side-chain or backbone functionalities. *J. Biomater. Sci. Polym. Edn.* **2005**;16(2):267-284.

Steffensen B, Hakkinen L, Larjava H. Proteolytic events of wound- healing – coordinated interactions among matrix metalloproteinases (MMPs), Integrins and extracellular matrix molecules. *Crit Rev Oral Biol Med* **2001**;12(5):373-398.

Stokes K and McVenes R. Polyurethane elastomer biostability. *J Biomater Appl.* **1995**;9:321-354.

Stokes KB. Polyether polyurethane pacemaker leads: The contribution of clinical experience to elucidation of failure modes and biodegradation mechanisms. In: Clinical studies of medical devices and diagnostics: principles and approaches. Ed. Witkin KB, Totowa, NJ: Humana press;**1997**.p233-255.

Swantek JL, Cobb MH, Geppert TD Jun N-terminal kinase/ stress activated protein kinase (JNK/SAPK) is required for lipopolysaccharide stimulation of tumor necrosis factor α (TNF-α) translation: glucocorticoids inhibit TNF-α translation by blocking JNK/SAPK. *Mol.Cell Biol.* **1997**;17:6274-6282.

Takahara A, Coury AJ, Hergenrother RW, Cooper SL. Effect of soft segment chemistry on the biostability of segmented polyurethanes. I. *In vitro* oxidation. *J Biomed Mater Res* **1991**;25:341-356.

Takahara A, Hergenrother RW, Coury AJ, Cooper SL. Effect of soft segment chemistry on the biostability of segmented polyurethanes. II. *In vitro* hydrolytic degradation and lipid sorption. *J Biomed Mater Res* **1992**;26:801-818.

Tang YW, Labow RS, Santerre JP. Enzyme induced biodegradation of polycarbonate-polyurethanes :dose dependence effect of cholesterol esterase. *Biomaterials* **2003**;24:2003-2011.

Tang YW, Labow RS, Santerre JP. Enzyme-induced biodegradation of polycarbonate polyurethanes: Dependence on hard segment concentration. *J Biomed Mater Res* **2001**[a];56:516-528.

Tang YW, Labow RS, Santerre JP. Enzyme-induced biodegradation of polycarbonate-polyurethanes: Dependence on hard-segment chemistry. *J Biomed Mater Res* **2001**[b];57:597-611.

Tang YW, Santerre JP, Labow RS, Taylor DG. Application of macromolecular additives to reduce the hydrolytic degradation of polyurethanes by lysosomal enzymes. *Biomaterials* **1997**;18:37-45.

Territo MC, Ganz T, Selsted ME, Lehrer R. Monocyte-chemotactic activity of defensins from human neutrophils. *J Clin Invest* **1989**;84:2017-2020.

Tracey KJ, Cerami A. Tumor necrosis factor: a pleiotropic cytokine and therapeutic target. *Annu Rev Med* **1994**;45:491-503.

Tuyt LM, Dokter WH, Birkenkamp K, Koopmans SB, Lummen C, Kruijer W, Vellenga E. Extracellular-regulated kinase, Jun N-terminal kinase, and c-Jun are involved in NF-κB dependent IL-6 expression in human monocytes. *Journal of immunology* **1999**;162:4893-4902.

Valledor AF, Borras FE, Cullell-Young M, Celada A. Transcription factors that regulate monocyte/macrophage differentiation. *J leukocyte Biol* **1998**;63:405-417.

Voet D and Voet JG. Biochemistry 2nd edition. John Wiley &sons Inc., NewYork. **1995**;1207-1234.

Vuori K and Ruoslathi E. Activation of protein kinase C preceeds α5β1 integrin mediated cell spreading on fibronectin. *J Biol Chem* **1993**;268:21459-21462.

Wagner MS, Horbett TA, Castner DG. Characterizing multicomponent adsorbed protein films using electron spectroscopy for chemical analysis, time-of-flight secondary ion mass spectrometry and radiolabelling: capabilities and limitations. *Biomaterials* **2003**;24:1897-1908.

Wagner VE, Bryers JD. Monocyte/macrophage interactions with base and linear- and star-like PEG-modified PEG-poly(acrylic acid) co-polymers. *J Biomed Mater Res* **2003**;66A:62-78.

Ward WK, Slobodzian EP, Tiekotter KL, Wood MD. The effect of microgeometry, implant thickness and polyurethane chemistry on the foreign body response to subcutaneous implants. *Biomaterials* **2002**;23:4185-4192.

Warren JS, Kunkel SL, Cunningham TW, Johnston KJ, Ward PA. Macrophage-derived cytokines amplify immune complex-triggered O2- responses by rat alveolar macrophages. *Am J Pathol* **1988**;130:489-495.

Wary KK, Mainiero F, Isakoff FJ, Marcantonio EE, Giancotti FG. The adaptor protein Shc couples a class of integrins to the control of cell cycle progression. *Cell* **1996**;87:733-743.

Wenig BM, Heffner DK, Johnson FB. Teflonomas of the larynx and neck. *Hum. Pathol.* **1990**;21:617-623.

Werthen M, Sellborn A, Kalltorp M,Elwing H, Thomsen P. *In vitro* study of monocyte viability during the initial adhesion to albumin-and fibrinogen coated surfaces. *Biomaterials* **2001**;22:827-832.

Williams DF and Roaf R. Reconstructing the body.Implants in surgery. Volume I. Liverpool University Press **2000**. pg 207-244.

Wilson K, Stuart SJ, Garcia A, Latour RA. A molecular modeling study of the effect of surface chemistry on the adsorption of a fibronectin fragment spanning the 7-10th type III repeats. *J Biomed Mater Res* **2004**;69A:686-698.

Wu C, Chung AE, McDonald JA. A novel role for $\alpha 3\beta 1$ integrins in extracellular matrix assembly. Journal of cell science **1995**;108:2511-2523.

Wu Y, Sellitti, Anderson JM, Hiltner A, Lodoen GA, Payet CR. An FTIR-ATR investigation of *in vivo* poly (ether urethane) degradation. *Journal of Applied Polymer Science* **1992**;46:201-211.

Wu Y, Zhao Q, Anderson JM, Hiltner A, Lodoen GA, Payet CR. Effect of some additives on the biostability of a poly(etherurethane) elastomer. *J Biomed Mater Res* **1991**;25:725-739.

Xi T, Sato M, Nakamura A, Kawasaki Y, Umemura T, Tsuda M, Kurokawa Y. Degradation of polyetherurethane by subcutaneous implantation into rats. I. Molecular weight change and surface morphology. *J Biomed Mater Res* **1994**;28: 483-490.

Xia Z and Triffitt JT. A review on macrophage responses to biomaterials. *Biomed Mater* **2006**;1:R1-R9. doi:10.1088/1748-6041/1/1/ROI.

Yang M, Santerre JP. Utilization of quinolone drugs as monomers:characterization of the synthesis reaction products for (polynorfloxacin diisocyanatododecane polycaprolactone) *Biomacromolecules* **2001**;2(1):134-141.

Zdrahala RJ, Zdrahala IJ. Biomedical applications of polyurethanes: A review of past promises, present realities, and a vibrant future. *Journal of Biomaterials Applications* **1999**;14:67-90.

Zhao Q, Agger MP, Fitzpatrick M, Anderson JM, Hiltner A, Stokes K, Urbanski P. Cellular interactions with biomaterials: *in vivo* cracking of pre-stressed Pellethane 2363-80A. *J Biomed Mater Res* **1990**;24:621-637.

Zhao Q, Topham N, Anderson JM, Hiltner A, Lodoen G, Payet CR. Foreign-body giant cells and polyurethane biostability: *In vivo* correlation of cell adhesion and surface cracking. *J Biomed Mater Res* **1991**;25:177-183.

Zhao QH, Anderson JM, Hiltner A, Lodoen GA, Payet CR. Theoretical analysis on cell size distribution and kinetics of foreign body giant cell formation *in vivo* on polyurethane elastomers. *J Biomed Mater Res* **1992**;26:1019-1038.

Zhao QH, McNally AK, Rubin KR, Renier M, Wu Y, Rose-Caprara V, Anderson JM, Hiltner A, Urbanski P, Stokes K. Human plasma α2-macroglobulin promotes *in vitro* oxidative stress cracking of Pellethane 2363-80A: *In vivo* and *in vitro* correlations. *J Biomed Mater Res* **1993**;27:379-389.

Zreiqat H, Howlett CR, Zannettino A, Evans P, Schulze-Tanzil G, Knabe C, Shakibaei M. Mechanisms of magnesium-stimulated adhesion of osteoblastic cells to commonly used orthopaedic implants. *J Biomed Mater Res* **2002**; 62:175-184.

Zuckerman ST, Kao WJ. Effect of surface-adsorbed proteins and phosphorylation inhibitor AG18 on intracellular protein expression in adherent macrophages. *Biomaterials* **2006**;27:3745-3757.